



Basic principles of ship propulsion

MAN Energy Solutions

Future in the making

Optimisation of hull, propeller, and engine
interactions for maximum efficiency

Future in the making



This paper will explain the most elementary terms used regarding ship types, dimensions and hull forms, and clarify some of the parameters pertaining to hull resistance, propeller conditions, main engine capabilities, and environmental regulations. The interdependencies between these illustrate the complexity of optimising the hull as well as the interaction with the propulsion plant.

Based on the explanations given, the reader will be able to work through the engine selection spiral described in this paper. This will facilitate selection of the right main engine(s) for the right hull in order to support the ambition of creating a sustainable future.

This paper is divided into five chapters which, with advantage, may be read in close connection to each other, providing the reader with an understanding of how the hull and propeller affect the engine running conditions and vice versa. The chapters can also be read independently. Therefore, some important information mentioned in one chapter may appear in another chapter as well.

The present edition of the paper has been revised compared to previous editions. In the previous 2018 edition, a description of the environmental regulations implemented over the past decade as well as their effect on designs of modern ship propulsion plants was added in Chapter 4. This chapter has been further extended in this revision, reflecting recent developments.

Numerous updates have been made to chapters 1 to 3, to reflect and highlight specific impacts of the implemented regulation and topics in increased need of consideration as a result hereof.

Chapter 1 describes the most elementary terms used to define ship sizes and hull forms such as, for example, the ship's displacement, deadweight, draught, length between perpendiculars, block coefficient, etc. Other terms described include the calm water resistance, which consist of frictional, residual and air resistance, along with the influence of these resistances in service.

Chapter 2 deals with ship propulsion and the flow conditions around the pro-

PELLER(S), and describes the main parameters related hereto. The operating conditions of a propeller according to the propeller law are described for free sailing in calm weather. The influence of the propeller size and speed is considered along with different philosophies for optimising hull and propeller interactions.

Chapter 3 explains the basic principles related to diesel engines. Two engine selection spirals for, respectively, fixed and controllable pitch propellers are introduced. Also, the principles of the engine layout diagram are explained, along with the link to the propeller curve and a description of the principles behind optimum matching of engine and propeller.

The engine load diagram, the effect of heavy running, and the necessity of a propeller light running margin are explained. Special considerations are given to the possibilities for including a shaft generator for both propeller types. Sections on the engine loading during acceleration, impact of various types of power limitations and initiatives to increase the area of the load diagram has been added for this edition.

Chapter 4 describes some of the environmental regulations governing shipping, especially pertaining to the layout of the propulsion plant. An overview of the possible measures allowing for fulfilment of the Energy Efficiency Design Index (EEDI) and reduction of the Carbon Intensity Indicator (CII) as per design are given. Finally, requirements for

minimum propulsion power of bulk carriers and tankers are considered along with its impact towards the layout of the propulsion plant.

Chapter 5 contains examples of the application of the engine selection spirals under consideration of EEDI phase 3. The examples underline the importance of optimum matching of engine and hull in order to minimise emissions.

In general, the interdependencies between different hull, propeller, and engine related parameters described throughout the chapters are complex, and several different paths for optimising the ship can be taken by the ship designer, all depending on the priorities of the project. This also explains why two tender designs for the same ship never look the same.

It is considered beyond the scope of this publication to explain how propulsion calculations, i.e. power predictions as such are carried out, as the calculation procedure is complex. The reader is referred to the specialised literature on this subject, for example as stated in the final section "References".

Contents

Chapter 1

Ship definitions and hull resistance p 7

- Hull dimensions and load lines p. 7
- Size determining factors p. 9
 - Displacement, deadweight and lightweight p. 9
 - Coefficients related to the hull p. 9
- Ship types with engine applications in overview p. 10
- Efficiencies affecting the total fuel consumption p. 11
- Resistance and influencing parameters p. 11
 - Components of resistance p. 11
 - Parameters influencing resistance and optimisation hereof p. 13
 - Added resistance in various conditions p. 14
 - Resistance margins in a slow steaming environment p. 15

Chapter 2

Propeller propulsion p 17

- Definitions of parameters p. 17
- Propeller types and geometry p. 18
- Flow conditions p. 20
- Propeller coefficients p. 21
- Slip p. 22
- Cavitation p. 22
- Efficiencies and influencing parameters p. 22
 - Influence of propeller diameter and pitch/diameter ratio example p. 24
 - Different approaches for optimising the propulsive efficiency p. 25
- Energy saving devices p. 26
- “Propeller law” and power/speed curves p. 27
- Acceleration, barred speed range, manoeuvring speed and propeller rotation p. 27
 - Manoeuvring speed p. 29
 - Direction of propeller rotation p. 29
 - Manufacturing accuracy of the propeller p. 30

Chapter 3

Engines for marine propulsion plants p 31

- Two-stroke uniflow crosshead diesel cycle engines p. 31
 - Engine efficiency parameters p. 32
 - GI, GA and LGI dual fuel engines p. 32
- Engine selection spiral for FP-propeller p. 34
 - 2. Light propeller curve p. 34
 - 3. Propulsion margins, including light running margin p. 35
 - 4. Engine layout diagram with SMCR, derating p. 36
 - 5. Select engine p. 38
 - 6. Passage of the barred speed range p. 38
 - 7. Engine load diagram and considerations of PTO p. 39

- 8. Compliance with regulations p. 42
- Engine selection spiral for CP-propeller p. 43
 - 2. Possible propeller operation for CPP and required power p. 43
 - 3. CPP operating principles for inclusion of PTO p. 44
 - 4. Propulsion margins for CPP p. 44
 - 5. Engine layout diagram with SMCR for CPP p. 45
 - 6. Select engine for CPP p. 45
 - 7. Engine load diagram for CPP and considerations of PTO power p. 45
 - 8. Compliance with regulations p. 46
- Engine tuning p. 46
- Rpm extended load diagram p. 46
- Constant ship speed curves p. 47
- Engine loading during acceleration p. 48
 - Acceleration from standstill p. 48
 - Acceleration during free sailing p. 49
- Power limitations of main engines p. 49
 - Impact of an index limitation for power limitation of MC engines p. 49
 - Impact of a power limitation of ME engines p. 50
- Extensions to the standard engine load diagram for acceleration and encounters of adverse weather p. 50
 - Dynamic limiter function (DLF) p. 50
 - Adverse weather condition (AWC) functionality p. 51
- Degradation of light running margin on a ship in service, example p. 52
- Power functions and logarithmic scale for engine diagrams p. 53

Chapter 4

Environmental regulations p 55

- Sulphur oxides p. 55
- Nitrogen oxides p. 56
 - Exhaust gas recirculation p. 57
 - Selective catalytic reduction p. 57
- Emission control areas p. 58
- Energy efficiency design index p. 58
 - EEDI reducing measures p. 60
 - EEDI and light running margin p. 60
- Energy efficiency existing ship index p. 62
- Carbon intensity indicator p. 62
- Minimum propulsion power p. 63

Chapter 5

Examples of engine selections

for selected ship types p 65

- Example 1 - MR tanker p. 65
- Example 2 - container carrier p. 68
- Example 3 - ro-ro cargo p. 71
- Closing remarks p. 75
- References p. 75
- List of abbreviations p. 76

Chapter 1

Ship definitions and hull resistance

Hull dimensions and load lines

This chapter starts by giving the definitions of the expressions used in various situations for length, draught and breadth, followed by the definitions of load lines, which describe how much of the hull that is submerged.

Lengths

The overall length of the ship L_{OA} is normally of no consequence when calculating the hull's water resistance. The determining factors used are the length of the waterline L_{WL} and the so-called length between perpendiculars L_{PP} . The dimensions referred to are shown in Fig. 1.01.

The length between perpendiculars is the length between the foremost perpendicular, i.e. usually a vertical line through the stem's intersection with the waterline, and the aftmost perpendicular

lar which, normally, coincides with the rudder stock. Generally, this length is slightly shorter than the waterline length, and it can often be expressed as

$$L_{PP} = 0.96 - 0.98 \times L_{WL}$$

Draught

The ship's draught, typically denoted T in literature, is defined as the vertical distance from the waterline to the point of the hull which is deepest in the water, see Figs. 1.01 and 1.02. The foremost draught T_F and aftmost draught T_A are typically the same when the ship is in the loaded condition, i.e. no trim.

The "scantling draught" is the maximum draught at which the hull can meet the strength requirements. It may

be coinciding with the summer load line draught, the distance from the keel to the summer load line, see the section "Load lines". If the hull is prepared for e.g. a later lengthening, the scantling draught will often exceed the summer load line draught.

Ballast draught is the draught of the ship with no cargo but adequate ballast water to ensure the stability of the ship.

Generally, the most frequently occurring draught between the scantling and the ballast draught is used as the "design draught". The design draught is typically applied as the basis for the design of the propulsion plant and hereby the prediction of the propulsion power required to attain the design speed at this loading condition.

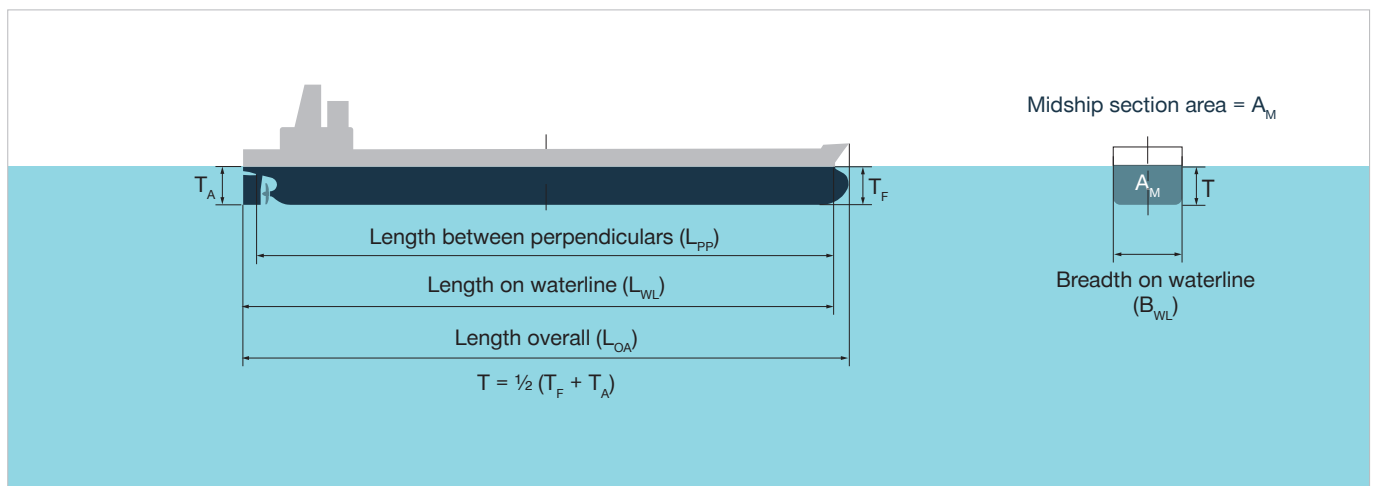


Fig. 1.01: Hull dimensions

Breadth

Another important factor is the hull's largest breadth on the waterline B_{WL} , see Fig. 1.02.

Depth

The depth describes the distance from the keel to the underside of a given deck of the ship and is typically denoted D . The moulded depth describes the distance from the keel to the freeboard deck measured at the ship side.

Load lines

Painted halfway along the ship's side is the load line mark (also known as the Plimsoll Mark after its inventor), see Fig. 1.03. The lines and letters of the load line mark, which conform to the freeboard rules laid down by the IMO and local authorities, indicates the draught to which the ship may be loaded, considering its stability. The term freeboard refers to the minimum distance from the lowest watertight deck of the ship to the waterline, i.e. when fully loaded, the load line.

There are, e.g. load lines for sailing in freshwater and seawater, respectively, accounting for the difference in the mass density of water and the corresponding difference in buoyancy depending on the salinity. Further divisions for tropical conditions and summer and winter sailing are given. The deadweight at the summer load line is for most ships defined as the capacity utilised for calculating the EEDI and CII. See Chapter 4.

The winter freeboard draught is less than that valid for summer because of the increased risk of bad weather. Correspondingly, a lower freeboard can be allowed in tropical waters. A further description of a ship's freeboard and stability is outside the scope of this paper.

Owing to ease of docking and avoiding damages if running soft aground, appendages of merchant ships are typically not designed to protrude to a deeper draught than the baseline of the hull.

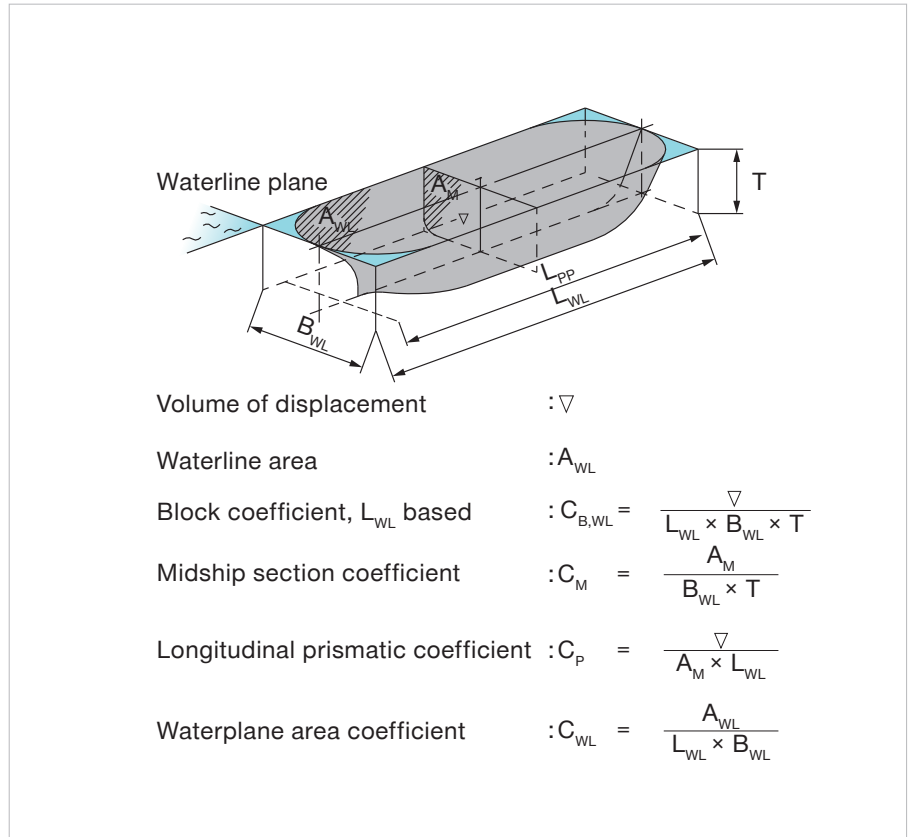


Fig. 1.02: Hull coefficients

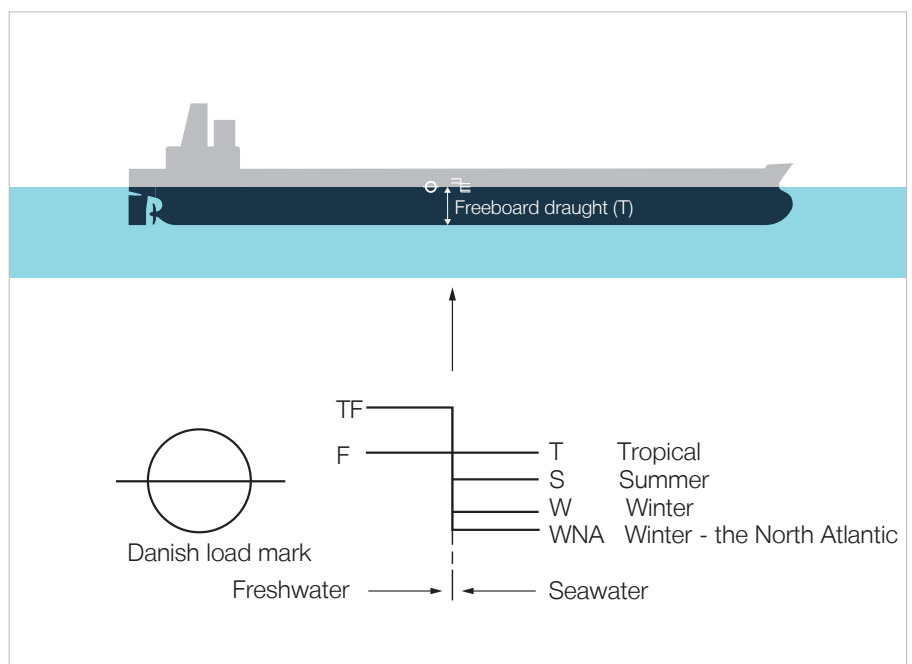


Fig. 1.03: Load lines

Size determining factors

Displacement, deadweight and lightweight

When a ship in loaded condition floats at an arbitrary water line, its displacement is equal to the relevant mass of water displaced by the ship. Displacement is thus equal to the total weight, of the relevant loaded ship, normally in seawater with a mass density of 1.025 t/m³.

Displacement comprises the ship's lightweight and its deadweight, where the deadweight is equal to the ship's loading capacity, including bunkers and other supplies necessary for the ship's propulsion. The deadweight at any time thus represents the difference between the actual displacement and the ship's lightweight, all given in tons.

EQ 1

$$\text{deadweight} = \text{displacement} - \text{lightweight}$$

The word "ton" does not always express the same amount of weight. Besides the metric ton (1,000 kg), there is the English ton (1,016 kg), which is also called the "long ton". A "short ton" is approx. 907 kg.

The deadweight tonnage (dwt) is based on the ship's loading capacity including the fuel and lube oils, etc. required for the operation of the ship. The dwt is often used as an indication of size, referring to the loading capacity when the ship is loaded to the summer load line.

Sometimes, the deadweight tonnage may also refer to the ship's loading capacity at the design draught, if so, this will typically be mentioned.

The lightweight of a ship describes the weight of the ship itself in light condition, i.e. without load on the ship. The lightweight tonnage (lwt) is normally not used to indicate the size of a ship.

Table 1.01 indicates the rule-of-thumb relationship between the ship's, deadweight tonnage (at summer freeboard/scantling draught) and lightweight tonnage.

The designation "payload" describes the weight that can be loaded onto the ship, excluding bunkers and supplies necessary for the ship's propulsion.

Gross and net tonnage

Without going into detail, it should be mentioned that there are also such measurements as the dimensionless gross tonnage (gt) and net tonnage (nt), which are calculated on the basis of the ship's volume and a multiplier defined by the IMO in the International Convention on Tonnage Measurement of Ships. Gross tonnage describes the entire enclosed ship space, whereas net tonnage covers only the cargo spaces. These measurements often form the basis for different regulatory requirements from the IMO.

Gross and net tonnage should not be confused with the older pre-convention terms gross register tons (grt), and net register tons (nrt) where 1 register ton corresponds to 100 English cubic feet, or 2.83 m³.

Coefficients related to the hull

The measures of length, breadth, draught, and depth as well of weights can with some additional measures be used for calculating some dimensionless coefficients.

Block coefficient

Various form coefficients are used to express and assess the shape of the hull. The most important of these coefficients is the block coefficient $C_{B,PP}$, which is defined as the ratio between the displacement volume ∇ and the volume of a box with dimensions $L_{WL} \times B_{WL} \times T$, see Fig. 1.02.

$$C_{B,PP} = \frac{\nabla}{L_{PP} \times B_{WL} \times T} \quad \text{EQ 2}$$

In the case cited above, the block coefficient refers to the length on waterline L_{WL} . However, shipbuilders often use block coefficient $C_{B,PP}$ based on the length between perpendiculars, L_{PP} , in which case the block coefficient will, as a rule, be slightly larger because L_{PP} is normally slightly shorter than L_{WL} .

$$C_{B,PP} = \frac{\nabla}{L_{PP} \times B_{WL} \times T} \quad \text{EQ 3}$$

Table 1.01 shows typical block coefficients for different categories of ships, indicating a strong correlation between ship speed and block coefficient.

Water plane area coefficient

The water plane area coefficient C_{WL} expresses the ratio between the ship's waterline area A_{WL} and the product of the length L_{WL} and the breadth B_{WL} of the ship on the waterline, see Fig. 1.02.

$$C_{WL} = \frac{A_{WL}}{L_{WL} \times B_{WL}} \quad \text{EQ 4}$$

Generally, the water plane area coefficient is some 0.10 higher than the block coefficient.

EQ 5

$$C_{WL} \cong C_B + 0.1$$

This difference will be slightly larger on fast ships with small block coefficients where the stern is also partly immersed in the water and thus becomes part of the "water plane" area.

Midship section coefficient

A further description of the hull form is provided by the midship section coefficient C_M , which expresses the ratio between the immersed midship section area A_M (midway between the foremost and the aftmost perpendiculars) and the product of the ship's breadth B_{WL} and draught T , see Fig. 1.01.

$$C_M = \frac{A_M}{B_{WL} \times T} \quad \text{EQ 6}$$

In general, the midship section coefficient for merchant (displacement) ships is high, in the order of 0.95-0.99. Low values, within the range, are found for fast ships such as container ships, whereas high values are found for the

slower bulkers and tankers. Fast ferries and naval ships can have significantly lower values.

Prismatic coefficient

The longitudinal prismatic coefficient C_P expresses the ratio between displacement volume ∇ and the product of the midship frame section area A_M and the length of the waterline L_{WL} , see also Fig. 1.02.

$$C_P = \frac{\nabla}{A_M \times L_{WL}} = \frac{\nabla}{C_M \times B_{WL} \times T \times L_{WL}} = \frac{C_{B,WL}}{C_M} \quad \text{EQ 7}$$

The prismatic coefficient describes how voluminous the fore and aft parts of the ship are. A low prismatic coefficient indicates a voluminous midship section compared to the fore and aft parts.

Finesness ratio alias length/displacement ratio

The length/displacement ratio or finesness ratio, C_{LD} , is defined as the ratio between the ship's waterline length L_{WL} , and the length of a cube with a volume equal to the displacement volume.

$$C_{LD} = \frac{L_{WL}}{\sqrt[3]{\nabla}} \quad \text{EQ 8}$$

Longitudinal centre of buoyancy

The LCB expresses the position of the centre of buoyancy and is defined as the distance between the centre of buoyancy and the midpoint between the ship's foremost and aftmost perpendiculars, termed "midships". The distance is normally stated as a percentage of the length between the perpendiculars.

Whether LCB is positive fore of the midpoint between perpendiculars, midships, or abaft midships is not stringent. The Holtrop Mennen, Ref. [1.3], power prediction method defines LCB positive fore of midships, whereas the method of Ref. [1.2] defines LCB positive abaft midships.

For a ship designed for high speeds, e.g. container ships, the LCB will, normally, lie abaft midships, whereas for slow-speed ships, such as tankers and bulk carriers, it will normally be forward of midships. The LCB is generally found at -3% to $+3\%$ of the L_{PP} around midships.

Longitudinal centre of flotation

LCF is the geometrical centre of the waterplane area, which does not necessarily coincide with the midship position, due to the ship usually not being symmetrical around this point in the longitudinal direction. The ship trims

about LCF and not LCB if not loaded to an even keel.

Ship types with engine applications in overview

Depending on the nature of their cargo, and also the way the cargo is handled, ships can be divided into different categories, some of which are mentioned in Table 1.01 along with typical number of propeller(s) as well as engine type.

The three largest categories of ships are container ships, bulk carriers (for bulk goods such as grain, coal, ores, etc.) and tankers, which again can be divided into more precisely defined sub-classes, sizes, and types.

Furthermore, Table 1.01 includes general cargo ships, where different kinds of cargo is brought onboard in pieces, and roll-on/roll-off (ro-ro) ships carrying lorry trailers and other cargoes that can be rolled on board. Rolling cargo in the form of cars and lorries are also combined with passenger transport in ro-pax ships.

Table 1.01 provides only a rough outline. In reality, there are many sub-types of ships, as well as combinations of these sub-types, i.e. ships carrying ro-ro cargo in the hull and containers stacked on deck.

Category	Type	Propeller	Main engine type	Size factor	C_B	V, kn	lwt/dwt
Tanker	Crude oil carrier	1 FP	2-stroke	dwt	0.78-0.83	13-17	0.13-0.20
	Gas tanker / LNG carrier	1 FP	2-stroke, steam turbine	dwt / cubic meter (cbm)	0.65-0.75	16-20	0.30-0.50
	Product	1 FP	2-stroke	dwt	0.75-0.80	13-16	0.15-0.30
	Chemical	1 FP	2-stroke	dwt	0.70-0.78	15-18	0.30-0.50
Bulk carrier	Ore carrier	1 FP	2-stroke	dwt	0.80-0.85	14-15	0.11-0.15
	Regular	1 FP	2-stroke	dwt	0.75-0.85	12-15	0.13-0.30
Container ship	Liner carrier	1 FP or 2 FP	2-stroke	teu	0.62-0.72	20-23	0.28-0.34
	Feeder	1 FP or 1 CP	2 or 4-stroke	teu	0.60-0.70	18-21	0.34-0.41
General cargo ships	General cargo	1 FP	2 or 4 stroke	dwt / nt	0.70-0.85	14-20	
	Coaster	1 FP or 1 CP	2 or 4 stroke	dwt / nt	0.70-0.85	13-16	
Roll-on/roll-off cargo ship (ro-ro)		1 CP or 2 CP	2 or 4 stroke	Lane meters (lm)	0.55-0.70	18-23	0.6-1.4
Passenger-cargo ship (ro-pax)		2 CP	2 or 4-stroke	Passengers / lm	0.50-0.70	18-23	
Passenger ship	Cruise ship	2 CP	4-stroke	Passengers / gt	0.60-0.70	20-23	
	Ferry	2 CP	4-stroke	Passengers / gt	0.50-0.70	16-23	

Table 1.01: Typical characteristics of different ship types.

As seen in Table 1.01, two-stroke engines are broadly used as main propulsion engines. Two-stroke diesel cycle engines have the highest efficiencies amongst mechanical means of propulsion, see Chapter 3.

This is reflected in the fact that two-stroke engines practically are the only engine of choice for ship types where fuel prices represent the main running costs, for example tankers, bulk carriers and container ships engaged in liner traffic between the continents but also for most container feeders.

For specialised ships, such as ferries and cruise ships, other parameters can constitute the main economic factors. The higher power density and lower height of four-stroke engines can make them more attractive in such cases.

For large ocean-going ships, fixed pitch propellers (FPP) are the most common choice, whereas controllable pitch propellers (CPP) are often utilised for smaller ships calling on smaller ports which demand increased manoeuvrability. In the case of a two-stroke main engine, it is possible to couple the propeller directly to the main engine, as an engine with a speed matching the optimum propeller speed can be found. For four-stroke engines, the higher speed of the engine requires a reduction gearbox. Propeller and engine matching is elaborated in Chapter 3.

Efficiencies affecting the total fuel consumption

The total fuel power, P_{fuel} , required for propelling a ship through water is governed by the fuel equation. This section describes the parameters included in the equation, and references are made to other parts of this paper where these are explained in detail.

$$P_{\text{fuel}} = \frac{R_T \times V}{\eta_H \times \eta_O \times \eta_R \times \eta_S \times \eta_E} \quad \text{“Fuel equation”} \quad \text{EQ 9}$$

The resistance of the hull, R_T , is influenced by multiple parameters as described in the following section “Resis-

tance and influencing parameters”. In general, the resistance is proportional to the speed to the power of $i = 2$ to 3 , $R \propto k \times V^i$, depending on speed. This means that when increasing the speed with the power of 1 (linearly), the power required will increase with the speed to a higher power, $P \propto k \times V^{i+1}$.

These relations are further discussed in Chapter 2, section “Propeller law and power/speed curves”.

The design speed of the ship is typically set according to the desire of the owner, if not limited due to e.g. EEDI regulations. In the fuel equation, the product of the resistance and speed is divided by the efficiencies of all of the components involved in propelling the ship - remembering all the efficiencies to consider is straight forward, as the indices combined spells HORSE.

η_H is the hull efficiency. It takes into account the difference in the effective (towing) power and the thrust power that the propeller must deliver to the water because the hull accelerates the water and the propeller “sucks” water past the hull. This is further elaborated in Chapter 2, section “Flow conditions”.

η_O is the open water efficiency of the propeller (not behind the hull), giving the efficiency of the propeller working in a homogeneous wake field with flow perpendicular to the propeller. η_O is further investigated in Chapter 2, section “Efficiencies and influencing parameters”.

η_R is the relative rotative efficiency of the propeller, accounting for the changes in water flow to the propeller behind the ship relative to the open water flow conditions, as further described in Chapter 2, section “Rotative efficiency”.

η_S accounts for the efficiency of the shaft connecting the main engine and propeller. It depends on the length of the shaft, whether gearing is necessary, etc. This is further described in Chapter 2, section “Shaft efficiency”.

η_E describes the efficiency of the en-

gine, depending on type of design and a variety of other parameters described in Chapter 3.

Resistance and influencing parameters

The total magnitude of resistance on the ship’s hull, R_T , is naturally paramount for the power required to move the ship (as seen in the fuel power equation) and hereby the fuel consumption.

The following section will explain the physical phenomena giving rise to the different components of the total calm water resistance, also termed the source resistances, and quantify their contribution to the total resistance.

Components of resistance

A ship’s calm water resistance is particularly influenced by its speed, displacement, and hull form. The total resistance R_T consists of many source-resistances R , which can be divided into three main groups, viz.:

1. Frictional resistance, R_F
2. Residual resistance, R_R
3. Air resistance, R_A

The influence of frictional resistance depends on the wetted surface of the hull, whereas the magnitude of residual resistance describes the energy lost by the ship setting up waves, eddies and by the viscous pressure resistance, which all depend on the hull lines. For slow moving ships such as tankers and bulkers, the frictional resistance is often of the greatest influence (70-90%) whereas for fast going ships, such as panamax container carriers, the frictional resistance may account for as little as half of the combined resistance.

This phenomena is reflected in the hull design for these different ships. For slow moving ships operating at a low relative speed, it is sought to maximise the cargo intake relative to the wetted surface area of the hull, and hereby frictional resistance, by a high block coefficient. For fast ships a balance between frictional and residual resistance is reflected in a lower block coefficient, see Table 1.01.

Air resistance normally represents about 2% of the total resistance, however, with a significant increase up to approx. 10% for ships with large superstructures such as container ships with containers stacked on deck. If wind resistance is considered, the figures may increase.

Water with a speed of V and a density of ρ has a dynamic pressure of:

$$p_{\text{dyn}} = \frac{1}{2} \times \rho \times V^2 \text{ "Bernoulli's law"} \quad \text{EQ 10}$$

Thus, if water is being completely stopped by a body, the water will react on the surface of the body with the dynamic pressure, resulting in a dynamic force on the body.

This relationship is used as a basis when calculating or measuring the source-resistances R of a ship's hull, by means of dimensionless resistance coefficients C . Thus, C is related to the reference force K , defined as the force that the dynamic pressure of water with the ship's speed V exerts on a surface which is equal to the hull's wetted area A_s . The rudder surface is also included in the wetted area. The general data for resistance calculations are thus based on the following two important relations:

Reference force: $K = \frac{1}{2} \times \rho \times V^2 \times A_s$

Source resistances: $R = C \times K$

On the basis of many experimental tank tests, and with the help of pertaining dimensionless hull parameters, methods have been established for calculating all the necessary resistance coefficients C and, thus, the pertaining source-resistances R at an early project stage without testing, Ref. [1.2] and [1.3].

In practice, the approximate calculation of a particular ship's resistance, which is required for the initial dimensioning, is often verified and optimised by testing a model of the ship in a towing tank.

Frictional resistance, R_F

The frictional resistance R_F accounts for two effects: Firstly the friction of a flat plate of the same length as the hull and an area equivalent to the hull's wetted surface area, A_s . Secondly the frictional resistance caused by the curvature of the ship's hull compared to a flat plate, see Fig. 1.05. The magnitude of the frictional resistance increases with

the fouling of the hull, i.e. by the growth of algae, sea grass and barnacles.

$$R_F = C_F \times K \quad \text{EQ 11}$$

The wetted surface area A_s can be estimated based on Mumford's formula. As

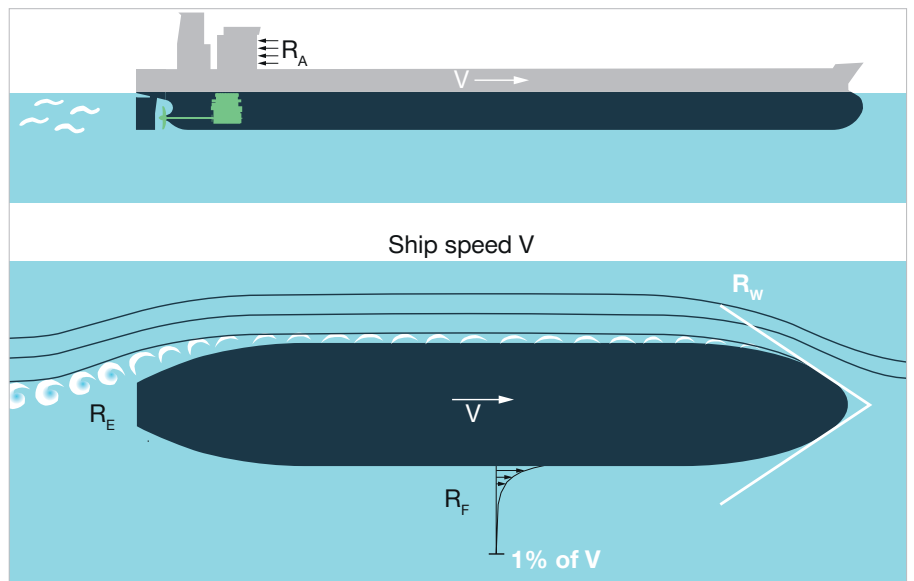


Fig. 1.04: Components of resistance on a ship

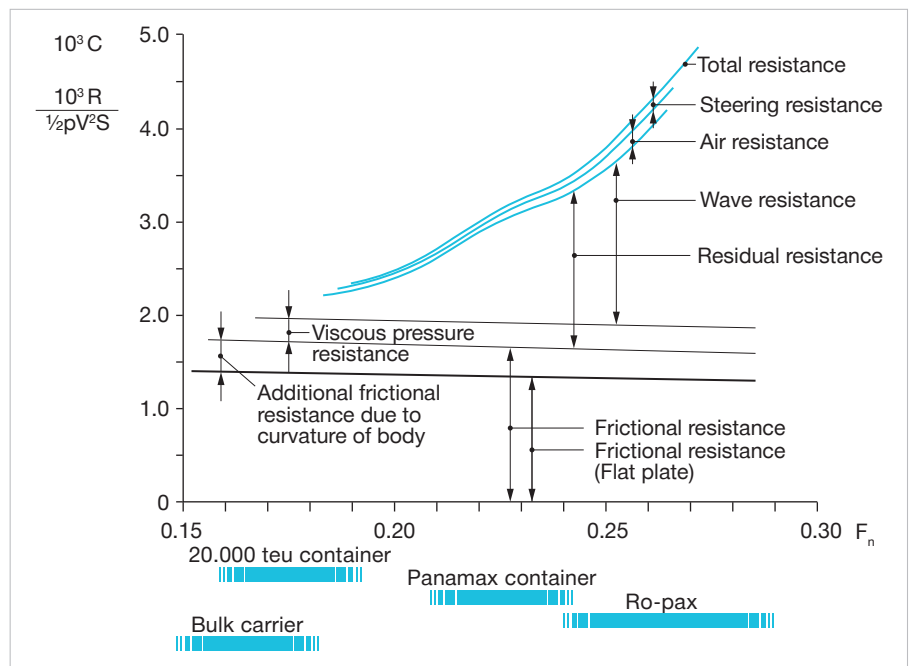


Fig. 1.05: Components of the total resistance as function of the Froude number from Ref. [1.2]

a rule of thumb, it can be estimated by this formula within 15% accuracy.

$$A_S = 1.025 \times L_{PP} \times (C_B \times B + 1.7 \times T) = 1.025 \times \left(\frac{\nabla}{T} + 1.7 \times L_{PP} \times T\right) \tag{EQ 12}$$

Residual resistance, R_R

Residual resistance R_R comprises wave making resistance and viscous pressure resistance. Sometimes the additional frictional resistance due to the curvature of the ship’s hull are also included in the residual resistance.

Wave making resistance refers to the energy lost by the setting up waves during the ship’s propulsion through water, and will typically, depending on the ship speed, form the greater part of the residual resistance, see Fig. 1.05.

The viscous pressure resistance is usually a small part of the total resistance. It arises from separation losses in the boundary layer and the increased thickness hereof along the ship’s side. The result of increased boundary layer thickness is a lower pressure on the aft of the ship than on the fore part, which gives rise to resistance. The concept of the boundary layer is explained in Chapter 2, section “Flow conditions”.

Generation of eddies when the flow separates from the hull surface is a special part of the viscous pressure resistance, which results in separation losses, sometimes referred to as eddy resistance. Eddies are created both due to separation in the boundary layer and on the aft part of the ship, due to the abrupt changes in curvature found here.

The procedure for calculating the specific residual resistance coefficient C_R is described in specialised literature, Ref. [1.2].

$$R_R = C_R \times K \tag{EQ 13}$$

The residual resistance is typically very limited at low ship speeds, see the sec-

tion “The Froude number”, but it can be significant at elevated ship speeds.

This results in the combined resistance growing by as much as the cubic of the speed or even more. Accordingly, the required power and, hence, fuel consumption can be proportional to the speed to the power of four, P ∝ k × V⁴ or even more, for fast ships. See also “Propeller law and speed power curves” in Chapter 2.

Air resistance, R_A

In calm weather, air resistance is, in principle, proportional to the square of the ship’s speed, and the cross-sectional area of the ship above the waterline. It is important to distinguish air resistance from wind resistance, air resistance only accounts for the resistance from moving the ship through the air with no wind.

The air resistance can, similar to the foregoing resistances, be expressed as a coefficient times a reference force, R_A = C_A × K_A. Using a drag coefficient C_A and an area of the ship above the waterline A_{air}, the resistance can be expressed as:

$$R_A = \frac{1}{2} \times \rho_{air} \times C_A \times A_{air} \times V^2 \tag{EQ 14}$$

Typically, the drag coefficient can be estimated at approx. C_A ≈ 0.9 depending on the shape of the superstructure, whereas the area above the waterline, on which the wind acts, must be calculated because the area depends on the wind direction. Further investigations on air resistance have been done in Ref. [1.4].

Parameters influencing resistance and optimisation hereof

Numerous parameters influence the total calm water resistance of a ship, and the nature of the influence can differ significantly depending on the speed of the ship. The following section provides an overview of the influencing parameters and a brief introduction to their relation. For in-depth understanding the reader is advised to consult special literature such as Ref. [1.2].

The Froude number

The Froude number is a dimensionless coefficient especially important for the residual resistance of ships. Ships with a similar Froude number will experience similar relative amounts of source resistance (relation between C_F, C_R, C_A.) despite not being the same size and moving at different absolute speeds.

$$Fn = \frac{V}{\sqrt{g \times L_{WL}}} \tag{EQ 15}$$

The total calm water resistance, and thus fuel consumption, increases when the Froude number increases. This is because the wave making resistance increases significantly when the Froude numbers exceed approx. Fn = 0.16 to 0.17, as can be seen in Fig. 1.05 from Ref. [1.2]. From this figure it is also clear that the friction is practically the only influencing parameter at Fn < 0.15.

In order to exemplify the influences of the different terms in the Froude number, a parameter sweep is displayed in Table 1.02.

	speed, kn						
Length, m	14	16	18	20	22	24	26
100	0.23	0.26	0.30	0.33	0.36	0.39	0.43
150	0.19	0.21	0.24	0.27	0.30	0.32	0.35
200	0.16	0.19	0.21	0.23	0.26	0.28	0.30
250	0.15	0.17	0.19	0.21	0.23	0.25	0.27
300	0.13	0.15	0.17	0.19	0.21	0.23	0.25
350	0.12	0.14	0.16	0.18	0.19	0.21	0.23
400	0.11	0.13	0.15	0.16	0.18	0.20	0.21

Table 1.02: Froude number as a function of the hull length and ship speed

When considering the formula for the Froude number, it becomes evident that by increasing the length of the ship, the value of the Froude number will decrease. Of course, this does not come without a cost, as it increases the wetted surface area of the ship, and hereby the frictional resistance. Depending on the speed of the ship, this increase in absolute frictional resistance may be meaningful in a compromise between resistance components.

Typically, the length of the ship is the most costly parameter to adjust with regards to building costs, due to the resulting increased stresses on the hull girder, but considering the EEDI regulations as described in Chapter 4 an increased length can be necessary if a specific speed is required for a special trade. This must be considered along any practical limits to maximum dimensions that may be imposed by harbour and canal dimensions etc.

Due to the continuously increasing residual resistance by increasing Froude numbers, it is important to realise that the exponent, i , of the speed power curve, $P \propto k \times V^i$, is not constant for a fixed design but increases with increased ship speed.

Influence of wetted surface area

The wetted surface area is paramount for the frictional resistance of the ship, which is seen to be predominant at $F_n < 0.15$ in Fig. 1.05.

By increasing the block coefficient, the wetted surface area is reduced relative to the cargo amount that can be carried, which is why slow-going ships such as tankers and bulkers have a high block coefficient.

The wetted surface area can be estimated by Mumford's formula, see section "Frictional resistance, R_F ".

Influence of block coefficient

The block coefficient describes the overall fullness of the hull. It is a good and easy-to-calculate indicator of a hull's resistance and capabilities with regard to speed. However, the other parameters described in this section

may have a relatively larger influence, specifically on the resistance, than small changes to the block coefficient. In general, fast ships, for which the wave making is the primary resistance parameter, demand small block coefficients, whereas slower ships, for which the friction against the hull is the main resistance parameter, are most effective with a higher block coefficient.

Influence of the fineness ratio alias length/displacement ratio

The fineness ratio describes the length of the ship relative to the displacement, and influences the resistance, especially for faster ships. When increasing the fineness ratio for constant displacement the residuary resistance decreases. However, at the same time the wetted surface area is increased.

The optimum length of the specific hull, with its specific design speed, must be found with due consideration to the limitations imposed by canal passages, harbours, building costs etc.

Influence of the prismatic coefficient

The prismatic coefficient is an important measure for describing how well the ship displaces the water while moving through it. The optimum for the prismatic coefficient changes greatly with the Froude number of the ship, and the reader is advised to consult specialised literature.

Added resistance in various conditions

Shallow water

In general, shallow water will have no influence when the water depth is more than 10 times the ship draught. Shallow water may increase the calm water resistance of the ship significantly for a variety of rather complex reasons listed below. The reader is advised to consult special literature e.g. Ref. [1.5].

The pressure set up by the ship's motion through the water will be greater as the flow of the water is restricted, thereby retarding and increasing the size of the wave system set up by the ship, and resulting in added resistance. This effect is primarily for $F_n > 0.2$.

In addition, water will flow back around the ship due to the restriction of the waterway caused by the presence of the ship (similar to an increase in velocity due to a local obstruction in a pipe). Furthermore, the propeller will to some extent suck water faster past the ship surface than in deep water due to the restricted volume of water. Both these effects increase flow velocities and, therefore, also the resistance.

In addition, the so-called squat effect may occur. The squat effect means that the pressure underneath the ship is reduced as the limited gap between the seabed and the ship results in friction on the water under the hull, see Bernoulli's law. The squat effect results in a larger than normal draught and hereby increased resistance. This is also primarily seen at elevated Froude numbers.

Weather, heavy seas

Waves created by high winds and swells can have a significant effect on the resistance experienced by the ship. Especially if the ship length and wave length are about equal.

The waves will set the ship in motion and lead to added resistance as more water is affected by the movement of the ship. Additionally the waves from the seaway will reflect on the hull, and thereby increase the resistance as well.

In combination, this is termed the wave drift force or added wave resistance. The influence hereof can be seen if an object is left to float freely in the waves. Such an object would slowly move in the direction of the wave propagation.

Furthermore, rudder corrections will be much more frequently needed to stay on course. The use of the rudder will of course result in increased resistance, this effect being most predominant for small ships ($L_{PP} < 135 \text{ m} \approx 20,000 \text{ dwt}$) due to their lower directional stability. Additionally, the shape of the stem can greatly influence the ship's ability to "cut through" heavy seas.

The relative magnitude of the added wave resistance resulting from waves

compared to the calm water resistance increases by lower ship speeds, reducing the exponent, i , of the combined calm water and added wave resistance, $R \propto k \times V^i$, at lower speeds [1.6].

This is important to consider when evaluating power reductions by reducing speeds in actual conditions, as power savings will reduce compared to considering calm water resistance only.

Weather, wind

It is important to distinguish between air and wind resistance. Air resistance only accounts for the calm weather resistance from moving the ship through the atmosphere without any wind. Wind resistance is calculated in the same way as air resistance but takes into account the combined speed of the ship and the wind.

For large ocean-going ships, wind resistance will normally be significantly lower than the wave resistance, but for ships intended for trade in sheltered waters without large wave resistance, e.g. ferries, the wind resistance can be the most significant added resistance in heavy weather.

Fouling

Fouling can result in a substantial increase in frictional resistance. Extreme cases have been seen where fouling had increased the frictional resistance by as much as 100%, normally up to 20-30%.

Before IMO banned TBT (tributyl tin) for new applications from 2003, and the full ban from 2008, marine growth on the hull was slower, but TBT was banned as it is extremely toxic to the marine environment. This means that the management of the ship with regard to dry-docking, hull cleaning and propeller polishing must be optimised, and that the cost of mechanical cleaning measures and the cost of added fuel consumption due to fouling must be balanced.

When designing the ship, especially for trade in warmer seas where growth is fast, some margin must be included for fouling, see p. 50 for example measure-

ments. Similar to the fouling, the increased roughness of the hull over time, arising from rust and dents from interactions with the quay, etc., will increase the resistance of the hull.

Ice

Ships sailing in ice will experience significantly higher frictional resistance. Designing for icy conditions is a specialist area. The reader is advised to consult the separate paper "Ice Classed Ships" and special literature on resistance in ice. An rpm extended engine *load* diagram can be of relevance to ice classed ships, especially if equipped with fixed pitch propellers, see "Rpm extended load diagram" in Chapter 3.

Designing for added resistance

All types of increased resistance on the hull, leads to increased heavy running of the propeller compared to calm water conditions: More torque is required to maintain the same rotational speed as more thrust is needed to overcome the increased resistance. As a directly coupled main engine cannot change gear, it is important to layout the propulsion plant and main engine with a margin for heavy running, see the later section "Light running margin" in Chapter 3.

Resistance margins in a slow steaming environment

To account for average weather, a relative resistance margin (called a sea margin) has traditionally been added to the power requirement for propelling the ship in calm waters at the design speed, as given, for example, in Ref. [1.2]. The ship design speeds have been lowered as a result of the increased focus on fuel consumption and environmental impact, see Chapter 4. This has led to a lower power requirement and, therefore, smaller engines. If the traditional relative resistance margins are applied to these smaller engines, the resulting absolute power margin will also be smaller.

Nevertheless, the weather does not know whether a ship of the same size is designed for a reduced service speed or not. The absolute added resistance

experienced on the hull in a given sea state will be the same. Therefore, it is important for the ship designer to consider resistance margins for the specific project. The designer must secure that the engine selected can ensure safe manoeuvring in all relevant conditions, and that all relevant operating points (power, rotational speed) for the propeller are inside the engine's *load* diagram. See the engine selection spirals in Chapter 3 as well as Chapter 4 for further guidance on this, touching upon the IMO requirements towards minimum propulsion power.

Further insights to these aspects are provided in the separate paper "Improved efficiency propulsion plants - optimisations for EEDI phase 3". This as well provides insights to how the manoeuvrability is maintained despite a power reduction.



Chapter 2

Propeller propulsion

The traditional agent employed to move a ship is a propeller. It is typically applied as a single-screw plant or, sometimes, as a twin-screw plant. In rare cases more than two propellers can be found on naval ships and high speed ferries.

This chapter starts by giving a series of definitions on the geometry of the propeller, followed by considerations on the flow conditions around a propeller. Next, the parameters affecting the propeller efficiency are investigated, along with philosophies for optimising the hull and propeller interactions. In conclusion, acceleration performance and manoeuvring are discussed.

Definitions of parameters

Diameter

With a view to obtaining the highest efficiency and lowest fuel consumption, the largest possible propeller diameter, d , will normally be preferred.

In general the propeller is, similar to appendages, not allowed to extend below the baseline of the hull on merchant ships, and typically a small margin is included to ensure that the propeller is not damaged in the event of a grounding, during dry docking or similar. Interference between the propeller and seabed, or a rock, can damage not only the propeller, but also the propeller shaft, the gearbox (if installed), and the main engine itself.

Furthermore, the propeller size is limited by the distance between the propeller-tip and the bottom of the hull, as a propeller being too close to the hull can result in both high vibrations and noise.

In all operating conditions the propeller must be fully submerged in the water. Especially for bulkers and tankers, often operating in ballast condition, this sets a limit on the propeller diameter. See Table 2.01 for a comparison of a rule-of-thumb typical maximum draught T and diameter d ratios.

Container ships operate with a more constant displacement, as the mix between empty and full containers today is almost constant regardless of journey. This allows for increasing the propeller size relative to the draught.

Volume ships carrying low-density cargo, such as ro-pax ships, can typically have larger d/T ratios as they have a more constant displacement,

as the lightweight is relatively high. Such large ratios will require special consideration to the design of the aft ship.

Pitch diameter ratio

The pitch diameter ratio p/d expresses the ratio between the propeller's pitch (angle) p and its diameter d , see Fig. 2.01. The pitch p is the distance the propeller "screws" itself forward through the water per revolution, provided that there is no slip, see "Slip".

As the pitch varies along the blade's radius, the ratio is normally calculated for the pitch at $0.7 \times r$, where $r = d/2$ is the propeller's radius. The optimum pitch depends on the rate of revolution and propeller diameter.

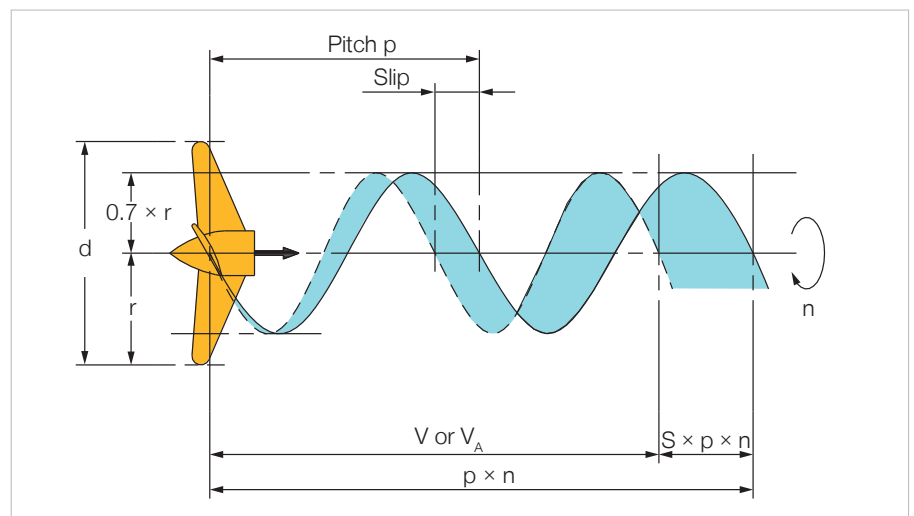


Fig. 2.01: Propeller pitch and slip

Bulkers and tankers	$d/T_d \approx 0.65$
Container ships	$d/T_d \approx 0.75$
Volume ships, high speed (i.e. ro-pax)	$d/T_d \approx 0.85$

Table 2.01: Approximate upper limit of ratio between propeller diameter and draught

Disk area coefficient

The disk area coefficient (sometimes referred to as expanded blade area ratio) defines the developed surface area of the propeller in relation to its disk area. This area must be sufficiently large to avoid harmful cavitation that can lead to erosion, see “Cavitation”, but not too large, as this will increase the frictional drag on the propeller. A ratio of 0.40 to 0.60 is typical for normally loaded 4-bladed propellers. Highly loaded single screw container ships can see values as high as 1.0. In order to accommodate this, the blade number must be increased.

Blade number

Propellers can be manufactured with 2, 3, 4, 5, 6 or 7 blades. In general, the fewer the number of blades, the higher the propeller efficiency will be. However, for reasons of strength and vibrations, 4, 5 and 6-bladed propellers are normally used on merchant ships, with 4 blades being the most common. 3-bladed propellers see an increased

application for low powered ships as bulkers and tankers and especially for twin-screw LNG carriers showing low propeller loads.

The lower limit of the blade number is typically set by the varying magnitudes of the forces experienced by the blades when moving through the “shadow” of the hull when in top, and in the less restricted flow at the bottom. The flow conditions behind the hull are typically described as the “wake field”, see the section “Flow conditions”. A sufficient number of blades are required to smoothen the load.

Ships with a relatively large power requirement and heavily loaded propellers, e.g. fast single-screw container ships, may need 5 or 6-bladed propellers in order to have a sufficient area for transferring the load without cavitating.

The optimum propeller speed depends on the number of blades. Thus, for the same propeller diameter, a 6-bladed

propeller has an about 10% lower optimum propeller speed than a 5-bladed.

For vibrational reasons, propellers with certain numbers of blades may be avoided in individual cases in order not to give rise to the excitation of natural frequencies in the ship’s hull or superstructure, Ref. [2.1].

Propeller types and geometry**Fixed pitch propellers**

Propellers of the fixed pitch (FP) type are cast in one block and are normally made of a copper alloy. The position of the blades is once and for all fixed, with a given pitch. This means that when operating in, for example, heavy weather conditions, the propeller performance curves, i.e. the combination of power and speed (rpm) points, will change according to the external conditions, see “Light running margin” in Chapter 3.

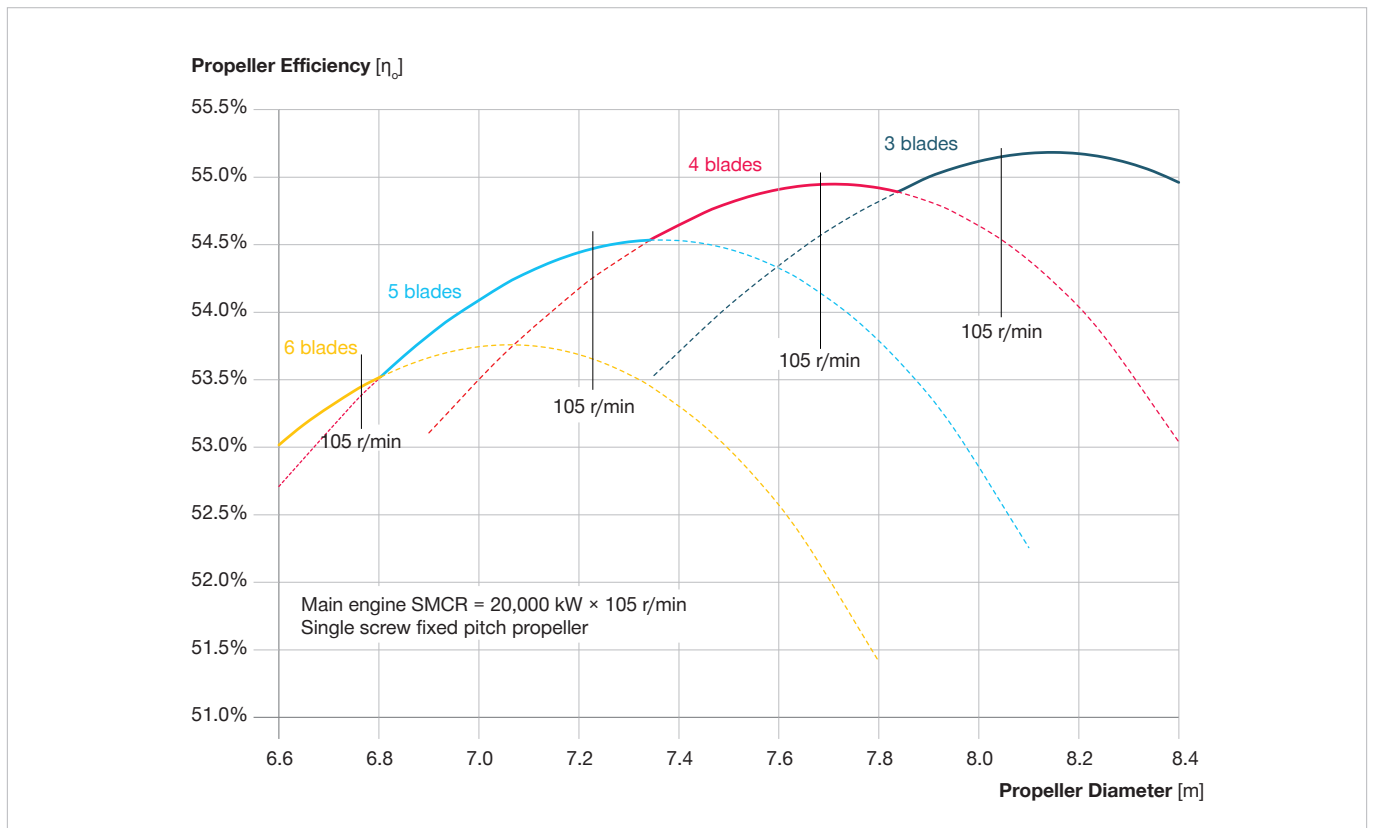


Fig. 2.02: Propeller efficiency and blade number. Notice that the speed is constant and therefore the diameter must be increased to achieve optimum. For constant diameter, the optimum speed decreases with the propeller blade number.

FP-propellers are simple and allow for the highest number of blades and blade area ratio. However, a drawback is that the engine must be stopped and reversed if reversal of the propeller is needed for deaccelerating the ship or to go astern. Note that the electronically controlled two-stroke engine mirrors the engine valve timing in astern, and is therefore equally capable of running astern as ahead.

Most ships that do not need a particularly good manoeuvrability, such as ocean-going container ships, tankers and bulk carriers are equipped with a FP-propeller, as it offers the highest efficiency. This is due to a small hub/diameter ratio of 0.15-0.20. See Fig. 2.03 for the conceptual differences to a CP-propeller.

Controllable pitch propellers

Propellers of the controllable pitch (CP) type have a relatively larger hub compared with the FP-propellers because the hub must accommodate the hydraulically activated mechanism to control the pitch. Therefore the CP-propeller is more expensive than a corresponding FP-propeller.

The great advantage of the CP-propeller is that it allows for operating the engine at any revolution or load desired, depending on the capabilities of the propeller control system. It also decouples the direction of thrust from the rotational direction of the engine, as the blades can be turned for going astern, thereby enabling swift manoeuvring without reversing the engine.

Because of the relatively larger hub, approx. a hub/diameter ratio of 0.22-0.30, the propeller efficiency is slightly lower, typically 1 to 2%.

The application of a well-designed rudder bulb, see “Energy saving devices”, would reduce the difference between the efficiency of a FP and CP propeller significantly in most cases, as a rudder bulb eliminates the low pressure behind the hub.

Any deficiency of the CP-propeller can in most cases be regained as it is

more adaptable to different operating conditions – ballast versus loaded, fouled hull versus clean, heavy weather, etc.

The blade area ratio and blade number are limited, in order to allow for the rotation of the blades about their own axis. For a medium sized 4-bladed propeller, a disk area coefficient of approx. 0.78-0.80 can be regarded a limit.

Rake and skew

Fig. 2.04 illustrates the concept of rake and skew. For normal merchant ships the blades are typically raked aft to increase the clearance between the hull and the propeller hereby reducing pressure pulses on the hull. Skew is introduced to improve vibration characteristics, as the blades will then meet any changes in the wake field progressively, see “Flow conditions”.

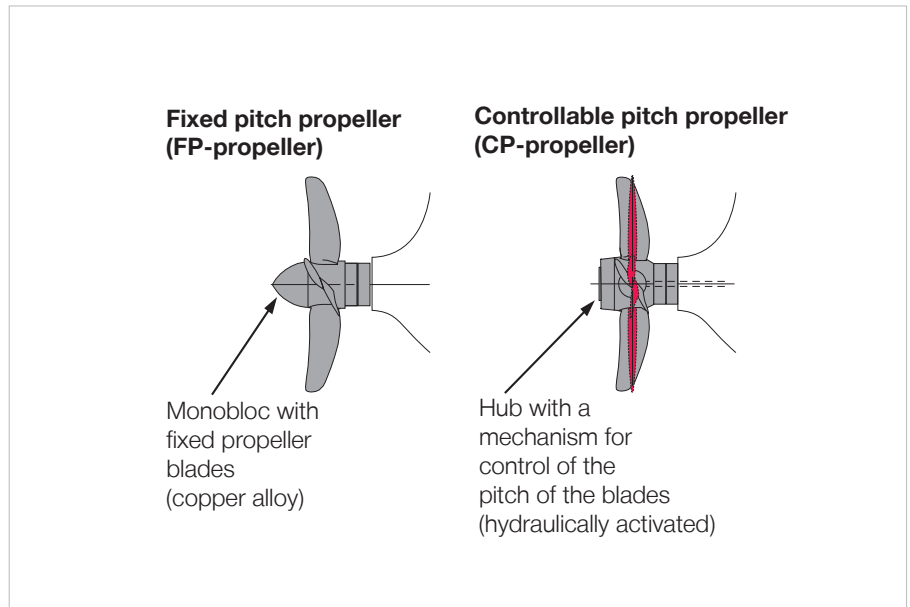


Fig. 2.03: Propeller types

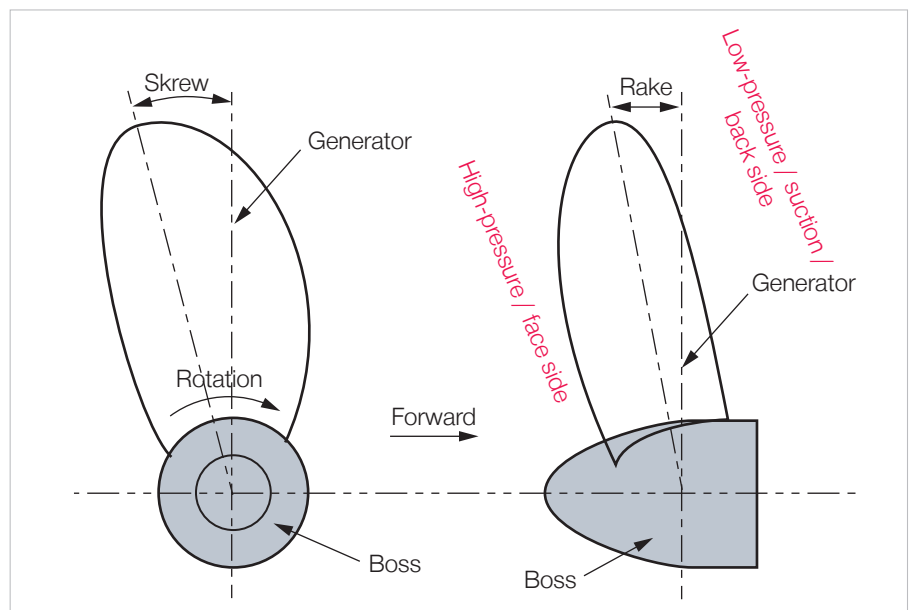


Fig. 2.04: Rake and skew

Special geometry propellers - the Kappel propeller

The Kappel propeller applies a special design where the tip of the blade is curved towards the suction side of the blade (i.e. in the forward direction), which minimise the size of the tip vortices, see “Open water efficiency”. This design is able to reduce the required engine power by 3-6%, especially for rather loaded propellers, see Fig. 2.05. In addition, the Kappel design lowers the propeller-induced pressure pulses to the ship’s hull which may allow for smaller clearance to the hull and hereby a larger propeller diameter.

Flow conditions

Boundary layer and wake

When the ship is moving, the friction of the hull will create a so-called boundary layer around the hull. In this boundary layer, the velocity of the water on the surface of the hull is equal to that of the ship, and reduces with the distance from the surface of the hull. At a certain distance from the hull, and, per definition, equal to the outer “surface” of the boundary layer, the water velocity is unaffected by the ship, see Fig. 1.04.

This “dragging” along of water on the ships surface is what creates the frictional resistance discussed in “Resistance and influencing parameters” in Chapter 1.

The thickness of the boundary layer increases with the distance from the fore end of the hull. The boundary layer is therefore thickest at the aft end of the hull, Ref. [2.1]. This means that the pressure is lower on the aft body of the ship compared to the fore part, resulting in the viscous pressure resistance described in Chapter 1.

Additionally, the ship’s displacement of water will set up wake waves both fore and aft.

The combined effects implies that the propeller will be working in a wake field.

Wake fraction coefficient, w

Mainly due to the boundary layer, the water flowing to the propeller will have

an effective wake velocity V_w which has the same direction as the ship’s speed V , see Fig. 1.04. This means that the velocity of arriving water V_A at the propeller (given as the average velocity over the propeller’s disk area and equal to the speed of advance of the propeller), is V_w lower than the ship’s speed V .

The effective wake velocity at the propeller is therefore equal to $V_w = V - V_A$ and may be expressed in dimensionless form by means of the wake fraction coefficient w , by Taylor defined as:

$$w = \frac{V_w}{V} = \frac{V - V_A}{V} = 1 - \frac{V_A}{V} \quad \text{EQ 16}$$

The value of the wake fraction coefficient depends on the shape of the hull (related to the 3D effects of the hull’s frictional resistance), and it can greatly influence the working conditions and,

hereby, the efficiency of the propeller. The larger the block coefficient, the larger the wake fraction coefficient.

Typical values of w are shown in Table 2.02 (p. 22), a first estimate can be given by $w = 0.5 \times C_B - 0.05$, Ref. [2.2]. For large d/T ratios (propeller diameter to draught of the ship) the size of the wake fraction will be reduced.

Thrust deduction coefficient, t

The action of the propeller causes the water in front of it to be “sucked” towards the propeller. This results in extra resistance on the hull normally termed “augment of resistance” or, if related to the total required thrust force T on the propeller, “thrust deduction fraction” F , see Fig. 2.06. This means that the thrust force T of the propeller has to overcome both the ship’s towing resistance R_T and the extra resistance on the hull due to the sucking action of the propeller.



Fig. 2.05: Kappel propeller



Fig. 2.06: Propulsion power

The thrust deduction fraction F may be expressed in dimensionless form by means of the thrust deduction coefficient t :

$$t = \frac{F}{T} = \frac{T - R_T}{T} = 1 - \frac{R_T}{T} \quad \text{EQ 17}$$

The thrust deduction coefficient t can be calculated by models set up in special literature, Ref. [1.2] and [1.3] or by CFD simulations.

Typical values of t are shown in Table 2.02 (p. 22), a first estimate can be given by $t = 0.27 \times C_B$ or by $t = 0.60 \times w$, again considering that the value of t will reduce for large d/T ratios.

Propeller coefficients

Propeller performance is described in systematic model tests, but to facilitate the practical use of these tests, certain dimensionless propeller coefficients have been introduced in relation to the diameter d , the rate of revolution n , and the water's mass density ρ .

Advance number

The advance number is a dimensionless expression of the propeller's speed of advance, V_A :

$$J = \frac{V_A}{n \times d} \quad \text{EQ 18}$$

For a given propeller pitch the advance number expresses the angle of the incoming water flow relative to the propeller blades, see Fig. 2.07. For a given propeller and pitch, knowledge of the advance number is sufficient to determine propeller thrust, torque and efficiency in any condition.

Thrust coefficient

Thrust force T , is expressed dimensionless, with the help of the thrust coefficient K_T :

$$K_T = \frac{T}{\rho \times n^2 \times d^4} \quad \text{EQ 1}$$

Torque coefficient

The propeller torque $Q = P / (2\pi n)$ is expressed dimensionless with the help of the torque coefficient K_Q , see Fig. 2.08:

$$K_Q = \frac{Q}{\rho \times n^2 \times d^5} \quad \text{EQ 19}$$

Thrust loading coefficient

The thrust loading coefficient describes the loading degree of the propeller, as the pressure of the propeller is related to the dynamic pressure of the incoming water flow to the propeller, i.e. thrust is divided by the speed of advance and diameter squared:

$$C_{th} = \frac{p_{propeller}}{p_{dynamic}} = \frac{\frac{T}{\frac{\pi}{4} d^2}}{\frac{1}{2} \rho V_A^2} = \frac{T}{\frac{1}{2} \rho V_A \frac{\pi}{4} d^2} = \frac{8K_T}{\pi J^2} \quad \text{EQ 20}$$

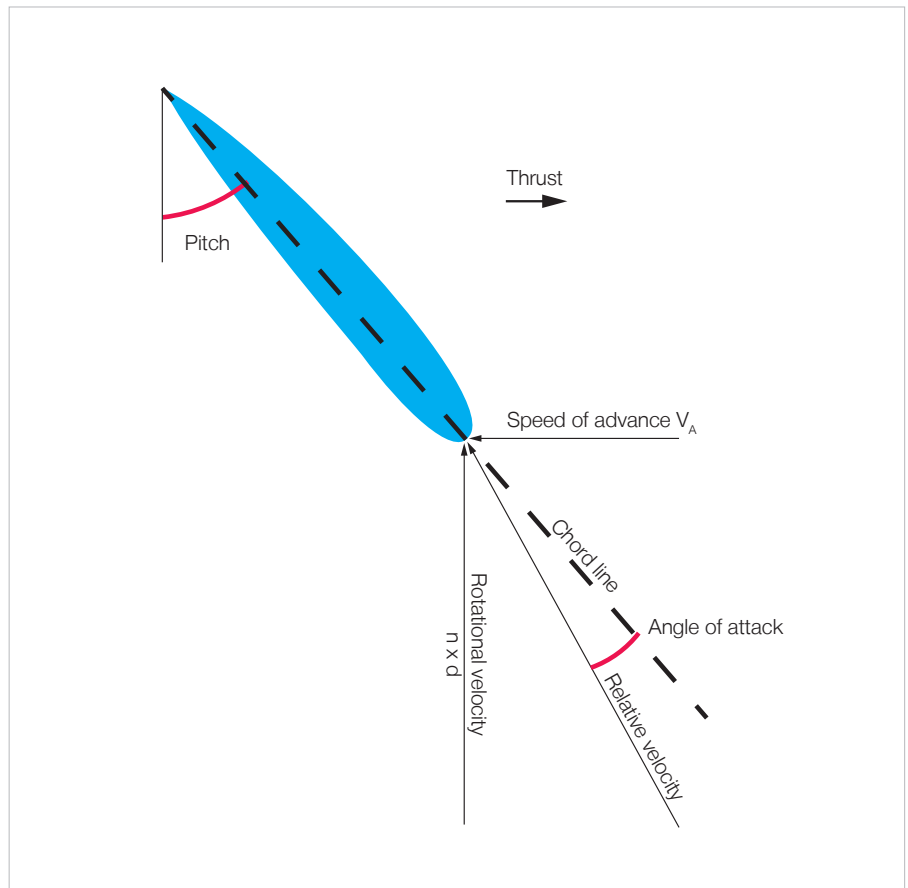


Fig. 2.07: Advance number

Slip

Sometimes the propeller is referred to as a screw, drawing on its similarity to a screw moving through a solid material. If this was the case, the propeller would move forward at a speed of the pitch times the rate of revolution, $V = p \times n$, see Fig. 2.01.

As water is not a solid material, the water yields (accelerates aft) due to the thrust of the propeller and therefore the propellers speed forward decreases compared to the non-yielding case. This difference is termed the slip.

Two terms describe the slip, the apparent slip S_A based on the speed of the ship, V , and the real slip S_R based on the speed of the water arriving at the propeller V_A , see Fig. 2.01. Both in principle quantify the ratio between the apparent/real advance per rotation and advance without water yielding:

$$S_A = \frac{p \times n - V}{p \times n} = 1 - \frac{V}{p \times n} \quad \text{EQ 21}$$

$$S_R = 1 - \frac{V_A}{p \times n} = 1 - \frac{V \times (1-w)}{p \times n} \quad \text{EQ 22}$$

The apparent slip can be calculated by the crew in order to provide an indication of the propeller load. Typically, the real slip cannot be calculated by the crew as V_A is not known but as the speed of advance V_A is smaller than V , it will be greater. The load is proportional to the slip on the propeller, i.e. the higher the slip, the higher the load and vice versa.

This implies that under increased resistance, the rate of revolution of the propeller must be increased to keep a constant ship speed.

Extra thrust is required to overcome the increased resistance, requiring extra torque from the main engine. Due the increased resistance, resulting slip and dropping propeller efficiency at higher load, it is only possible to deliver the in-

creased torque to a certain extent, and in severe weather the speed of a FP-propeller will drop when encountering the load limits of the engine. This will limit the possible power output of the main engine, see "Propulsion margins, including light running margin" in Chapter 3 as well as the considerations on minimum propulsion power in Chapter 4. Depending on the capabilities of the control system of a CP-propeller, the pitch can be lowered to enable the engine to maintain its speed and hereby power in severe conditions. However, at a reduced propeller efficiency, stemming from the reduced propeller pitch required to maintain the shaft speed.

When performing bollard pull, i.e. $V = 0$ and high thrust, the slip will be equal to one. All the water will yield (accelerate aft) as all the thrust delivered by the propeller will be used to accelerate the water and not the ship.

Remembering that the advance number is $J = V_A / (n \times d)$, the slip is considered in the advance number through the inclusion of V_A .

Cavitation

Cavitation occurs when the local pressure of the fluid drops below the vapour pressure of the fluid. Depending upon the location on the propeller blade, cavitation can be categorized either as back or face cavitation. Back cavitation occurs on the low-pressure (forward) side of the blade, and face cavitation occurs on the high-pressure (aft) side of the blade. The most know cavitation patterns and place of formation are:

- Sheet cavitation: on the low-pressure side of the blade surface near the nose of the blade
- Tip vortex: on the tip of the propeller
- Propeller-hull vortex: between the propeller blade tip and the hull
- Root: on the propeller blade root
- Cloud and bubble: on the low-pressure side of the blade surface
- Hub vortex: on the face surface of propeller hub
- Pressure side: on the high pressure side of the blade surface

If the vapor phase of the fluid/cavitation bubbles implodes on any surface of the propeller or rudder, they may cause erosion, performance breakdown, noise and vibration. Cavitation on the face side, shall be avoided as it is highly erosive.

A limited level of sheet cavitation on the suction / back side of the propeller blade may be accepted, in order to attain optimum efficiency, as long as it does not cause an unaccepted level of noise, vibration, and erosion. The reader is recommended to consult specialist literature for further information on propeller cavitation, i.e. [2.2] and [2.6].

Efficiencies and influencing parameters

The fuel equation in Chapter 1 describes the combined fuel power required to propel the ship. It is strongly dependent on the individual efficiencies of the propulsion plant components, which is discussed in the following, recalling that:

$$\eta_{\text{tot}} = \eta_H \times \eta_O \times \eta_R \times \eta_S \times \eta_E \quad \text{EQ 23}$$

Open water efficiency

The propeller efficiency η_O is related to working in open water, i.e. the propeller works in a homogeneous wake field with no hull in front of it. The propeller efficiency depends, especially, on the speed of advance V_A , the thrust force T , the diameter d , and on the design of the propeller, such as the number of blades, disk area ratio, and pitch/diameter ratio, as previously explained.

The ideal, and not reachable, efficiency, is given by the thrust loading coefficient:

$$\eta_{O,\text{ideal}} = \frac{2}{1 + \sqrt{1 + C_{th}}} \quad \text{EQ 24}$$

As seen, the lighter that the propeller is loaded (low C_{th}), the higher the ideal efficiency will be. In practice, there is a

lower limit of load, below which the efficiency will decrease again, as frictional losses will become relatively larger than the savings on other losses attained by the lighter propeller load, see Fig. 2.08, that provides an example of both the usable power/efficiency and the losses occurring on the propeller.

This limit is typically not met for practical applications, see specialist literature on propellers.

The two principal means to minimise the load include either to increase the diameter within the limits previously mentioned, or to increase the speed of advance. When working behind the ship, the hull can be optimised to decrease the wake fraction coefficient, hereby increasing V_A , see “Different approaches for optimising the propulsive efficiency” or some devices altering the flow can be installed, see “Energy saving devices”.

For a wide beam bulk carrier, with a low V_A , and a relatively small propeller, the load expressed by C_{th} will be high. On the other hand a twin-screw container or LNG carrier will have lightly loaded propellers.

The C_{th} -based approach to propeller efficiency given above does not take into account the propeller rotational speed. Therefore it is often more convenient to express the propeller efficiency as a function of the advance number J as well as the non-dimensional thrust and torque coefficient explained previously. These are obtainable from various propeller-series, see Fig. 2.08 for an example.

$$\eta_o = \frac{P_T}{P_D} = \frac{T \times V_A}{Q \times 2\pi \times \eta} = \frac{K_T}{K_Q} \times \frac{J}{2\pi} \quad \text{EQ 25}$$

Depending on the propeller loading and design, an open water efficiency of $\eta_o = 0.55 - 0.70$ is typically attained.

The axial losses account for most of the loss at low J and frictional losses at high J . Rotational losses as well as tip and hub vortex losses (usually small compared to others) constitute the rest, see Ref. [1.2] and [2.2].

Rotative efficiency

The actual velocity of the water flowing to the propeller behind the hull is neither constant nor at right angles to the propeller’s disk area, but has a kind of rotational flow described by the wake

field of the hull. Therefore, compared with when the propeller is working in open water, the propeller’s efficiency is affected by the propeller’s relative rotative efficiency, η_R , which can be interpreted as, Ref. [2.2]:

$$\eta_R = \frac{\text{power absorbed in open water at } V_A}{\text{power absorbed in wake behind ship at } V_A} \quad \text{EQ 26}$$

On ships with a single propeller, the rotative efficiency η_R is normally around 1.0 to 1.07. The rotative efficiency η_R on a ship with a conventional hull shape and with two propellers will normally be less, approx. 0.98, whereas for a twin-skeg ship with two propellers, the rotative efficiency η_R will be around 1.0. In the initial stage of a project, η_R can be set equal to 1.

Efficiency, working behind ship

The term behind efficiency describes the efficiency of the propeller when working behind the ship, considering the open water and rotative efficiency:

$$\eta_B = \frac{P_T}{P_D} = \eta_o \times \eta_R \quad \text{EQ 27}$$

Hull efficiency

The hull efficiency η_H is defined as the ratio between the effective (towing) power $P_E = R_T \times V$, and the thrust power delivered to the water by the propeller $P_T = T \times V_A$, i.e.:

$$\eta_H = \frac{P_E}{P_T} = \frac{R_T \times V}{T \times V_A} = \frac{\frac{R_T}{T}}{\frac{V}{V_A}} = \frac{1 - t}{1 - w} \quad \text{EQ 28}$$

This efficiency explains the complex relationship between the thrust deduction coefficient and the wake fraction coefficient. If the wake fraction coefficient w is larger than the thrust deduction coefficient t , which is normally the case, the hull efficiency will become larger than one, thereby reducing the overall power required to propel the ship. However, reality is far more complex than this single formula indicates, as the parameters affecting the hull efficiency to a

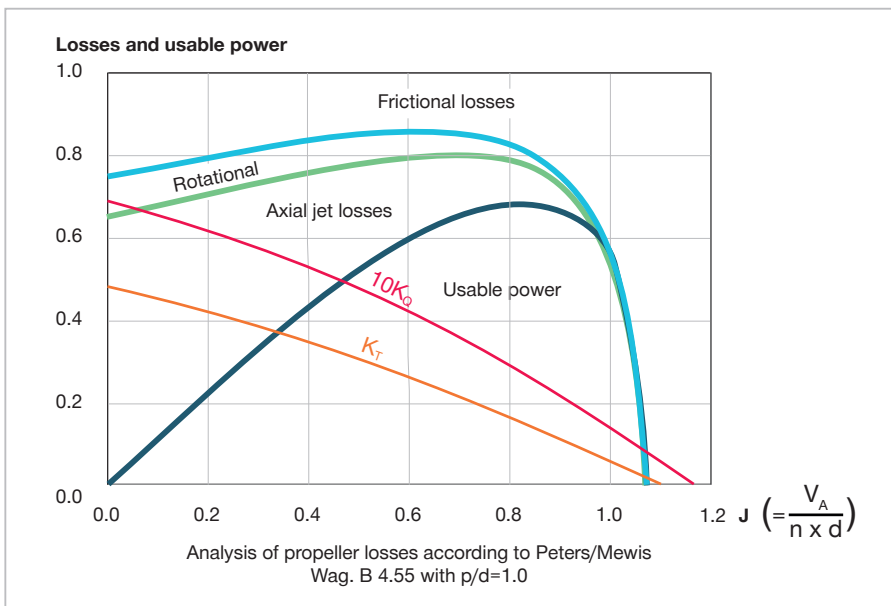


Fig. 2.08: Propeller losses. Note that this is only an example, various combinations of speed and pitch exist in different propeller-series. Courtesy of HSVA, Ref. [2.3]

large extent will affect the open water efficiency of the propeller.

If the wake fraction coefficient is increased, the speed of advance, or water arriving at the propeller, will be lower (remember that $w = 1 - V_A/V$). This means that the open water efficiency of the propeller will be reduced, see Fig. 2.08.

Table 2.02 shows the typical values of the hull efficiency depending on the propeller arrangement. In general, the hull efficiency will be higher for ships with a high block coefficient, creating a large wake fraction coefficient - and large hull resistance. These full body ships also tend to demonstrate a lower propeller efficiency due to the restrictions on propeller diameter set by the ballast condition.

Propulsive efficiency

The term “propulsive efficiency” describes the combined efficiency of the hull and propeller – excluding the engine and shaft connection:

$$\eta_D = \eta_H \times \eta_O \times \eta_R \tag{EQ 29}$$

Traditionally, the influence of the propulsive efficiency, η_D , on the engine efficiency η_E and vice versa has not received much attention, but it is important to stress that there are strong interdependencies, which is why an optimal ship cannot be reached by optimising these independently.

The process of matching hull and engine for the overall best efficiency is described in Chapter 3.

Shaft efficiency

The shaft efficiency η_S is not related to the propeller, but is included here for

completeness. It depends, among other factors, on the alignment and lubrication of the shaft bearings and on the reduction gear, if installed. It is defined as the ratio between the power delivered to the propeller P_D and the brake power of the main engine P_B :

$$\eta_S = \frac{P_D}{P_B} \tag{EQ 30}$$

For directly coupled two-stroke engines with a short shaft $\eta_S \approx 0.99$, for long shafts $\eta_S \approx 0.98$, and if a reduction gear is installed, $\eta_S \approx 0.95$ to 0.96 .

Influence of propeller diameter and pitch/diameter ratio example

As already mentioned, the highest possible propulsive efficiency at a given ship speed is in general obtained with the largest possible propeller diameter d , in combination with the corresponding, optimum pitch/diameter ratio p/d .

As an example for an 80,000 dwt crude oil carrier, with a service ship speed of 14.5 knots and a propeller diameter of 7.2 m, this influence is seen in Fig. 2.09.

According to the blue curve, the maximum possible propeller diameter of 7.2 m may have the optimum pitch/diameter ratio of 0.70, and the lowest possible shaft power of 8,820 kW at 100 rpm. If the pitch for this diameter is changed, the propulsive efficiency will be reduced, i.e. the necessary shaft power will increase, see the red curve.

The blue curve shows that if a bigger propeller diameter of 7.4 m is possible, the necessary shaft power will be reduced to 8,690 kW at 94 rpm, i.e. the bigger the propeller, the lower the optimum propeller speed.

For the same engine the bigger propeller though reduce the extent to which the engine can be derated. This influence on the engine efficiency is some-

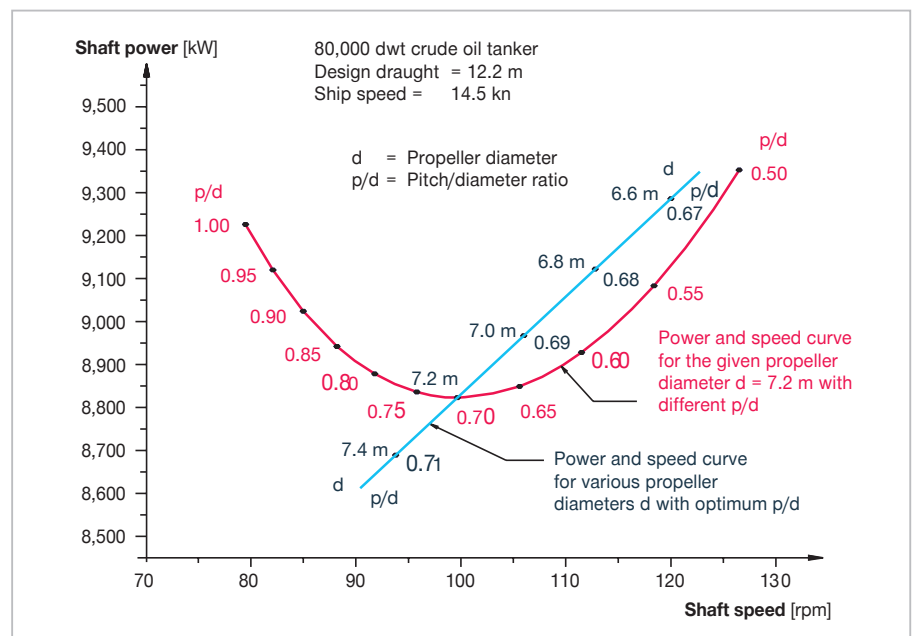


Fig. 2.09: Example of influence of diameter and pitch

Propeller arrangement	Wake fraction coefficient, w	Thrust deduction coefficient, t	Hull efficiency, η_H
Single-screw	0.20-0.45	0.10-0.30	1.1-1.3
Twin-screw, single skeg	0.10-0.25	0.05-0.15	0.95-1.15
Twin-screw, twin skeg	0.15-0.35	0.05-0.25	1.05-1.25

Table 2.02: Typical approximate propulsion coefficients

times not considered when designing the propulsion plant and, depending on the specific project, it can be well worth sacrificing 0.5% of propeller efficiency for gaining a larger increase in engine efficiency, see Chapter 3.

Depending on the hull geometry, the maximum propeller diameter is sometimes not the limiting factor. For some reason, there might be an engine limitation with regard to the lowest possible rotational speed instead. In such cases, as the red curve shows, it may still be worth applying the largest possible propeller, and instead decrease the pitch in order to increase engine speed. The benefit of the larger propeller will typically be significantly larger than the small decrease in efficiency from the lower pitch, see Fig. 2.09.

Different approaches for optimising the propulsive efficiency

As described above, many different aspects affect the overall efficiency of the propulsion plant (including the engine). These aspects may also affect the hull resistance. Therefore, the designer must find a balance, and as great variety exists among ship types and designers, one size does not fit all, and different approaches can lead to the same combined efficiency.

A short example of such considerations can be given for a large ≈ 20.000 teu container ship, where different designs exist with one and two propellers, typically twin-skeg. A single-screw ship will offer the best efficiency of the engine as the engine is larger. Furthermore, the single-screw ship will have the smallest

wetted surface area, hereby reducing the frictional hull resistance.

On the other hand, the propeller of the single-screw ship will be higher loaded than on the twin-screw ship, which in itself decreases its efficiency. Furthermore a high disk area coefficient and hereby greater blade number must be employed in order to avoid cavitation, further decreasing the efficiency of the propeller for the single-screw ship.

In this case, the greatly improved propeller efficiency of a twin-skeg ship will not only level out the other losses, but usually lead to an overall increase in propulsive efficiency.

Velocities

- Ship's speed : V
- Arriving water velocity to propeller..... : V_A
(Speed of advance of propeller)
- Effective wake velocity : $V_W = V - V_A$
- Wake fraction coefficient..... : $w = \frac{V - V_A}{V}$

Forces

- Towing resistance : R_T
- Thrust force : T
- Thrust deduction fraction : $F = \frac{T - R_T}{T}$
- Thrust deduction coefficient : $t = \frac{T - R_T}{T}$

Power

- Effective (Towing) power : $P_E = R_T \times V$
- Thrust power delivered
by the propeller to water : $P_T = P_E / \eta_H$
- Power delivered to propeller : $P_D = P_T / \eta_B$
- Brake power of main engine : $P_B = P_D / \eta_S$

Efficiencies

- Hull efficiency : $\eta_H = \frac{1 - t}{1 - w}$
- Propeller efficiency - open water : η_O
- Relative rotative efficiency : η_R
- Shaft efficiency : η_S
- Engine efficiency : η_E
- Propeller efficiency - behind hull : $\eta_B = \eta_O \times \eta_R$
- Propulsive efficiency : $\eta_D = \eta_H \times \eta_B$
- Total propulsive efficiency : η_{prop}
- $\eta_{prop} = \frac{P_E}{P_B} = \frac{P_E}{P_T} \times \frac{P_T}{P_D} \times \frac{P_D}{P_B} = \eta_H \times \eta_B \times \eta_S = \eta_H \times \eta_O \times \eta_R \times \eta_S$
- Total efficiency : η_{tot}
- $\eta_{tot} = \eta_{prop} \times \eta_E = \eta_H \times \eta_O \times \eta_R \times \eta_S \times \eta_E$

Table 2.03: Collection of equations relevant for ship propulsion and efficiencies

Energy saving devices

Energy saving devices (ESDs), or sometimes efficiency improving devices, is a term covering different devices designed for optimising the flow to, around or after the propeller. The devices are primarily designed to alter the wake field or eliminate the losses arising on the propeller, see “Open water efficiency”. Table 2.04 categorises different devices according to their working principle.

Fig. 2.10, illustrates the savings that can be gained by employing the devices individually. It is important to note that savings cannot just be added. An individual analysis of the effect in the specific wake of the hull must be per-

formed. Experience has shown that it is unlikely to achieve combined savings of more than 10% compared to a standard design.

When choosing the optimum ESD (or a combination hereof), the operating conditions of the ship must be considered.

For instance, the Kappel propeller provides the largest savings for highly loaded (high C_{th}) propellers. The wake equalising duct (and similar duct systems) works best for ships with large block coefficients, as it equalises and reduces the wake fraction coefficient.

Contra-rotating propellers have high costs, not only due to the cost of two propellers, but also the complex me-

chanical construction required for powering both propellers. In addition, careful maintenance is required why it is not commonly applied.

In general, hub vortex reducing measures (see Table 2.04) provide a rather simple, maintenance-free (other than cleaning) solution and are amongst the most popular. These factors also apply for pre-swirl fins and twisted rudders.

For all ESDs, their potential savings must always be evaluated against the added wetted surface and the resistance created by its presence. This is accounted for in Fig. 2.10.

It is important to evaluate the impact of any ESD towards the propeller light

Working principle, reducing	Device	Saving potential
Rotational losses	Pre-swirl fins	3-5%
	Twisted rudder	1-2%
	Contra rotating propellers	4-7%
Rotational losses and separations in the aft body	Wake equalising duct	3-8%
Hub vortex losses	Efficiency rudders	2-6%
	Rudder bulb	2-5%
	Hub cap fins	2-5%
Tip vortex losses	Kappel propeller	3-6%

Table 2.04: Working principles of various energy saving devices including individual saving potential, Ref. [2.4]

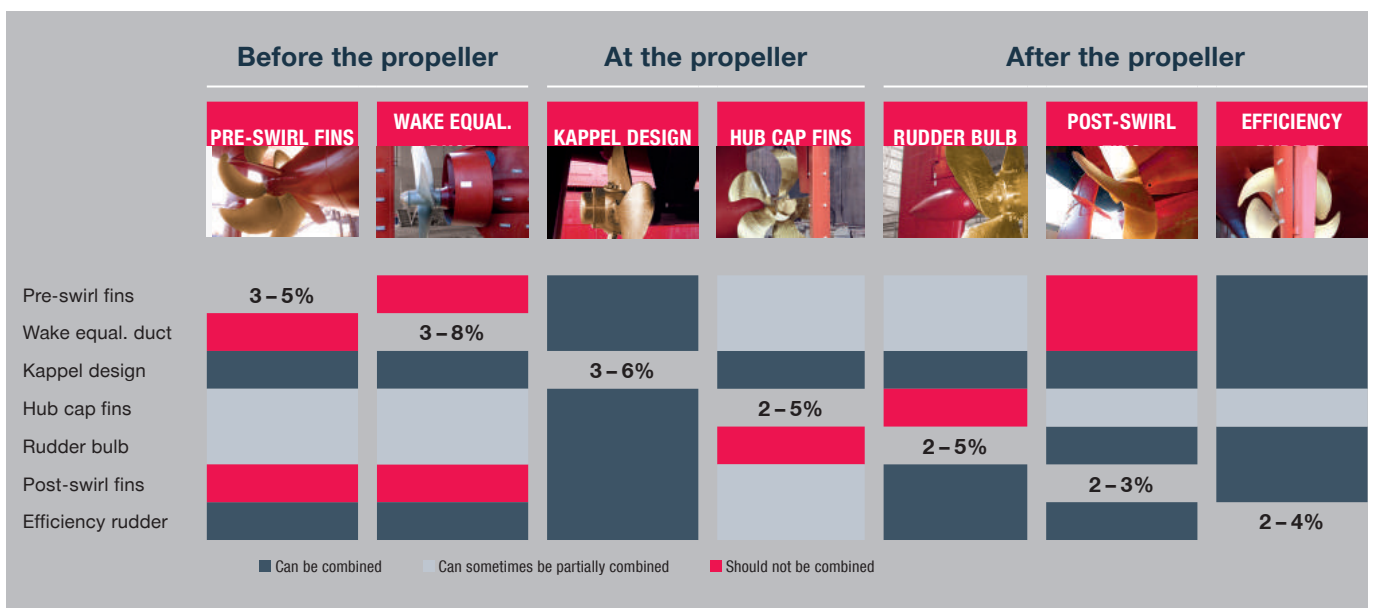


Fig. 2.10: Possibilities for combining energy saving devices, including individual saving potential

running margin, especially for retrofit, see “Light running margin” in Chapter 3. Additionally, when evaluating stated saving potentials for specific devices, the designer must take care whether the savings are attained at model or full scale, as scaling effects can be significant.

“Propeller law” and power/speed curves

As explained in Chapter 1, the resistance of a ship can be expected to increase by the square of the speed, $R = \frac{1}{2} \times \rho \times A_S \times C \times V^2$ at lower Froude numbers

$$F_n = \frac{v}{\sqrt{g \times L_{WL}}} \quad \text{EQ 31}$$

where the resistance is purely frictional. As power is the force of resistance times speed, $P = V \times R$, this results in a required power and hereby fuel consumption proportional to the cubic of the speed, $P \propto k \times V^3$.

This proportionality is termed the Propeller law, and despite it being termed a law that the required power is proportional to the cubic of the speed, it is only an assumption applicable at lower Froude numbers. At elevated Froude numbers, where the wave making resis-

tance must be taken into account, the required power can be proportional to the speed to a power of four or even larger, $P \propto k \times V^4$. This is exemplified in Table 2.05 for different ships.

Explanations regarding the concept of a heavy running propeller and light running margin in Chapter 3 will be based on the propeller law, $P \propto V^3$.

Acceleration, barred speed range, manoeuvring speed and propeller rotation

Acceleration is an important parameter for the manoeuvring performance of the ship. In addition, there is a link between acceleration performance and ship performance under increased resistance: If the ship can produce a high thrust force for acceleration at low ship speed, it can also produce a high thrust force for overcoming high resistance at low speed in heavy weather conditions.

Two important aspects of acceleration are acceleration of the ship itself, and shaft acceleration past a barred speed range. The bollard pull propeller curve is introduced before the discussion of shaft acceleration past a barred speed range (BSR).

Application of a CP-propeller will provide more flexibility with respect to

achieving good acceleration performance. This is not treated further in this section, see the engine selection spiral for CP-propellers in Chapter 3.

Ship acceleration capability is mostly governed by the power to displacement ratio of the ship, P_B / Δ . In other words, how much power there is to push a ship with a certain displacement.

The trend towards increasingly larger ships is rooted in the fact that a large ship, compared to a smaller one, has less wetted surface relative to the cargo capacity, and thereby less resistance and fuel consumption relative to cargo capacity. Therefore, the large ship will be equipped with less engine power relative to its displacement than the small ship. As a result, the large ship will accelerate slower than the small ship.

Focus on lowering the fuel consumption and still tighter EEDI requirements may result in ships with quite low power-to-displacement ratios compared to earlier designs. It must be assured in the design phase that a ship has sufficient power for safe manoeuvring in all relevant conditions. The IMO Minimum Propulsion Power requirements address and regulate this issue, see Chapter 4.

Category	Propeller	Length, L _{PP}	Breadth, B	Draught, T _d	C _B	V, kn (=n)	V, kn (=n)	V, kn (=n)	V, kn (=n)
Tanker, product	1 FP	174	32.2	11.0	0.78	13 (3.2)	14 (3.4)	15 (3.6)	16 (3.8)
Bulk carrier	1 FP	273	46.0	16.5	0.83	13 (3.0)	14 (3.1)	15 (3.3)	16 (3.6)
Container ship	1 FP	375	59	16.0	0.68	21 (3.2)	22 (3.3)	23 (3.3)	24 (3.4)
Container ship	2 FP, twin skeg	375	59	16.0	0.68	21 (3.1)	22 (3.2)	23 (3.2)	24 (3.3)
Ro-pax	2 CP, twin skeg	200	31.8	7.0	0.61	21 (3.4)	22 (3.7)	23 (4.1)	24 (4.8)

Table 2.05: Example ships with exponents to the power curve, $P = k \times V^n$, depending on the speed of the ship. The approximate exponent of the power equation corresponding to the speed is stated in parentheses, Ref. [2.5]

Bollard pull propeller curve for FPP

Fig. 2.11 shows the bollard pull propeller curve and the normal light propeller curve as a function of propeller rpm, which for a directly coupled propeller equals engine rpm. At the start of acceleration, from zero ship speed, the propeller will be heavy running and operating along the bollard pull curve.

The limits of the main engine is illustrated on Fig. 2.11 and is described in Chapter 3. It is clear that due to the heavy running of the propeller in bollard pull, 100% rpm cannot be reached in the bollard pull condition due to the limit of the engine power curve.

The exact value of heavy running in bollard pull condition is difficult to predict at the early ship design stage. In general, a heavy running factor of 15-20% relative to the light propeller curve have been experienced, i.e. an rpm reduction of 15-20% for the same power. This is equivalent to approx. 60-100% increase in power for the same rpm.

Considering Fig. 2.11, it is brought to the reader's attention that an engine with an FP-propeller can always accelerate to approx. 50% rpm along the bollard pull curve before encountering the load limits of the engine. At low rpm, the propeller curve is well within the limits of the engine diagram.

Shaft acceleration past a barred speed range for FPP

A barred speed range imposed by vibrations must be passed sufficiently quick in order not to damage the shafting due to vibrations resulting in excessive stresses.

What is meant by "sufficiently quick" depends on how high the stresses in the shaft are compared to the strength of the shaft material.

Furthermore, the definition of "sufficiently quick" depends on how often the barred speed range will be passed during the expected lifetime of the ship. For example, a feeder container ship with many port calls will pass the barred speed range more frequently than a large crude carrier that mostly performs ocean crossings.

In general, the barred speed range must be passed within seconds, not minutes. Classification societies have established methods for determining if a BSR passage is sufficiently quick, see i.e. [2.7].

The acceleration of the shaft line is governed by the difference in power delivered by the main engine and the hydrodynamic power required by the propeller. As long as the power provided by the engine is higher than the

power required by the propeller, the shaft line will accelerate.

During acceleration from ship standstill, the propeller curve is heavy running along the "bollard pull" propeller curve. This is comparable to a car going uphill at the same speed in the same gear as when driving on a flat highway. Thus, going uphill, the load on the engine will be greater as more work must be delivered to lift the mass of the car (in the case of the ship to accelerate the water at the propeller) even if the rotational speed is the same.

At some point, the bollard pull propeller curve will demand more power than the engine can deliver at low rpm as full engine power can only be delivered at full engine rpm. As there is no longer an excess of engine power relative to the bollard pull curve, the propeller and shaft speed will accelerate at a slower rate, namely the rate at which the ship is accelerating through water. It is important to note that the propeller in this case will continue to accelerate with the acceleration of the ship, though no longer at the maximum rate along the bollard pull curve.

With this acceleration of the ship, the actual propeller curve will gradually shift towards the light propeller curve and, at some point, the actual curve will be outside the barred speed range, as seen on Fig. 2.11. Thereby, the barred speed range is passed, but over longer time, i.e. not necessarily ensuring a sufficiently quick passage of the BSR.

In other words, if the bollard pull curve crosses the power limit of the engine at an rpm below or within the BSR, the BSR may not be passed sufficiently quick.

In order to avoid issues with slow passage of the BSR, the engine power and the propeller characteristics should be matched accordingly, see the engine selection spiral for FP-propeller plants in Chapter 3. Here, the capability to pass the BSR sufficiently quick can be evaluated by means of the barred speed range power margin, BSR_{PM} .

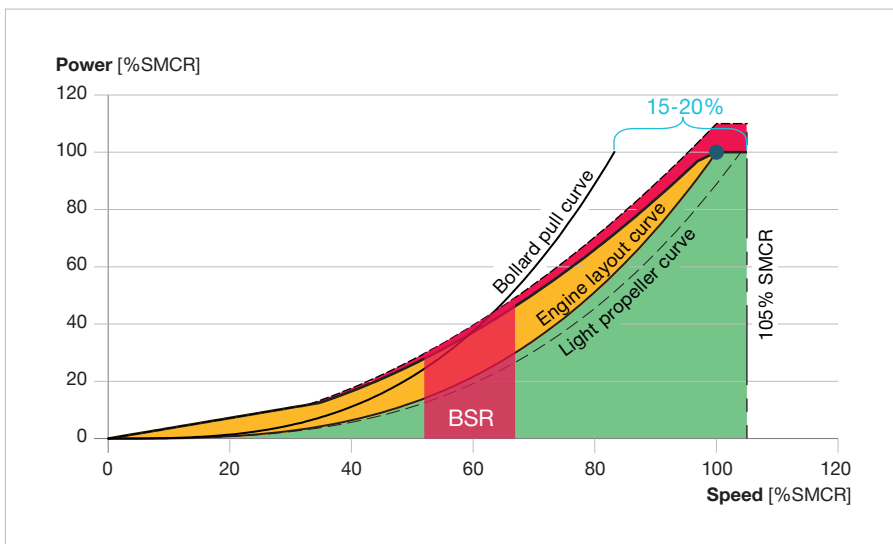


Fig. 2.11: Bollard pull curve. The two-stroke engine can always accelerate a propeller to about 50% rpm quickly. The BSR in the figure is placed high up in the rpm range and BSR passage may not be quick.

For a practical example on the interactions between the engine and propeller during acceleration of the ship, along with the impact of any power or torque limitation, see “Engine loading during acceleration” and “Power limitations of main engines” in Chapter 3.

In situations with very high resistance on the ship, such as in very rough weather, it may not be possible to accelerate the ship to speeds much higher than a few knots. If the ship does not have sufficient BSR_{PM} , it may not be possible to achieve a propeller speed above the BSR. Hence, the crew will be forced to reduce the rpm setting of the main engine to a value below the BSR, resulting in an even lower ship speed. A sufficient BSR_{PM} is therefore also important in other situations than acceleration. This needs to be included in considerations on minimum propulsion power as well, see Chapter 4.

Manoeuvring speed

Below a certain ship speed, referred to as the manoeuvring speed, the manoeuvrability of a ship will be insufficient due to the too low velocity of the water arriving at the rudder and flow along the sides of the ship. It is rather difficult to give a general figure for an adequate manoeuvring speed of a ship, but a manoeuvring speed of 2 to 4 knots is often applied.

Considering manoeuvring and minimum speed hereof, it is important to realise that it is not the rudder and the flow across it that turns the ship. The rudder provides the ship's sides with an angle of attack to the water flow along it, which generates the force to alter the course of the ship.

This is in principle similar to an aircraft where the elevators provide the wings with an angle of attack towards the airflow, increasing the lift and hereby changing the altitude of the aircraft.

It is furthermore worth noticing that effects of bow and stern thrusters reduce significantly at speeds above approx. 2 to 4 knots, depending on the plant specific flow conditions. The effect of the thrusters reduce as the wa-

ter flow to the thrusters is reduced due to the flow across the inlets, as well as the ejected jet attaches itself to the flow along the hull, as per the “Coanda” effect, see i.e. [2.8].

Direction of propeller rotation

When a ship is sailing, the characteristics of the wake field means that the propeller blades bite more in their lowermost position than in their uppermost position. The resulting side-thrust effect is larger the more shallow the water is as, for example, during harbour manoeuvres.

Therefore, a clockwise (looking from aft to fore) rotating propeller will tend to push the ship's stern in the starboard direction, i.e. pushing the ship's stem to port, during normal ahead running. This has to be counteracted by the rudder.

When reversing the propeller to astern running as, for example, when berthing alongside the quay, the side-thrust effect is also reversed and becomes further pronounced as the upper part of the propeller's slip stream, which is ro-

tative, strikes the aftbody of the ship. Awareness of this behaviour is very important in critical situations and during harbour manoeuvres, also for the pilot.

It has therefore been common that on a ship fitted with an FP-propeller, the propeller is always designed for clockwise rotation when sailing ahead.

CP-propellers always rotate in the same direction, without reversing the engine for going astern, rather the blades are turned. In order to obtain the same side-thrust effect when reversing to astern, CP-propellers are typically set for anti-clockwise rotation when sailing ahead. As the side thrust effect is strongest when going astern, this is the most critical situation, see Fig. 2.12.

Due to the recent years' developments in computational fluid dynamics, it has become a possibility to evaluate if the direction of rotation may offer an efficiency gain or a larger absolute thrust, moving away from the previous customs towards an individual setting for the specific plant.

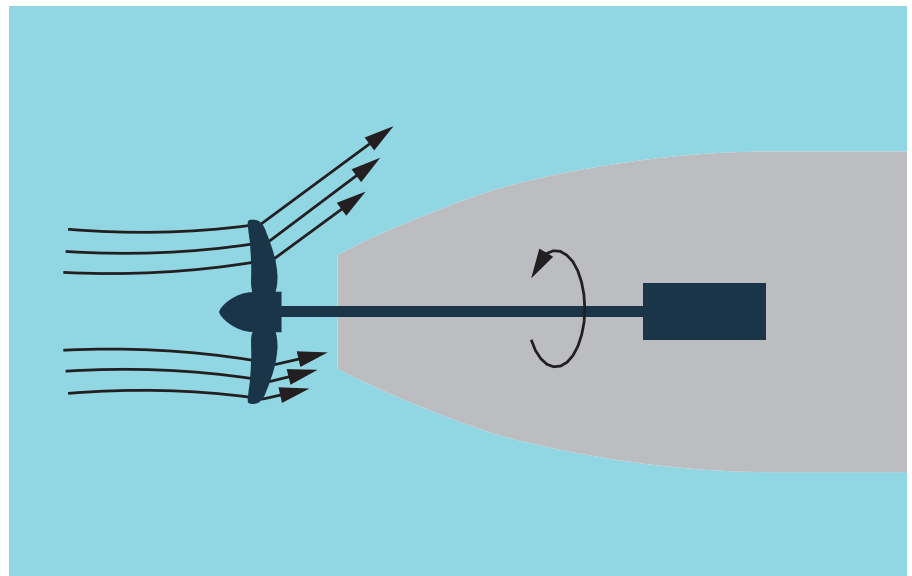


Fig. 2.12: Astern water flow

Manufacturing accuracy of the propeller

Before the manufacturing of the propeller, the desired accuracy class standard of the propeller must be chosen by the customer. Such a standard is, for example, ISO 484/1 – 1981 (CE), which has four different “Accuracy classes”, see Table 2.06. Typically class S is almost only used for naval ships, whereas class I is typically used for merchant ships. Class II and III are rarely used.

The manufacturing accuracy tolerance corresponds to a propeller speed tolerance of max. +/- 1.0%. When also incorporating the influence of the tolerance on the wake field of the hull, the total propeller tolerance on the rate of revolution can be up to +/- 2.0%. This

tolerance must also be borne in mind when considering the operating conditions of the propeller in heavy weather, and can explain why sister ships may have different propeller light running margins.

This chapter explains the basic working principles of a two-stroke crosshead engine, the parameters affecting its efficiency, the concepts for using alterna-

tive fuels, and how the loading of the propeller influences the engine layout and running conditions.

An engine selection spiral is introduced and provided in two editions, one for fixed pitch propellers and one for controllable pitch propellers. The engine selection spiral describes the method for selecting the optimum engine depending on the priorities of the project.

ISO 484/1 – 1981 (CE)

Class	Manufacturing	Mean pitch
S	Very high accuracy	+/- 0.5%
I	High accuracy	+/- 0.75%
II	Medium accuracy	+/- 1.00%
III	Wide tolerances	+/- 3.00%

Table 2.06: Manufacturing accuracy for propeller

Chapter 3

Engines for marine propulsion plants

This chapter explains the basic principles. For specific calculations for two-stroke engines, we recommend the on-line CEAS tool available from the MAN Energy Solutions website → Two-Stroke → CEAS Engine Calculations.

Two-stroke uniflow crosshead diesel cycle engines

Diesel cycle engines are characterised by the direct injection of fuel into the combustion chamber. The fuel is ignited by the high temperatures arising from the large mechanical compression of the air prior to fuel injection. For further details, see Ref. [3.1].

The power delivered from an engine depends on the torque it can develop at a given rotational speed (angular velocity, ω) and the rotational speed itself:

$$\text{SMCR}_{\text{speed}} = \text{PD}_{\text{speed}} \times \left(\frac{\text{SMCR}_{\text{power}}}{\text{PD}_{\text{power}}} \right)^{1/3} \times \left(1 - \frac{\text{LRM}}{100} \right) \quad \text{EQ 32}$$

Engines may work according to the two-stroke or the four-stroke principle. Both principles are utilised for mechanical propulsion of ships, as shown in Table 1.01 (p. 8) in Chapter 1.

Medium speed four-stroke engines have a higher power density than low speed two-stroke engines and requires less engine room height but a reduction gear to match the propeller speed. Low speed two-stroke crosshead engines offers superior fuel economy and a speed matching the optimum propeller speed.

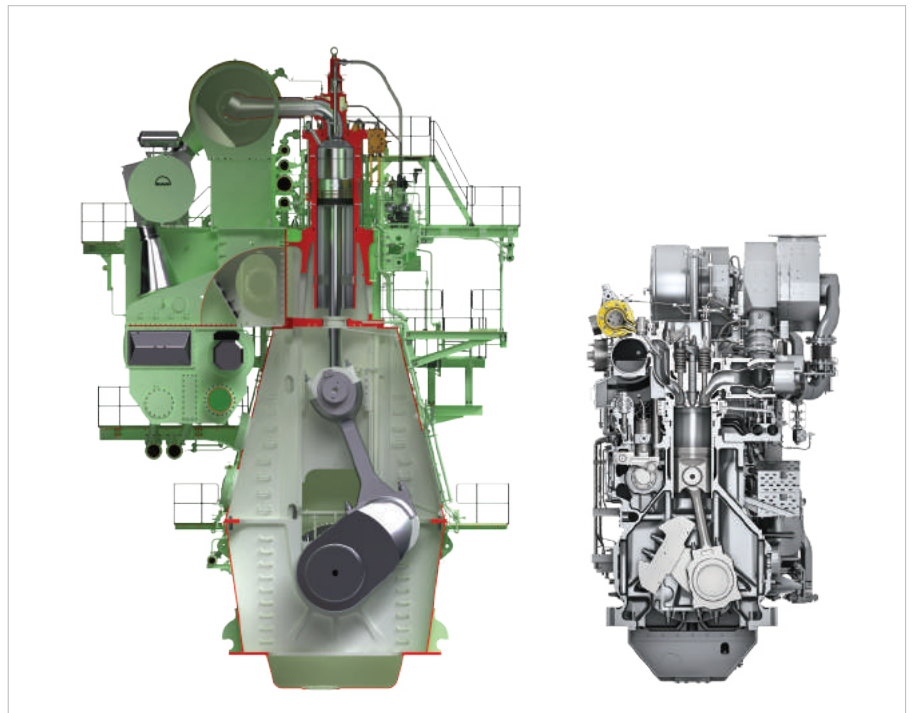


Fig. 3.01: Two-stroke crosshead engine and four-stroke trunk engine, not to scale

The principle of the crosshead is illustrated in Fig. 3.01. The crosshead allows a significantly larger stroke/bore ratio compared to its counterpart, the trunk engine, as the vertical-only movement of the piston rod allows it to be as long as required, without interfering with the cylinder liner.

The long stroke leads to both high efficiency, as well as a low speed, making it possible to couple the engine and propeller directly. This eliminates the complexity and losses in a reduction gearbox, and ensures further savings.

Performing a combustion each time the piston is at top also increases efficiency, as the relative frictional loss is reduced.

The scavenging (exchange of exhaust gas with fresh air) of the two-stroke uniflow engine is different from the cross-flow scavenging concept applied in two-stroke engines known for domestic use, i.e. in a lawn mower engine.

In the uniflow scavenging engine the pressurised charge air enters through scavenge air ports in the bottom of the cylinder liner as these are uncovered

when the piston is at its bottom position, see Fig. 3.02. The scavenging air pushes the remaining exhaust gas out through the exhaust valve in the middle of the cylinder cover at the top of the cylinder. The uniflow scavenging is applied both for the diesel and otto cycle marine two-stroke engines.

Electronically controlled engines

Ever since the first engine was built and up until the turn of the century, marine engines were mechanically controlled. This meant that the timing of the fuel injection and the opening of the exhaust valves were controlled by a camshaft. Today, most new engines are electronically controlled.

The camshaft-less ME engine enables dynamic optimising of combustion parameters such as injection timing, injection pressure, and shaping of the profile hereof as well as the timing of the exhaust valve actuation. The fuel oil injection pressure is decoupled from the engine speed which allows the injection pressure to be high for the whole load range, ensuring optimal efficiency and low soot formation.

On ME engines, the air amount trapped in the cylinder, and later compressed, is less dependent on the scavenge air pressure, as the closing time of the exhaust valve can be varied. Early closing during acceleration (to compensate

that during acceleration the scavenge air pressure is lower) i.e. ensures a better performance in manoeuvring compared to previous MC engines with camshaft control.

Engine efficiency parameters

The efficiency of a two-stroke diesel cycle engine is affected by many parameters, but a few main parameters important for an initial comparison of engines can be identified:

- Compression ratio:
The higher the compression ratio, or more importantly the corresponding high expansion ratio, the higher the end-temperature of the air in the cylinder when compressed. This ensures that the heat from the combustion is released at a high temperature level, and that a high degree of expansion of the hot gasses is possible before the exhaust valve needs to be opened. It is the expansion of the hot gasses that produces the power, and the high compression/expansion ratio of the diesel cycle engine is therefore a main contributor to the high efficiency of the diesel cycle engine.
- Cylinder bore:
For the same stroke/bore ratio, the larger the bore, the larger the engine. A larger bore will reduce the relative heat loss, as the surface through which heat can escape will be rela-

tively smaller compared to the combustion volume. This improves engine efficiency.

- Stroke/bore ratio:
For a uniflow two-stroke engine, a high stroke/bore ratio improves the efficiency of the scavenging process and thereby the efficiency of the engine.

As mentioned previously, the stroke length has an influence on the rate of revolution. Typically, the biggest improvement to ship efficiency by increasing the stroke length, is not from the engine itself. Instead the increased efficiency of the larger propeller that can be applied with the resulting lower rotational speed brings the largest improvement, see Chapter 2.

GI, GA and LGI dual fuel engines

Engines capable of operating on traditional bunker oil as well as alternative fuels are termed dual fuel engines. At present, liquefied natural gas (LNG), which primarily consists of methane, is the dominant alternative fuel, but methanol engine contracting has increased significantly since 2023, especially for large container vessels. Ethane and LPG engines are as of 2023 only applied on ships that carry the fuel as a cargo. Ammonia fueled engines are under development as per 2023.

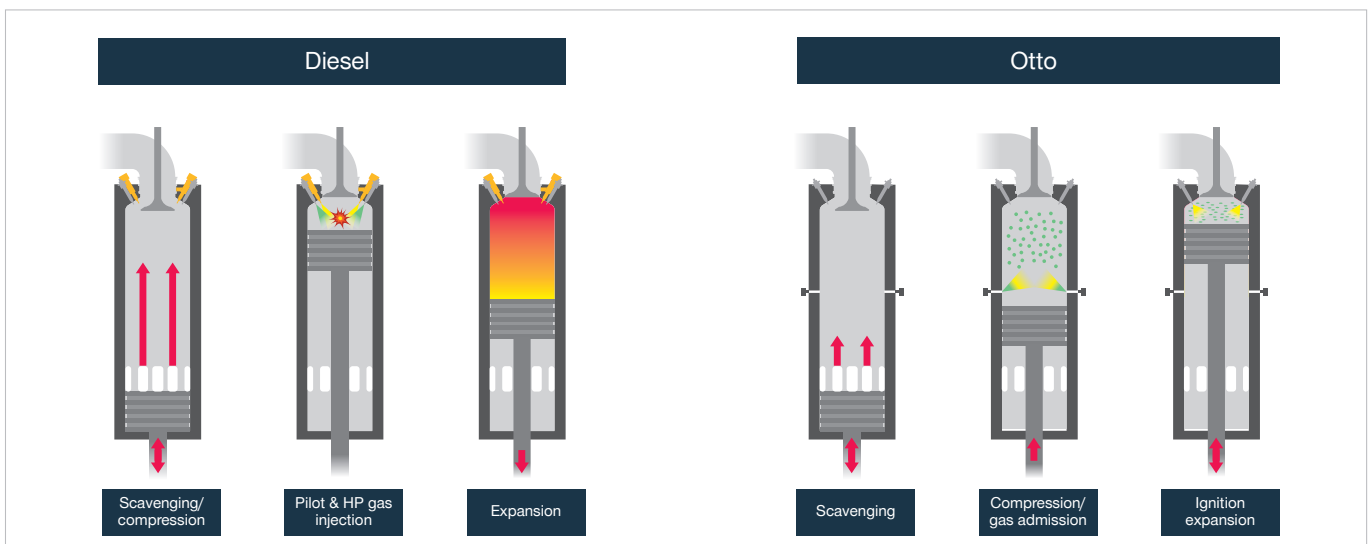


Fig. 3.02: Diesel and otto cycles for dual fuel uniflow scavenging two-stroke engines

LNG and ethane are for diesel combustion injected into the combustion chamber in gas form, giving rise to the GI (gas injection) engine type affix. LPG and methanol are injected in liquid form, giving the type affix LGI (liquid gas injection) with LGIM for methanol and LGIP for LPG.

For the otto cycle dual fuel engine for LNG as fuel, the affix GA is related to the gas *admission* concept, rather than the gas *injection* of the GI engine.

In general, these alternative fuels can be characterised as low-flashpoint fuels, as they have a low carbon-to-hydrogen ratio. The lower carbon content of these fuels is also what makes alternative fuels interesting climate-wise, as CO₂ emissions are also reduced hereby, see Chapter 4.

Due to its current dominance as an alternative fuel, the principle of an LNG dual fuel engine will be the base for explaining the two existing concepts for combustion of low-flashpoint fuels, see Fig. 3.02 as well:

- The diesel cycle:
When injected into the combustion chamber the Fuel is ignited by the temperature and burned in a diffusion flame. This is also termed a compression ignition engine.
- The otto cycle:
Air and fuel are premixed, for marine applications either in or outside the cylinder. The mixture is then compressed and later ignited by a release of heat, e.g. a spark in a petrol car engine, or pilot fuel oil in a marine engine.

The diesel and the otto cycles are both available for two-stroke crosshead engines. The diesel cycle offers a series of advantages besides being the most efficient operating principle:

- Methane slip is very limited by the diesel principle as the injected gas is burned directly in a diffusion flame. In an otto cycle engine, the total volume of the combustion chamber is not included in the volume swept by

the flame front during the combustion. Hereby not all of the fuel/air mixture is burned, which result in higher amounts of unburned methane that slips to the atmosphere. This is important as methane has a global warming potential that is 28-36 times as high as CO₂, Ref. [3.2]. However, exhaust gas recirculation (EGR) can be applied on an otto cycle engine to recirculate the exhaust gas and hereby reduce slip amongst others.

- Gas qualities with very large varieties in compositions can be burned in a diesel cycle engine. As the injected gas is burned directly, the methane number of the gas, indicating its resistance towards engine knocking (premature ignition), is of no significance.
- Heavy running capabilities and hereby acceleration performance and acceptance of external load variations, such as varying propeller load as a result of heavy sea are better for diesel cycle engines, as knocking is not an issue. For marine otto cycle engines diesel oil is, when the torque cannot be developed purely by the otto cycle without risk of engine knocking, injected directly into the combustion chamber in sufficient amounts to attain heavy running capabilities similar to a diesel cycle engine.
- No reduction of compression ratio. To avoid knocking, the compression ratio of an otto cycle engine is lower compared to a diesel engine, resulting in a lower efficiency of an otto engine when operating in diesel mode. The high compression ratio allows the diesel engine to operate with any mixing ratio of traditional fuel and LNG as well as traditional fuel only, at the same high efficiency.

In the diesel cycle ME-GI engine, the gas is operating at 300 bar, in order to overcome the compression pressure in the chamber. This is achieved by pressurising the LNG to the rated pressure and hereafter vaporise it to gas form, prior to injection.

In otto cycle engines the gas is admitted to the chamber at a pressure of 6 to 14 bar depending on maker and engine load, as the gas is admitted prior to the compression, where the pressure in the cylinder is low. The low gas admission pressure of the otto cycle ME-GA engine is relevant for LNG carriers where large amounts of boil of gas is available at ambient pressures.

For LNG carriers the diesel cycle GI engine will, despite some extra work needed for compressing the boil of gas, result in the overall lowest emission of CO₂-equivalents compared to the otto cycle ME-GA engine, as a result of the reduced methane slip and higher fuel efficiency. For diesel cycle plants, the boil of gas can be reliquified before being pressurised for injection, greatly reducing the work required hereto. The separate paper "LNGC-optimised designs of ME-GI engines and fuel gas supply systems" explains in detail how to outline a dual fuel plant for a diesel cycle engine.

For other ship types where the LNG is pressurised while in liquid form, directly from the bunker tanks, the advantages of the diesel cycle engine mentioned in general outweigh the advantages of low pressure gas admission. The higher efficiency of the diesel cycle engine outweighs the added work for compressing the LNG to the higher gas injection pressure. Therefore the ME-GI is the market leading LNG-fueled engine type for large merchant marine vessel types, with the only exception of LNG carriers.

With regard to layout of the propulsion plant, a dual fuel diesel cycle engine implies no changes. Occasionally engines of a larger bore or with an additional cylinder must be applied when applying the otto cycle, due to the lower mean effective pressure (see p. 34).

Engine selection spiral for FP-propeller

Selecting the right engine for a ship is an important parameter for achieving the lowest possible fuel oil consumption and emissions or fulfilling whatever other priorities of the project.

This section will introduce an engine selection spiral describing the process of selecting an engine to be combined with a FP-propeller. Later a separate section will describe the process for a CP-propeller.

The steps in the engine selection spiral in Fig. 3.03 are:

1. Establish the calm water resistance, possible propeller diameter and propeller working conditions, Chapters 1 and 2
2. Calculate the light propeller curve giving the required power at the design speed
3. Establish the sea margin, engine margin, and the propeller “light running” margin for the project in order to specify the maximum continuous rating (SMCR)
4. Plot SMCR on engine *layout* diagrams for various possible engine types for example by using the online calculation tool CEAS
5. Based on the CEAS results, select the engine depending on the priorities of the project
6. Check for quick passage of the barred speed range (BSR)
7. Check the engine *load* diagram of the selected engine, taking into consideration a possible shaft generator/PTO and PTI if desired for the project
8. Check compliance with regulations such as EEDI and Minimum Propulsion Power (MPP), see Chapter 4

In the following sections all steps of the selection spiral will be considered except step 1, as determining the calm

water resistance and propeller working conditions constitutes Chapter 1 and 2 respectively.

Depending on the outcome of step 6, 7 and 8, it can be necessary to re-enter the selection spiral at either step 1, 3 or 5.

Examples on the use of the engine selection spiral are given in Chapter 5, including the important considerations on SO_x, NO_x, EEDI, and manoeuvring capabilities as described in Chapter 4.

2. Light propeller curve

In the initial project stage, estimations of the necessary propeller power and propeller rotational speed (for a direct

coupled two-stroke engine equal to engine speed), are based on theoretical calculations of the calm water resistance for the loaded ship and the propeller working conditions behind the hull.

Resistance calculations are typically validated, and the design is further optimised by experimental towing tank tests and computational fluid dynamics (CFD) simulations, ultimately giving the final propeller curve for the project.

The combination of propeller speed and power obtained on the light propeller curve at the ship’s design speed can be termed the propeller design point (PD), see Fig. 3.04.

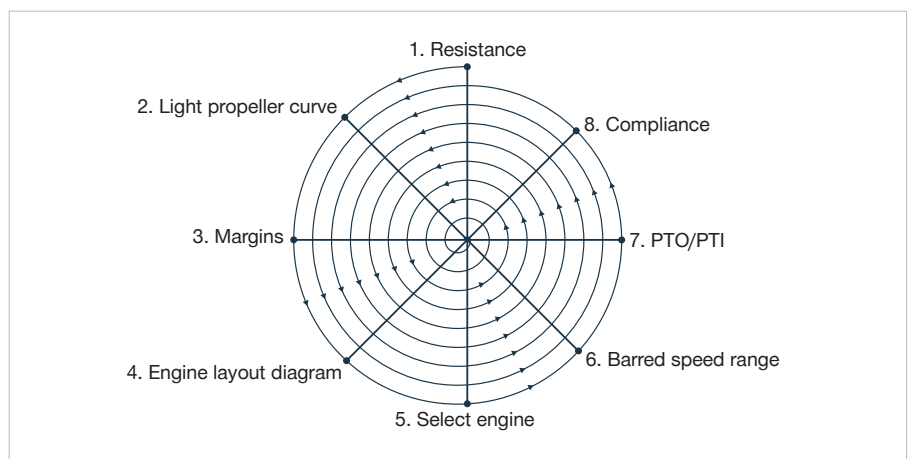


Fig. 3.03: FPP engine selection spiral

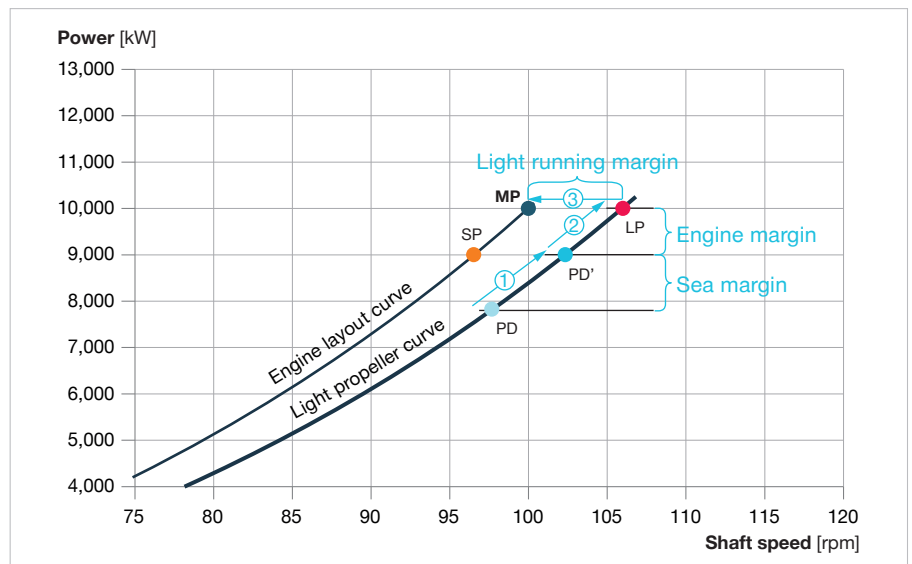


Fig. 3.04: Light propeller curve with added margins resulting in the engine layout curve

The influence of the combination of propeller diameter, ship speed and engine power is further exemplified in the later section “Constant ship speed curves”.

3. Propulsion margins, including light running margin

Traditionally, first a margin termed the sea margin followed by an engine margin have been added to the propeller design point (PD) along the light propeller curve. This is then shifted left with the light running margin to achieve the engine layout curve, see Fig. 3.04. These margins are explained in the following sections.

Sea margin

The sea margin (SM) is added to account for added resistance from expected average wind and waves as explained in Chapter 1, in order to make the ship capable of maintaining the design speed also in these average conditions.

A sensible sea margin must be established by the designer for the specific project, operational profile, and expected area of operation, typically in the range of 10 to 30%. Historically, 15% has been applied, and can be used as a first estimate.

It is important to note that often the propeller designer will design the propeller to the operating point including the sea margin, why the propulsion point including sea margin can also be termed the alternative propeller design point (PD’), see Fig. 3.04.

The location on the engine layout curve after having added the sea margin and the later light running margin is termed the service propulsion point (SP).

$$SMCR_{power} = PD_{power} \times \frac{100 + SM}{100} \times \frac{100}{100 - EM} \tag{EQ 33}$$

$$SMCR_{speed} = PD_{speed} \times \left(\frac{SMCR_{power}}{PD_{power}} \right)^{1/3} \times \left(1 - \frac{LRM}{100} \right) \tag{EQ 34}$$

Engine margin

Often, 100% utilisation of engine power is not desirable for normal operation due to the increased fuel consumption and a desire for a power reserve. Therefore, an engine margin is added. Historically, 10% has been applied, but the engine margin can typically vary between 10 to 30%, depending on the priorities of the project. A high engine margin (EM) is typically preferred for ships in scheduled traffic, in order for them to be able to catch up delays.

Today, the influence of IMO Minimum Propulsion Power Requirements (MPP), see Chapter 4, can also lead to higher than traditional engine margins in order to comply with these regulations, if compliance is attained through assessment level 1.

Light running margin (rpm margin)

In the ideal world, the light propeller curve on Fig. 3.04 with its added sea and engine margins would not require further considerations, and the weather, the hull, as well as the propeller would stay in a condition as on sea trial. This is not the case.

A fouled hull will add resistance and change the wake field as described in Chapter 2 section “Wake fraction coefficient”, reducing the speed of the arriv-

ing water and increasing the slip on the propeller, making it more heavy running, for a practical example on the development, see p. 50. Heavy seas will increase the resistance for a series of reasons as described in Chapter 1, section “Added resistance in various conditions”. As a rule of thumb, 20% increase in required power from added resistance corresponds to 1% heavy running, i.e. 1% lower speed for the same engine power.

There must be a margin in the layout of the propulsion plant to allow for this shift from the, light, propeller curve, n_L , towards a heavier curve, n_H when encountering increased resistance. This is termed the light running margin:

$$LRM = \frac{n_L - n_H}{n_H} \times 100\% \tag{EQ 35}$$

The propeller curve arising after having included the light running margin to the light propeller curve is termed the engine layout curve, as it will be decisive for the selection of the engine’s specified MCR (SMCR).

Fig. 3.05 illustrates the engine layout diagram including sea margin, engine margin, and light running margin, giving the engine layout curve with point MP which is the SMCR to be ordered.

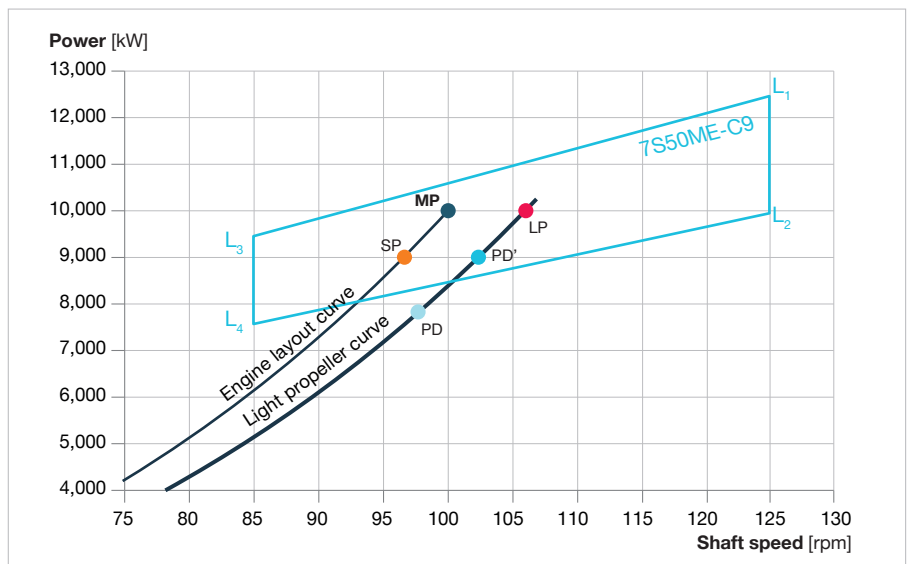


Fig. 3.05: Engine layout diagram with light propeller curve and engine layout curve

MAN Energy Solutions recommends a light running margin of 4 to 7%, depending on the specific ship and operational profile. In special cases up to 10%. High light running margins are relevant for ships where the expected relative increase in a ship's resistance from fouling, heavy weather, shallow water, ice, etc., is high and may also be relevant if a PTO is applied.

It is the responsibility of the ship designer to select an adequate propeller light running margin so that the desired operating points (power and speed) in all relevant conditions, will not fall inside a barred speed range (see step 6), nor outside the engine *load* diagram (see step 7). Furthermore, adequate light running margin is paramount for fulfilment of the IMO MPP requirements if compliance is attained through assessment level 2, see Chapter 4.

The desired light running margin (LRM) can be attained in several ways:

- If possible within the engine *layout* diagram (see Fig. 3.06 and step 4) the SMCR speed can be determined by shifting the speed at 100% power along the optimum light propeller curve by the LRM, see Fig. 3.04.
- If the above is not possible, the SMCR power can be increased in order to increase the margin from the optimum light propeller curve to the SMCR and hereby increase the LRM. With respect to the EEDI this may be unattractive.
- If neither of the above is possible, the LRM can be attained by a pitch reduction on the design propeller, to make it lighter running.

The recommended use of a relatively high light running margin for design of the propeller will, if attained by a pitch reduction, involve that a relatively higher propeller speed will be used for the layout design of the propeller. This, in turn, may involve a minor reduction of the propeller efficiency (see Fig. 2.09), and may possibly cause the propeller manufacturer to abstain from using a high light running margin.

However, this reduction of the propeller efficiency caused by the light running margin is actually relatively insignificant compared with the improved engine performance obtained when sailing in heavy weather and/or with fouled hull and propeller.

Even if attaining the light running margin by shifting the optimum light propeller curve by the LRM to determine the SMCR as per Fig. 3.04, this involves a compromise. The lower the speed of the SMCR, the higher will the mean effective pressure (mep) be, which implies that the engine is less mep derated, see the following section.

Determining the true optimum of the SMCR for the desired light running margin requires evaluation of the SMCR, with resulting mep-derating, along with the impact of a pitch adjustment on the propeller, i.e. a combination of the listed pathways. For ships attaining EEDI phase 3 compliance by a power reduction, see "EEDI and light running margin" in Chapter 4 for specific consideration on the LRM herefore.

If the light running of a specific operational point (P, n) is to be evaluated, this can be performed by considering the operational point relative to the SMCR point (P_{SMCR}, n_{SMCR}):

$$LR = \left(\frac{n}{n_{SMCR} \times \sqrt[3]{\frac{P}{P_{SMCR}}}} - 1 \right) \times 100\% \quad \text{EQ 35}$$

4. Engine layout diagram with SMCR, derating

Often more than one engine can deliver the SMCR calculated for the project. The location of the SMCR within the *layout* diagram for these engines will provide vital information as to which engine will be the most beneficial. The basic engine *layout* diagram is shown in Fig. 3.06. The engine can have its SMCR within the limits of L₁-L₂-L₃-L₄.

The lines L₁-L₂ and L₃-L₄ of the *layout* diagram limit the speed of the engine whereas the lines L₁-L₃ and L₂-L₄ are lines of maximum and minimum mep, respectively. Depending on engine type, the line L₂-L₄ will typically be 75 to 80% of maximum mep.

Mean effective pressure

The mean effective pressure (mep) is an important parameter for understanding the engine *layout* diagram. It is an expression for how much power (P_B) the engine delivers relative to the displacement volume of the engine (V_d) and rotational speed (n). For two-stroke engines it can be expressed as:

$$mep \propto \frac{P_B}{V_d \times n} \quad \text{EQ 36}$$

The mean effective pressure can be useful for comparing engines with a different bore, and indicate how hard an engine is loaded.

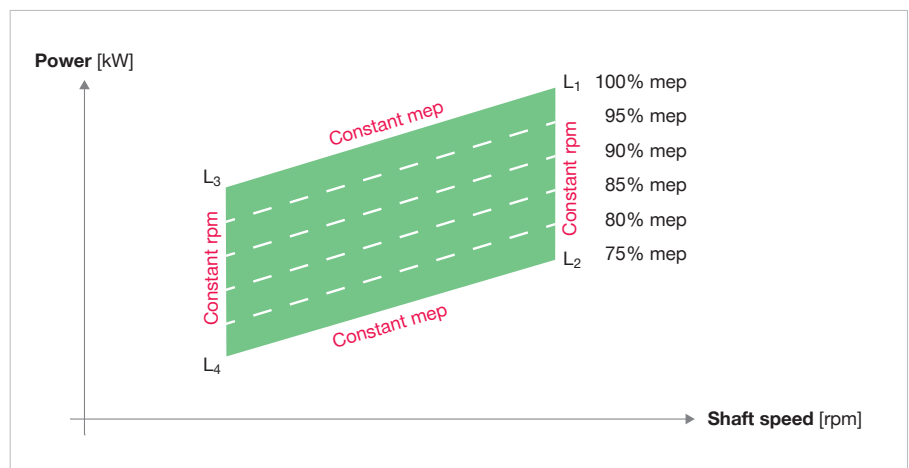


Fig. 3.06: Engine layout diagram with lines of constant mep and rpm

Maximum continuous rating

The maximum continuous rating (MCR) is the maximum power the engine can continuously deliver.

Nominal maximum continuous rating

The L₁ point designates the engine's nominal maximum continuous rating (NMCR) and is the maximum power the engine type can deliver (depending on the number of cylinders).

Specified maximum continuous rating

Within the layout diagram there are no restrictions to the location of the SMCR, point MP in Fig. 3.06.

The location of SMCR within the diagram will influence the fuel oil consumption of the engine as it influences the degree of derating.

Normal continuous rating

The normal continuous rating, S, is the power needed in service – including the specified sea margin and light running margin of the propeller – at which the engine is to operate. Point S is identical to the service propulsion point (SP) unless a main engine-driven shaft generator is installed, see step 7.

As the engine margin is not included in this figure, this point is sometimes also referred to as the continuous service rating.

Sometimes the normal continuous rating is defined without the light running margin, i.e. coinciding with point PD', the alternative propeller design point.

Engine mep-derating for reduced SFOC

A mep-derated engine, typically just termed derated, has its mep reduced relative to the maximum mep limited by the line L₁-L₃. A derated engine maintains its maximum cylinder pressure during combustion, but with an mep at SMCR, which is lower than the max. mep, fuel consumption is decreased.

It is important to note that derating is about reducing the mep, which is constant with lines parallel to L₁-L₃ and L₂-L₄. Moving the SMCR parallel with the lines L₁-L₃ and L₂-L₄ will therefore not bring any derating and associated reduction in fuel consumption.

Due to requirements of ship speed and possibly shaft generator power output, derating is often not achieved by reducing the SMCR power of an engine. Instead a larger engine is applied in order to be able to choose a lower mep rating with the same SMCR, for example an engine of the same type but with an extra cylinder, see Fig. 3.11.

Derating of an engine to a lower mep implies a series of physical changes to the engine. Shims are inserted under

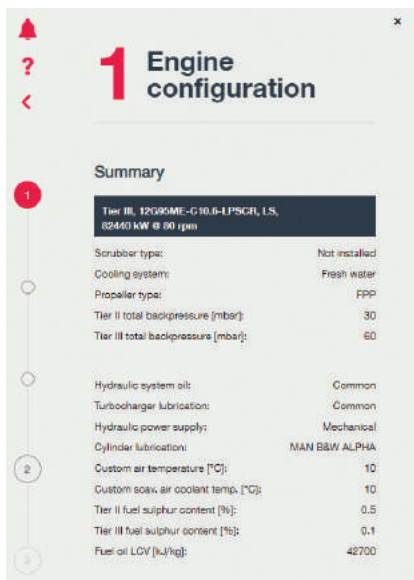
the piston to increase the compression ratio and, hence, the expansion ratio. The turbocharger is matched to the amount of exhaust gas generated. Fuel valve nozzles, cylinder liner cooling, lubrication, shafting system, as well as pump and cooler capacities are dimensioned for the SMCR.

Due to the mechanical changes implied by derating, an engine with an SMCR lower than the NMCR cannot operate at NMCR in service.

It can be an option to design the ship for a derated engine but with auxiliaries such as coolers, pumps and pipe dimensions, shafting etc., that are sufficient for a later uprating of the engine – provided that the EEDI regulations allow it. This is termed a dual rated engine. In such a case, and to avoid the more expensive in-ship testing of the engine, it is beneficial to perform the necessary testing to get the IMO technical file for the alternative SMCR, during shop testing of the engine before delivery.

CEAS

The online calculation tool CEAS, see Fig. 3.07, can be accessed from the MAN Energy Solutions website → Two-Stroke → CEAS Engine Calculations. CEAS can be used for plotting the calculated SMCR within the layout dia-



Engines

G95ME-C10.6	S95ME-C10.6
G95ME-C10.5	S95ME-C10.5
G90ME-C10.5	S90ME-C9.6
G80ME-C10.6	S90ME-C10.6
G80ME-C10.5	S80ME-C9.7
G70ME-C10.5	S90ME-C9.5
G70ME-C9.2	S49ME-C8.6
S70ME-C10.5	S49ME-C9.7
S95ME-C8.8	S40ME-C9.5
G60ME-C10.5	S95ME-C9.7

Cylinders

12	8
11	7
10	6
9	

Fig. 3.07: CEAS front page

gram of every engine design and cylinder number hereof present in the engine programme. Furthermore a range of options, including fuel type(s), emission reduction equipment, and possible turbocharger combinations, are displayed and can be selected.

An extensive report containing output about fuel consumption, capacity of auxiliary systems, etc. is generated. The tool is easy to use, efficient compared to manual calculations, and forms a superior basis for selecting the right engine.

5. Select engine

In Fig. 3.08 several *layout* diagrams of engines that include the example SMCR point are displayed. Different priorities of the project will result in different optimum engines.

The engine design capable of delivering the largest power at SMCR-speed can be derated the most, resulting in a reduced fuel consumption, but will typically also have the largest dimensions and highest initial cost.

Sometimes other parameters such as engine dimensions can have a greater priority than the fuel consumption. En-

gine length and width can be a challenge for smaller ships.

6. Passage of the barred speed range

As described in the section “Acceleration etc.” in Chapter 2, challenges may exist for passing the barred speed range (BSR) of the shaftline sufficiently quick to avoid shaft fatigue issues, especially for 5 and 6 cylinder engines. This situation, and the dynamic limiter function (DLF) dealing with it, is explained in the later section “Extensions to the standard engine load diagram for acceleration and encounters of adverse weather” and in detail in the separate paper “The dynamic limiter function”.

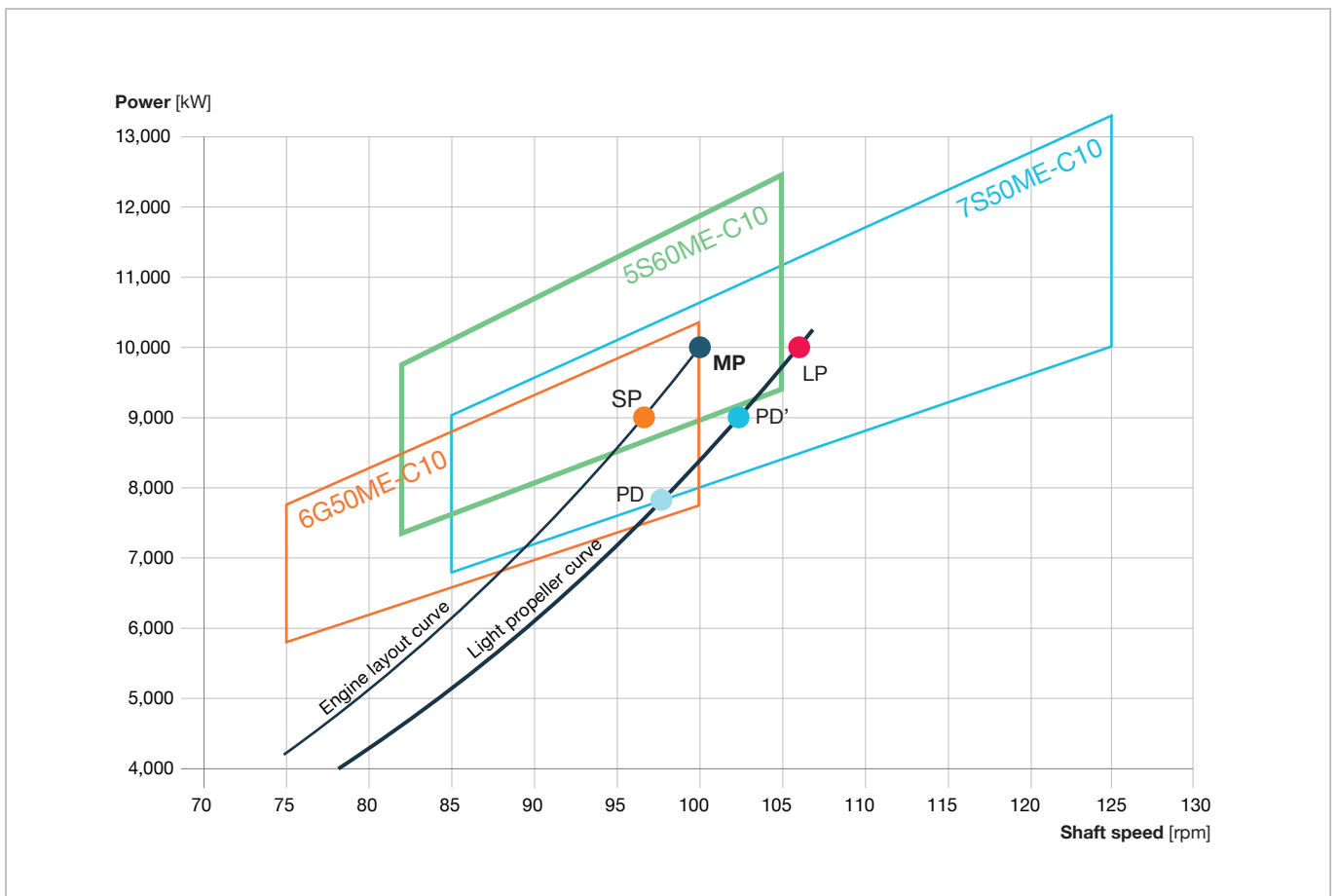


Fig. 3.08: Engine *layout* diagrams of selected possible engines, see the engine programme

The most basic guidance to avoid slow passing of the barred speed range is to avoid barred speed ranges that extend higher than to 60% engine rpm.

A more detailed approach is to ensure a BSR power margin, BSR_{PM} , of at least 10% in the design.

$$BSR_{PM} = \frac{P_L - P_P}{P_P} \times 100 \quad \text{EQ 37}$$

P_P is the power required by the bollard pull propeller curve at the upper end of the barred speed range, whereas P_L is

the engine power limit without DLF at the same rpm. As such, the BSR_{PM} expresses the excess engine power in the upper range of the barred speed range, and hereby the ship's capability to pass it. On Fig. 3.09 the BSR and BSR_{PM} is shown along with the engine layout diagram and the engine load diagram described in the subsequent step.

When accelerating, the propeller will be heavy running to various degrees, and the bollard pull curve, see Chapter 2, is used as a reference. Experience shows that the bollard pull curve will be between 15-20% heavy running rel-

ative to the light propeller curve, 17.5% is often used when better data is not available.

For a practical example on engine loading during acceleration of the ship, along with impact of any power or torque limitation, see the later section "Engine loading during acceleration and impact of power limitations".

7. Engine load diagram and considerations of PTO

The load diagram of the engine defines the power and speed limits of an actual engine built with a specified maximum continuous rating (SMCR) - point MP in

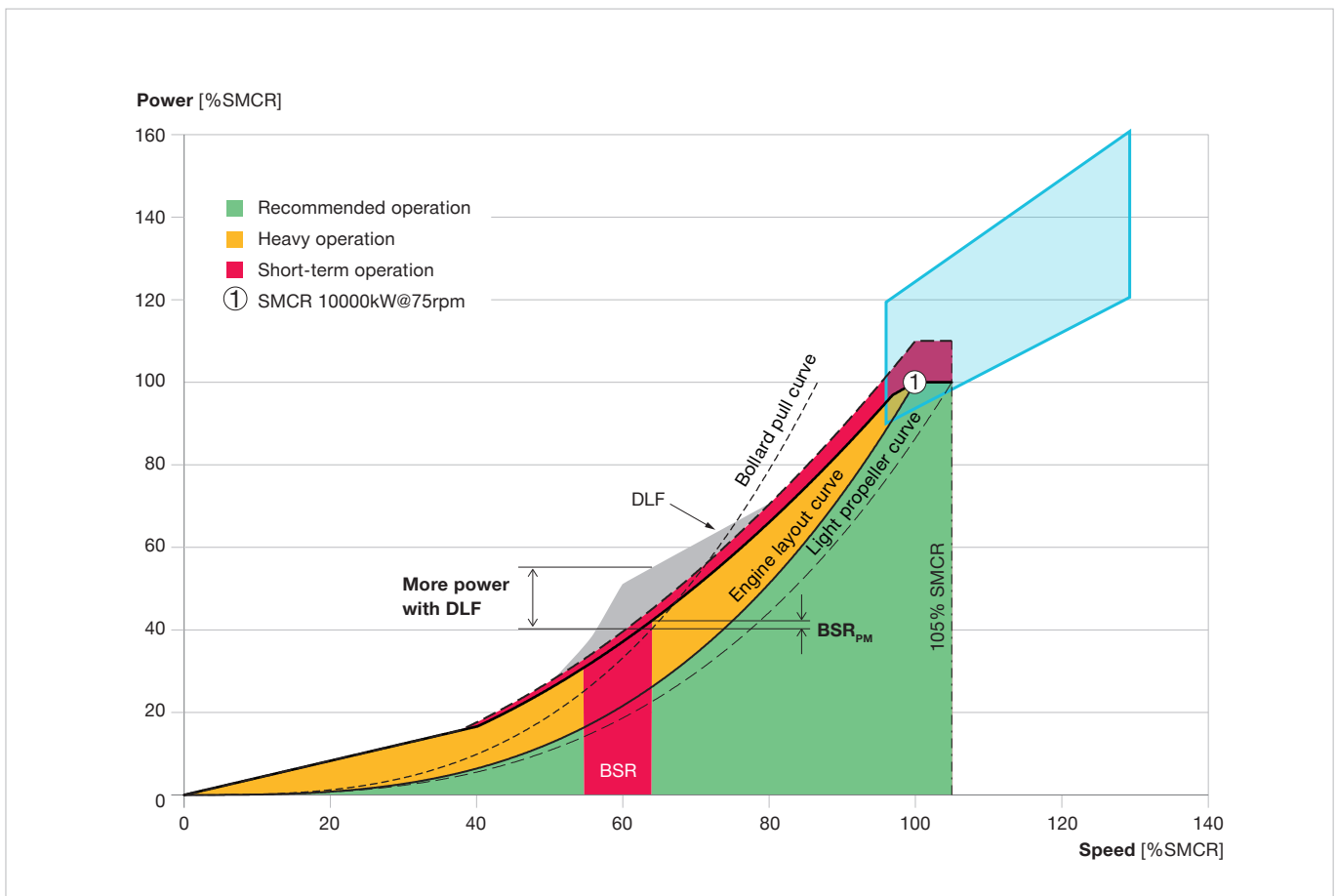


Fig. 3.09: An example of a BSR extending above 60% rpm and resulting small BSR_{PM} . In this example DLF was applied as a retrofit to reduce BSR passage time

the *layout* diagram - that conforms with the ship's power requirement.

The engine *load* diagram is important when investigating the possibility of installing a shaft generator/PTO. Additionally it provides the basis for underlining the necessity of the light running margin.

The standard engine *load* diagram is shown in Fig. 3.10, where different lines are numbered, setting the limits for operation of the engine. The location of the SMCR point within a *layout* diagram does not influence the appearance of the *load* diagram, see Fig. 3.11. Once the engine is constructed for its SMCR, it will not "know" of its *layout* diagram, only the *load* diagram resulting from the SMCR is decisive for the operational limitations of the engine.

Line 1: The engine layout curve, per definition moving through 100% SMCR speed and 100% SMCR power. This curve coincides with the "heavy propeller curve", line 2. An engine without PTO will typically operate to the right of this curve about 95% of the time.

Line 2: The heavy propeller curve is the light propeller curve (line 6) shifted with the light running margin to account for heavy weather and fouled hull.

Line 3: Maximum rpm for continuous operation. For engines with SMCR on the line L₁-L₂ in the *layout* diagram up to 105% of L₁-speed can be utilised.

If the SMCR is sufficiently speed derated, 110% of SMCR speed, but no more than 105% of L₁-speed, can be utilised, if permitted by the torsional vibration conditions.

For engines where 110% SMCR speed does not exceed 105% of L₁-speed, it is possible to choose an rpm extended *load* diagram. The engine and shafting can, considering the torsional vibration conditions, be constructed to run up to 105% of L₁-speed, see the separate section "Rpm extended engine *load* diagram" explaining this concept in further detail. A limit to this application is that, typically, class rules do not allow

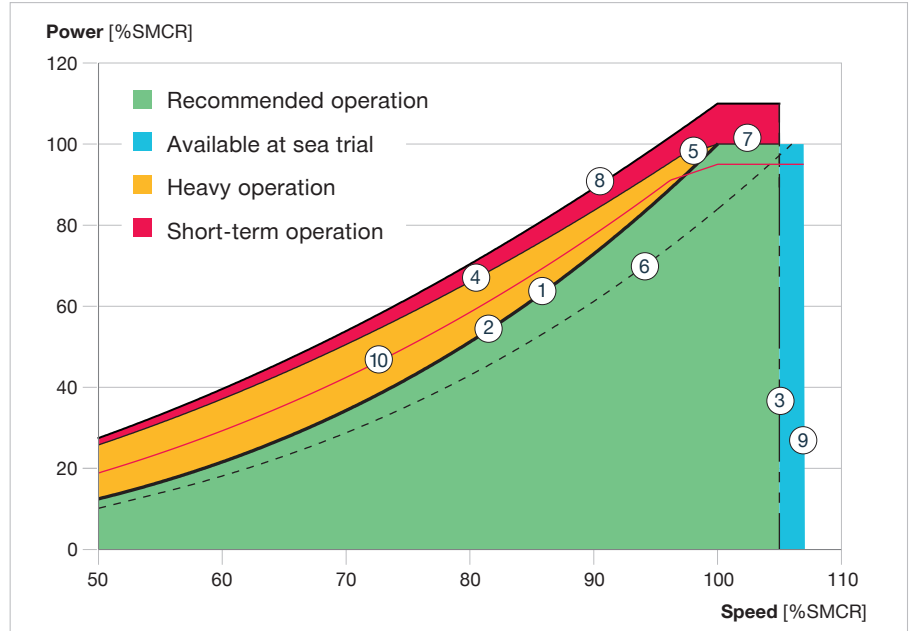


Fig. 3.10: Standard engine *load* diagram with marked lines

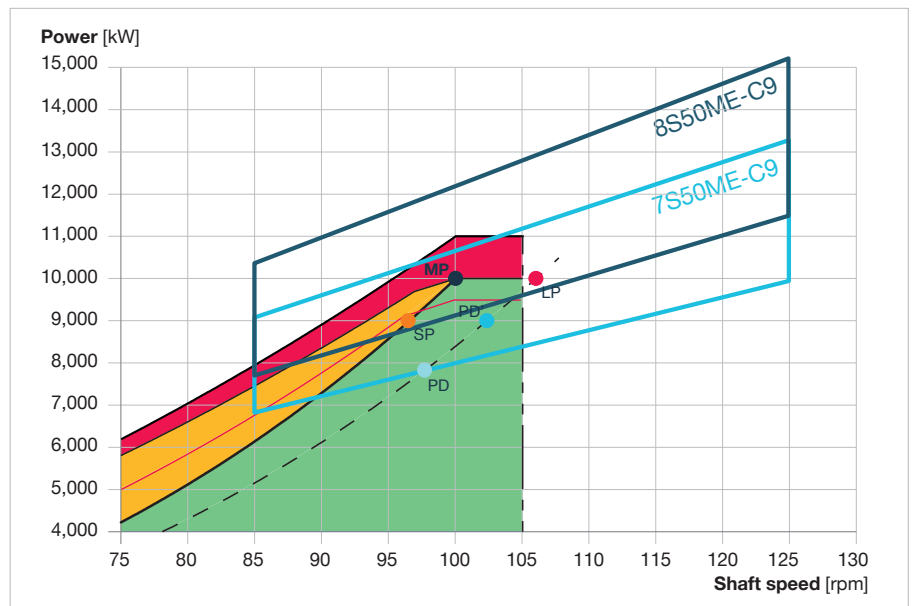


Fig 3.11: Engine *load* diagram, with different *layout* diagrams, note that the appearance of the *load* diagram is independent of the position of point MP within a *layout* diagram

an engine to run faster than 115% of the SMCR speed.

Line 4: Is the torque/speed limit of the engine, limited mainly by the thermal and bearing loads on the engine, preventing the engine from developing 100% torque when active.

Line 5: Represents the maximum mean effective pressure (mep) level acceptable for continuous operation, corre-

sponding to 100% torque. Note that this is only a limit at high loads and speeds. At lower speeds, line 4 is a stricter limit.

Line 6: The light propeller curve, for clean hull and calm weather. Often used for propeller layout. The speed margin (in percent) between the engine layout curve and the light propeller curve at 100% power is the light running margin, see step 3.

Line 7: Represents the maximum power for continuous operation. Note that when increasing rotational speed towards lines 3 and 9, the maximum power for continuous operation cannot exceed 100%.

Line 8: Represents the overload operation limit of the engine. Overload running is possible only for limited periods, 1 hour per 12 hours or when required in an emergency situation, as the resulting thermal load on the engine is high.

Line 9: Maximum acceptable engine rpm at trial conditions. 110% of SMCR speed, but no more than 107% of L₁-speed if permitted by the torsional vibrations.

Line 10: PTO_{layout limit}. This curve describes the maximum combined power required by the light propeller curve and PTO at a given rotational speed if a shaft generator/PTO is installed. This layout limit ensures some operational margin to line 4, see the subsequent section “Shaft generator/PTO”.

Recommendation for operation

The green area between lines 1, 3 and 7 is available for continuous operation without limitation.

The yellow area between lines 1, 4 and 5 is available for operation in shallow waters, in heavy weather, and during acceleration, i.e. for non-steady operation without any strict time limitation, as well as for PTO operation.

The red area between lines 4, 5, 7 and 8 is available for overload operation for 1 out of every 12 hours or when required in an emergency situation.

Limits for low-load running exist. An electronically controlled ME engine can operate down to around 15-20% of L₁-speed. A mechanically controlled MC engine can operate down to 20-25% of L₁-speed. The exact minimum speed for the specific plant is determined at sea trial. Continuous operation below 5% to 10% of engine load is not recommended, depending on engine type and operational profile.

Shaft generator/power take-off (PTO)

With the SMCR and knowledge about the load diagram, it is possible to calculate the maximum power take-off possible within the limits of the engine.

The maximum power demanded by the light propeller curve and PTO combined should not exceed a limit governed by the following equations. This set of equations determines line 10 on Fig. 3.10:

The maximum design PTO power at a given rotational speed is then found as the vertical difference between line 6, the light propeller curve, and line 10, the PTO_{layout limit} as marked in Fig. 3.10.

For reasons of governor/rpm stability, see the later separate section, the minimum speed permitted for PTO operation is 50% of the SMCR speed, whereas the maximum operating speed depends on the specific PTO plant.

If the full SMCR power is used for propulsion, the PTO naturally cannot take out any power.

Designing the power of the PTO not for the torque/speed limit (line 4) and mep limit (line 5) but instead the PTO_{layout limit} will ensure that the PTO can be operated also in conditions not as ideal, as ideal sea trial condition.

In case of fouling and/or heavy weather, the propeller curve will shift left towards the engine layout curve, exploiting the light running margin. With increased heavy running, the electric power taken out at the PTO must gradually be decreased (and taken over by the auxiliary engines) in order not to push the operational point outside the engine limits. An interface between the

onboard power management system (PMS) and engine control system (ECS) is available, informing the available PTO power to the PMS, see the Project Guide for further information.

In severe cases, fouling and sea conditions alone are enough to shift the propeller curve to line 4, see “Light running margin”. In such cases, the PTO cannot be utilised without overloading the engine and the auxiliary engines must deliver all the electric energy. The PTO can take up load again when weather conditions have improved.

Considering EEDI, see Chapter 4, a PTO can be an attractive solution as the EEDI reference speed is calculated at 75% engine load in trial condition, where there is a good margin for PTO power under the PTO_{layout limit}.

Governor/rpm stability with PTO

Traditionally, complicated gearing have for ships with FP propellers ensured a constant electric frequency from the PTO within a (narrow) range of varying engine speed. Gearing has to a wide extend been replaced by frequency converter, as power electronics have dropped significantly in price over recent decades.

For PTO plants connected to the onboard electric grid via a frequency converter, it is important to consider its impact towards governor stability.

When the generator is connected to the grid via a frequency converter, the mechanical torque from the generator required to maintain constant electric power is inversely proportional to the engine speed. I.e. if the engine speed is increased, the torque required to deliver the same power is reduced.

PTO layout limit	
RPM [% SMCR]	PTO_{layout limit} [% SMCR]
50 – 96.4	$100 \times (\text{rel. rpm} [\%] / 100\%)^{2.4}$
96.4 – 100	$95 \times (\text{rel. rpm} [\%] / 100\%)$
>100	95

Table 3.01: Equations for establishing the PTO layout limit.

This inverse proportionality destabilises the engine speed: If the electric power output needs to increase, the torque required from the PTO increases. The engine must respond to this increase in torque, and if the torque increase required is so big that the engine cannot increase the torque output instantaneously, the engine speed will reduce. This will result in a further increase of torque on the PTO in order to deliver the desired electric power, which may destabilise the engine speed further. Vice-versa if the electric power output reduces.

Similar behavior will be experienced, if the ship encounters a wave large enough to reduce the speed through water, reducing the propeller and shaft speed before the fuel index (amount) is increased. The increased torque on the PTO required to maintain constant electric power at a lower speed will amplify such a speed drop.

The control of the engine speed of a two-stroke low speed marine engine is relatively slow by nature, because of the relatively low firing frequency. This can make it difficult for the ECS system to maintain a constant engine speed if the generator power is large compared to the power required for propulsion.

For further information on the layout and integration of a PTO in the propulsion plant, please see the separate paper “Shaft generators for low speed main engines“, including examples. For further information on criteria for evaluating governor stability, please consult the Project Guide.

Considerations of shaft motor/PTI

For some trades it may be attractive to use a shaft motor, also termed a power take-in (PTI). In such cases, electric power from the gensets, waste heat recovery or other electric power sources are used to boost the propulsion of the ship.

When using PTI, the engine will typically deliver 100% power, but the propeller, and thus also the engine, will run at increased speed, along the propeller curve, due to the extra power delivered to the shaft by the PTI. For such type of operation, it can be necessary to consider an engine with an rpm-extended load diagram, see the later section.

8. Compliance with regulations

The selected engine’s compliance with the environmental legislation described in Chapter 4 must be considered. Considerations on NO_x reduction measures to fulfil IMO Tier III in ECA zones does not directly influence the attained EEDI, as this is calculated for Tier II only.

Having ensured that the ship complies with SO_x and NO_x legislation as well as EEDI, the ship’s capability to manoeuvre safely in all relevant conditions must be considered. This is termed minimum propulsion power (MPP) and is described in Chapter 4.

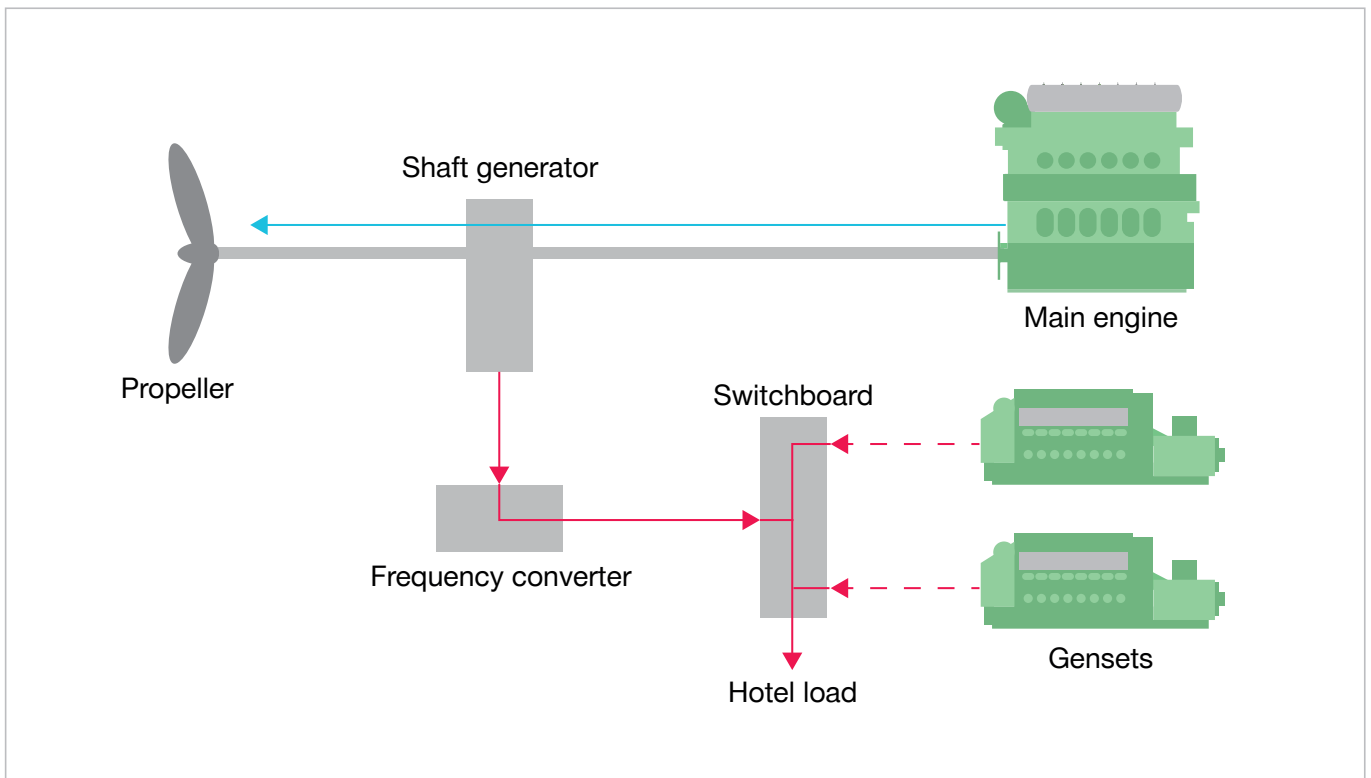


Fig. 3.12: Schematic view of the propulsion system with the shaft generator in PTO mode. The blue arrow represents the energy flow from the ME, and the red solid arrow represents the energy flow from the PTO. The dashed red arrows represent the energy flow from the gensets, when these operate in parallel, or when the ship operates at low speed without the PTO engaged.

Engine selection spiral for CP-propeller

This section will shortly elaborate on the engine selection spiral for a CPP plant, referring to and explaining the difference to the FPP engine selection spiral.

The steps in the CPP engine selection spiral in Fig. 3.13 can be written as:

1. Establish calm water resistance, propeller diameter and working conditions, see Chapters 1 and 2
2. Calculate the possible CP-propeller operation and the required power
3. Consider the operating principles of the CP-propeller for inclusion of possible PTO
4. Establish the sea margin, engine margin, and the speed / "light running" margin for the project" in order to specify the maximum continuous rating (SMCR)
5. Plot the SMCR on the engine layout diagrams for various possible engine types (use CEAS)
6. Based on the CEAS results, select an engine depending on the priorities of the project
7. The engine *load* diagram of the selected engine, considerations about shaft generator/PTO and PTI if desired for the project
8. Check compliance with regulations, EEDI and Minimum Propulsion Power (MPP), see Chapter 4

Depending on the outcome of considerations on a possible shaft generator in step 7 and regulations in step 8, it can be necessary to re-enter the design spiral at either step 1, 3, 4 or 6.

2. Possible propeller operation for CPP and required power

There are three options when operating a ship with a CP-propeller:

- Constant engine speed
- Follow a fixed combinator curve
- Control pitch and speed individually (typically based on some combinator curve)

The required power at the design speed will be practically the same, independent of the operational method,

but the required power at lower speeds will differ between the options.

Constant engine speed is only of interest if a PTO is to be included, as a frequency converter can be omitted if the PTO is matched to deliver the required frequency at the constant speed, see step 3. Constant speed operation eliminates the need for considerations of two important principles from the FPP selection spiral: light running margin and passage of the barred speed range.

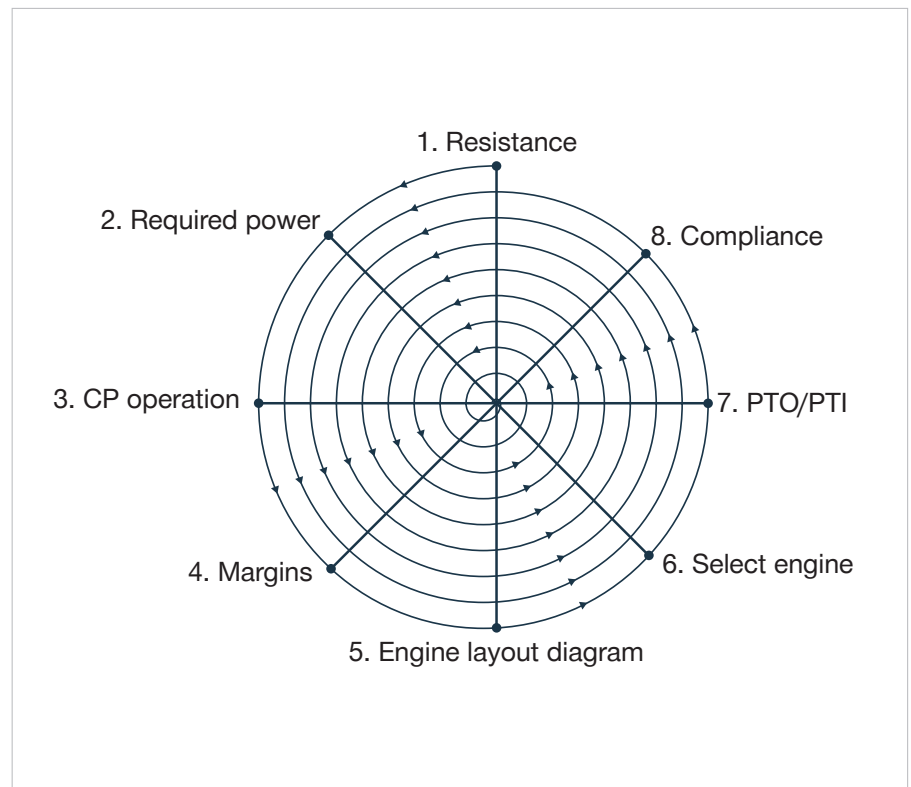


Fig. 3.13: CPP engine selection spiral

Operating on a fixed combinator curve means to follow a fixed set of pitch settings varying with the speed, generating the combinator curve. The fixed combinator curve is designed to take into account the cavitation patterns of the propeller, the operational profile of the ship, and to some extent the engine limits, see Fig. 3.14.

Operation along a fixed combinator curve would require considerations similar to a light running margin, see “Light running margin”, as the fixed combinator curve, similar to a fixed pitch propeller curve, will be heavy running during encounters of added resistance. Furthermore, sufficiently quick passage of the barred speed range, see step 6 in the FPP selection spiral, must be considered. Often considerations on the BSR are resolved by setting the idling speed of the shafting above the BSR, see Fig. 3.14.

The third option, to control the pitch and engine speed individually (typically based on some combinator curve) is, in principle, equivalent to fitting a variable gearbox between engine and propeller. Controlling the pitch allows for quick acceleration of the engine and shaft line, and therefore the barred speed range passage is not a

problem. Additionally, the engine can be loaded at any point within the engine *load* diagram, eliminating the need for a built-in light running margin.

Data on the specific fuel oil consumption of an engine along a combinator curve can be requested from MAN Energy Solutions by writing to Marine-ProjectEngineering2S@man-es.com.

3. CPP operating principles for inclusion of PTO

The advantage of operating at constant engine speed is that it allows for easy inclusion of a synchronous PTO.

The disadvantage of operating at constant engine speed is that, at low ship speeds, the frictional losses on the propeller and in the engine will be relatively higher than if a combinator curve were followed.

Even though the efficiency is low at low loads, so is the energy consumption, which results in a small penalty on the overall fuel consumption, therefore, constant speed can still be an option if a very simple system is desired.

It is of special interest that following a combinator curve, or controlling the

pitch and speed individually, means that the relative frictional losses are not increased at lower ship speeds. With the greatly reduced costs of frequency converters that can ensure constant frequency from electric generators at fluctuating speed, the previous disadvantage of operating along a combinator curve with a PTO, has been reduced.

4. Propulsion margins for CPP

The magnitude of the sea and engine margins is not changed for projects with CP-propellers. The light running margin (LRM) can still be necessary for CP-propellers, all depending on the capabilities of the propeller control system.

Traditionally, the combinator curve, as illustrated in Fig. 3.14, has been calculated and set for the propeller. This means that for a given propeller speed, the combinator curve has a given propeller pitch.

Operating along a fixed combinator curve, like for a fixed pitch propeller, the propeller may be heavy running in heavy weather, requiring a light running margin. See the FPP selection spiral.

The development within fixed combinator curves has been to calculate different combinator curves from which the crew can choose, depending on the degree of fouling and sea conditions. This reduces the need for a light running margin, but attention to the consequences of continuous heavy running is required from the crew, why including an LRM in the combinator curve(s) for free sailing still is recommended.

Some modern CP-propeller control systems allow for continuous adaptation of the propeller pitch, exploiting that in fact installing a CP-propeller is equivalent to having free gearing between the engine and the propeller. Inclusion of a light running margin can be avoided if automatic continuous pitch adaptation is applied, as the pitch can be decreased when the propeller shifts towards a heavier curve.

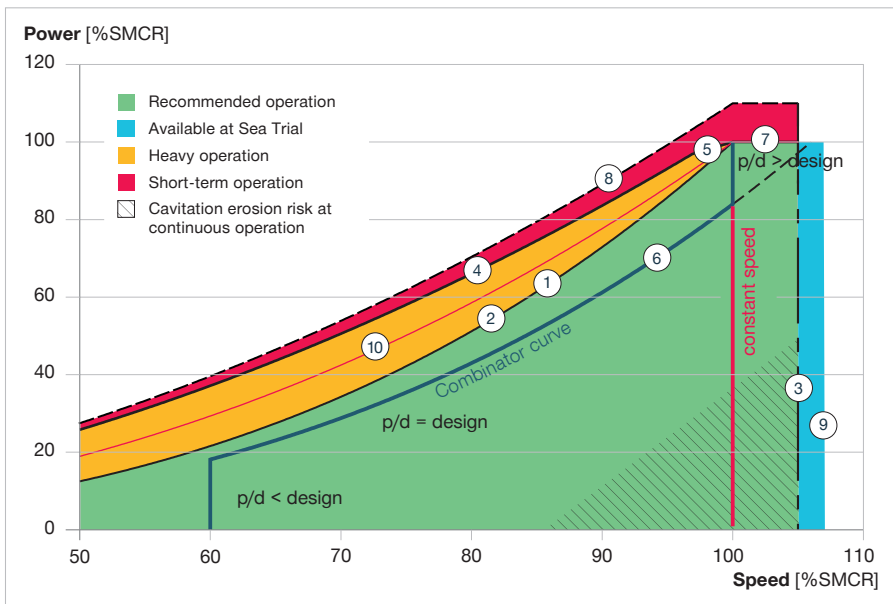


Fig. 3.14: Combinator curve with engine *load* diagram, see Ref. [3.3]. The constant speed curve can also be referred to as the generator curve

Control systems that continuously adapt the pitch will be able to load the engine at all points within the engine *load* diagram, and as such the engine can in principle deliver maximum power in any weather and fouling condition. However, margins towards the limits for continuous operation of the engine are recommended to be included in the propeller load controller.

The ship designer is advised to investigate the options offered by different propeller manufacturers with regard to the capabilities of the control of the CP-propeller.

5. Engine layout diagram with SMCR for CPP

The propeller type does not affect the *layout* diagram of the engine.

6. Select engine for CPP

The application of a CP-propeller does not imply any changes with regard to the selection of engine. The optimum choice with regard to derating, installation height, first cost, etc. will be similar to the situation for a FP-propeller.

7. Engine load diagram for CPP and considerations of PTO power

The engine *load* diagram is unaffected by the combination with a CP-propeller. Instead, the position of the operational point of the engine within the *load* diagram is in principle, depending on the capabilities of the propeller control system, set free.

When running at maximum rpm with zero pitch, the power required to turn the propeller is approx. 15-20% of SMCR.

Shaft generator/PTO and PTI

As described previously, more options for operating a shaft generator with a CP-propeller exist: Constant engine speed or (as with an FP-propeller) varying engine speed a frequency converter ensure constant frequency. The same considerations apply to inclusion of a PTI.

For CPP plants with a PTO connected to the onboard electric grid via a frequency converter, special attention must be given to governor stability as described in the FPP selection spiral:

As the pitch of a CP-propeller is reduced, so is the inertia of the propeller in water, as well as the damping provided by having to accelerate the mass of the ship itself to increase the water flow across the propeller. I.e. when the propeller is pitched out, only the shafting and not the ship itself is accelerated in response to any a torque increase on the engine.

These considerations are especially important in order to avoid overspeed, if ship maneuvering with a CPP plant is intended to be performed in constant speed mode with low propeller pitch and high PTO load, e.g. for driving thrusters. Therefore, governor stability

criteria for CPP plants are stricter than for FPP plants, for further information consult the Project Guide.

When considering the $PTO_{\text{layout limit}}$, line 10 on the engine *load* diagram in Fig. 3.14, it is evident that the most PTO power is available at relative high engine speeds. Here, the distance between the light propeller curve/combination curve and the $PTO_{\text{layout limit}}$ is largest.

CP-propellers can therefore be of interest if the electricity demand on the ship is high and the operational profile involves large variations in ship speed. If the engine speed is independent of the ship speed (by varying the pitch), then the engine speed can be kept high during low ship speeds, and thereby ensure a constant availability of full PTO power. This can typically be of interest for ships with many reefer units in and/or in scheduled liner traffic, e.g. feeders carrying fresh fruit from the Americas.

In such cases the increased efficiency of the main engine for generating electric power compared to the auxiliary engines will result in savings. Typically, these savings will be larger than the small losses implied by the slightly lower efficiency of the CP-propeller compared to an FP-propeller.

8. Compliance with regulations

Considerations on NO_x and SO_x eliminating measures do not change with the selection of a CP-propeller, and neither does the EEDI requirements.

As previously briefly discussed, CP-propellers can be an attractive solution for ship designs that have difficulties towards fulfilling the requirements for minimum propulsion power:

If the CP-propeller control system can control pitch and propeller speed individually, the engine will be capable of delivering its maximum power even at reduced ships speeds. However, it must be borne in mind that the propeller efficiency in such a condition reduce compared to optimum, see Chapter 4.

Engine tuning

This and the following sections are intended to provide further detail on some of the engine related parameters shortly described in the process of working through the engine selection spirals.

Engine tuning applies to an engine with a specified MCR – derated or not. As of 2023 three options exist for tuning a regular ME engine for Tier II:

- High-load tuning
- Part-load tuning
- Low-load tuning

Tier III engines do not offer the option for load tuning, neither in tier II or tier II mode, as the parameters controlling the combustion process are already fixed in order to meet both Tier II and Tier III demands.

The tuning of Tier II engines decides the shape of the SFOC curve as a function of engine load. High-load tuning has the lowest SFOC in the high-load range and low-load tuning has the lowest SFOC in the low-load range. Choice of tuning depends on the expectations for the operational profile of the ship. For a ship sailing a fixed schedule in a certain geographical area it is often possible to predict the required engine power quite accurately, allowing just

the adequate selection of engine SMCR power. In such a case, a high-load tuning is often a good choice. For a ship engaged in tramp trade, such as many bulk carriers, the engine load can differ greatly between voyages, and low-load tuning is then sometimes selected.

Rpm extended load diagram

For speed derated engines with an SMCR speed sufficiently below L₁-speed, the speed limits of the engine can be designed to extend beyond the normal maximum limit of 110% of the SMCR speed, but not more than 105% of engine speed at L₁ during normal operation (107% during sea trial). This can, as a result of the high light running margin allowed hereby, be of special interest especially to ships often operating in conditions implying increased resistance such as:

- ships sailing in areas with very heavy weather
- ships operating in ice
- ships with two fixed pitch propellers/ two main engines, where one propeller/one engine is blocked/declutched for some reason. Measurements

show an approximate 8-10% heavy running of the remaining propeller in operation for a twin-skeg ship.

This possibility for speed derated engines is described in the rpm extended load diagram in Fig. 3.15. Here, the engine layout diagram is plotted as well, showing the speed limits of the engine design.

In Fig. 3.15 it is seen that for a heavily speed derated engine with an SMCR at point MP, the rpm extended load diagram permits a substantial increase to the possible light running margin, in the extreme case depicted up to 23%.

Considering that the bollard pull propeller curve is rarely more than 15-20% heavy running, a light running margin higher than this will not bring any benefit. In addition, class rules typically does not allow an engine to run faster than 115% or 120% of SMCR-speed.

The speed limit can only be extended if the torsional vibration conditions permit this. Thus, the shafting, with regard to torsional vibrations, has to be approved by the classification society in question.

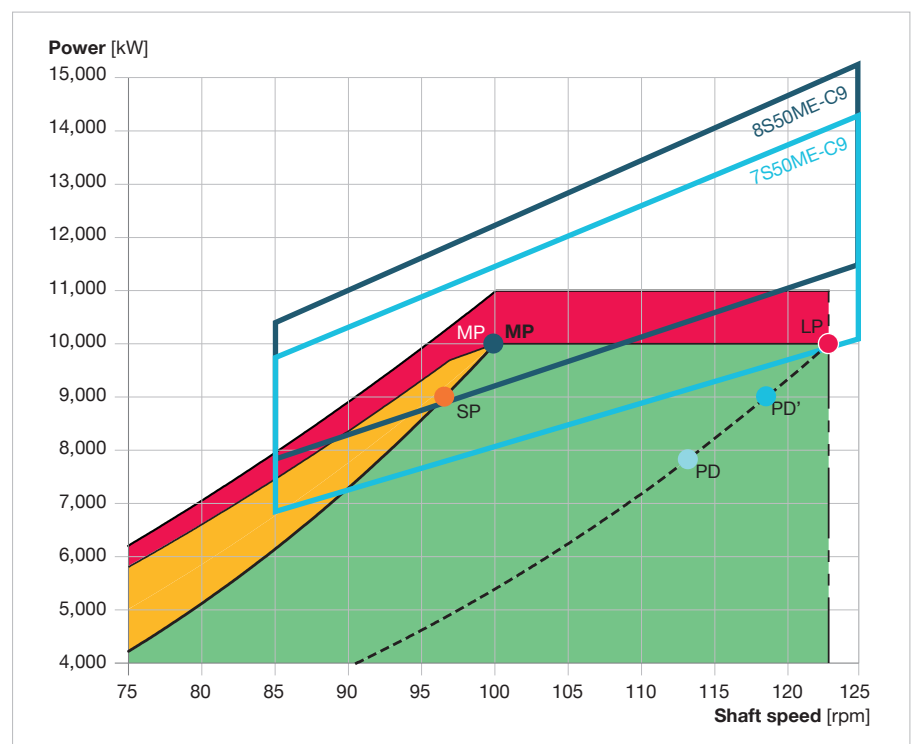


Fig. 3.15: Rpm extended load diagram, for an extreme case

Constant ship speed curves

As earlier described in Chapter 2, the larger the propeller diameter, the higher the propeller efficiency and the lower the optimum propeller speed. There is therefore a drive to optimise the aft-body and hull lines of the ship to accommodate the largest propeller diameter possible.

The constant ship speed curve, α , shown in Fig. 3.16 indicates the power required at various propeller diameters and, thereby, propeller speeds to keep the same ship speed, if at any given speed the optimum pitch diameter ratio is used, taking into consideration the total propulsion efficiency.

Normally, for a given ship with the same number of propeller blades but different propeller diameter, the following relation between necessary power

and propeller speed can be assumed:

$$P_2 = P_1 \times \left(\frac{n_2}{n_1}\right)^\alpha \quad \text{EQ 38}$$

where:

P = propulsion power
 n = propeller speed, and
 α = the constant ship speed coefficient.

For any combination of power and shaft speed, each point on the constant ship speed curve returns the same ship speed.

When such a constant ship speed line is drawn into the engine layout diagram through a specified MCR point 'M1', selected in the layout diagram, another specified propulsion MCR point 'M2' upon this line can be chosen to give the ship the same speed for the new combination of engine power and rpm.

Provided the optimum pitch/diameter ratio is used for a given propeller diam-

eter, the following data applies when changing the propeller diameter:

For general cargo, bulk carriers and tankers: $\alpha = 0.20 - 0.30$

Container and ro-ro: $\alpha = 0.15 - 0.25$

Fig. 3.16 shows an example of the required power speed point M1, through which a constant ship speed curve $\alpha = 0.28$ is drawn. Hereby point M2 with a lower engine power and a lower engine speed is achieved at the same ship speed.

Thus, for a handymax tanker, if the propeller diameter is increased, and going for example from the SMCR-speed of $n_{M1} = 125$ rpm to $n_{M2} = 100$ rpm, the required power will be $P_{M2} = (100/125)^{0.28} \times P_{M1} = 0.935 \times P_{M1}$, i.e. providing a power reduction of about 6.5%.

When changing the propeller speed by changing the pitch diameter ratio, the α constant will change.

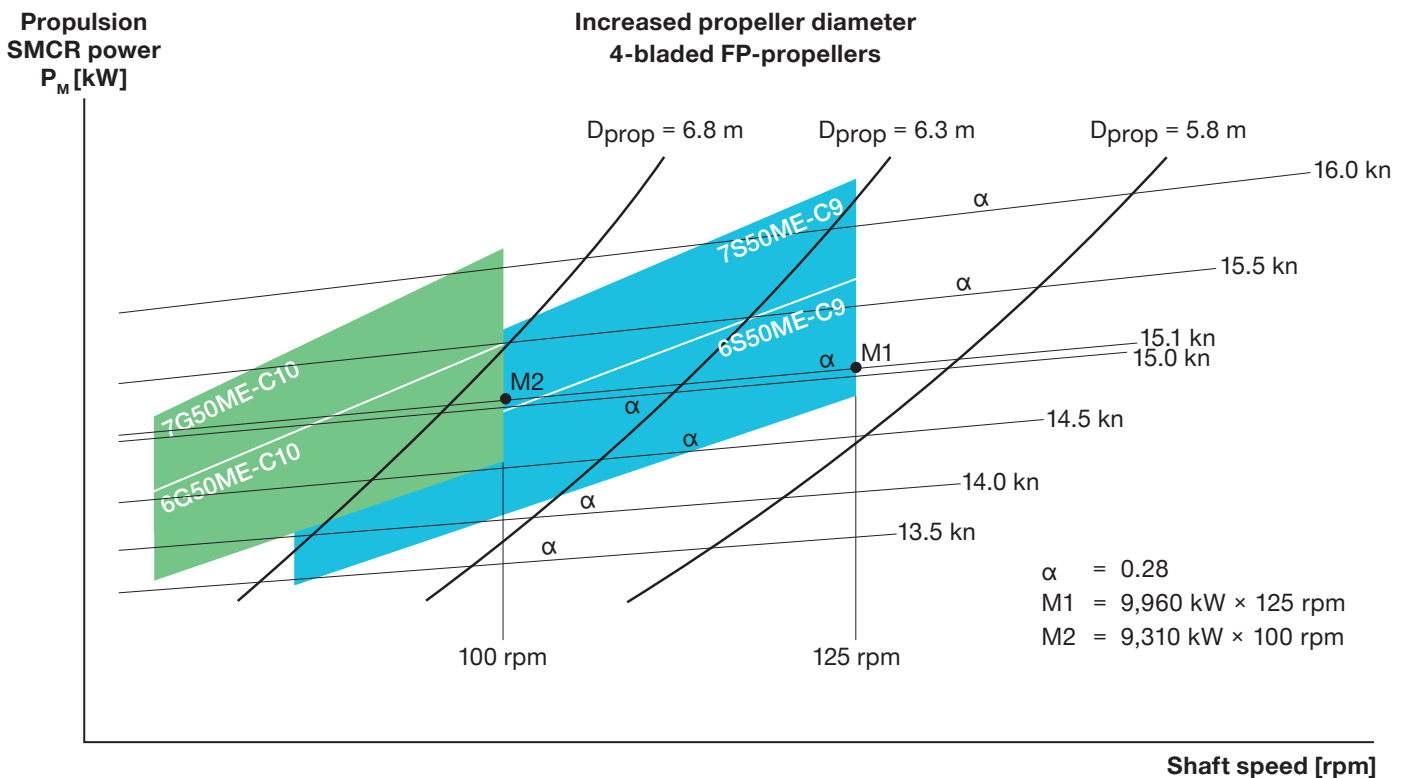


Fig. 3.16: Example of constant ship speed curves with selected engine layout diagrams

Engine loading during acceleration

In the section “Acceleration, barred speed range, manoeuvring speed and propeller rotation” in Chapter 2, the bollard pull curve and considerations of the passage of a barred speed range is introduced from a propeller perspective. Having introduced the engine load diagram in the previous section “Engine load diagram & considerations of PTO” of the present chapter, it is of interest to consider the engine loading during acceleration, illustrated in the engine load diagram.

Acceleration from standstill

On a FPP plant, imagine a scenario of acceleration from standstill, as depicted on Fig. 3.17. As the engine is started, initially with the starting air, the shaft and engine will in the beginning accelerate fast along the bollard pull propeller (BP) curve, e.g. the propeller curve for an advance number of zero / zero speed through water, see Fig. 2.08.

A. As the ship itself gains speed, the propeller curve will become slightly lighter, i.e. require less torque, than the BP curve: As the speed of water arriving at the propeller increases with the speed of the ship, the advance number increases, which reduces the torque required on the shaft, see Fig. 2.08.

B. At some point the BP curve (or due to the above mentioned phenomenon a propeller curve running almost as heavy as the BP curve) encounters the torque limit of the engine. At this point, the engine can no longer deliver the torque required to follow the heavy propeller curve. From this point the engine speed will increase at a slower rate, corresponding to the increase of ship speed and hereby increase of advance number with its resulting decrease of the torque required by the propeller.

C. The engine will accelerate along the torque limit until the desired engine speed is reached.

D. Hereafter the fuel index (fuel amount relative to maximum) decreases at constant engine speed until steady state sailing is reached, i.e. the ship speed corresponding to the set engine speed on the light propeller curve, is reached.

The light running margin previously described affects the margin from the light propeller curve towards the engine load limits and thereby the ability for fast acceleration.

For a CPP plant following a fixed combinator curve similar behaviour as for the FPP example will be observed. I.e.

if the propeller pitch is not reduced, the rate of acceleration will upon encounter of the engine load limitations reduce. The propeller load controller often applies pitch reduction upon encounter of the engine load limitations, in order to increase the engine speed (and hereby available power) at a faster rate than if accelerating the ship itself along the engine load limitations as for an FP propeller.

For a CPP plant following a generator curve, the load controller will gradually increase the propeller pitch, in order to increase the engine load at constant speed, see Fig. 3.14.

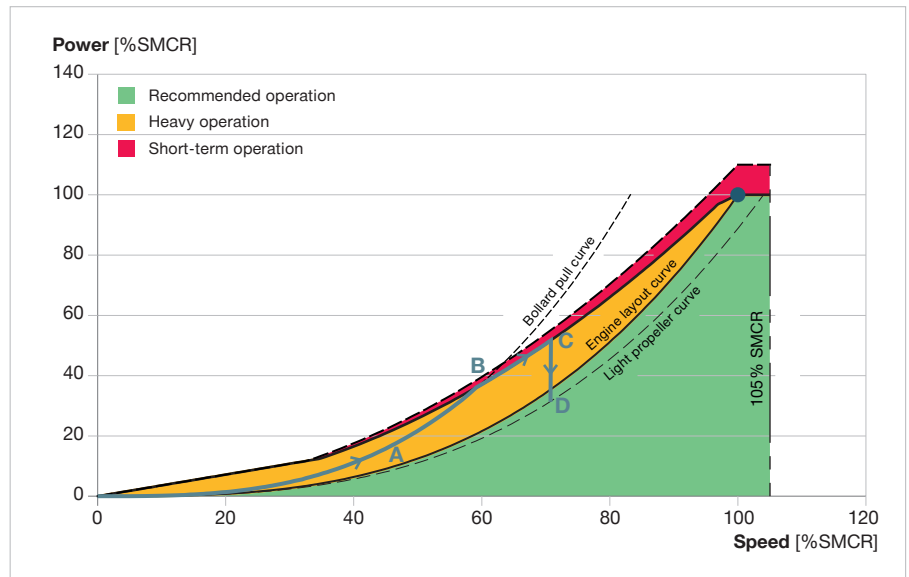


Fig. 3.17a: Engine loading in the engine load diagram from acceleration with an FPP plant from standstill, A-B-C-D (top), and from acceleration initiated while sailing, 1-2-3-4 (lower).

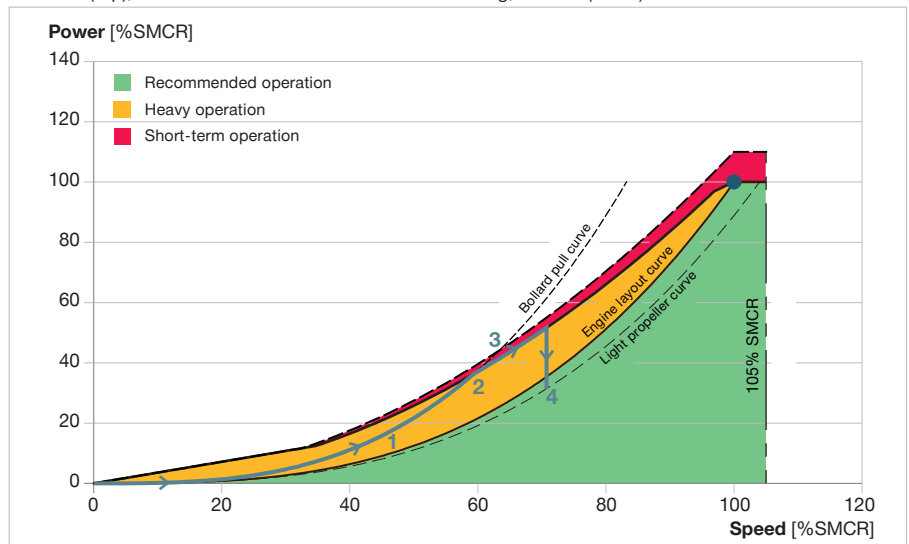


Fig. 3.17b: Engine loading in the engine load diagram from acceleration with an FPP plant from standstill, A-B-C-D (top), and from acceleration initiated while sailing, 1-2-3-4 (lower).

Acceleration during free sailing

On an FPP plant, imagine a scenario of acceleration from an example engine speed of “half” on the machinery telegraph, for which steady state has been reached, to “harbour full” on the machinery telegraph as illustrated on Fig. 3.17.

1. Fuel index and hereby engine power increases until the bollard pull curve, or in reality a propeller curve running almost as heavy as the BP curve, is encountered. No more torque can be absorbed by the propeller than along this line.
2. The engine and propeller shaft accelerates quickly along the BP curve, until the torque limit is encountered. The location of the BP curve is plant specific and its intersection with the torque limit is not necessarily found between “half” and “harbour full” which themselves are set individually for the specific plant.
3. The engine again accelerates along the torque limit. The engine will have to accelerate the ship itself to increase the advance number on the propeller in order to attain a reduction of the propeller torque required, and hereby allow for a higher shaft speed.
4. As the new engine speed set point is reached, the fuel index will gradually reduce until steady state is reached.

As seen, point 3 and 4 of an acceleration during free sailing corresponds to point C and D for an acceleration from standstill. In reality there will be an inclination to line 1 in Fig. 3.17 as the ship itself will experience some acceleration, and hereby increased speed of water arriving at the propeller.

For quick acceleration through a barred speed range of an FPP plant, it is prior to passage of the BSR recommended to reach steady state sailing at an engine speed just below the barred speed range. In other words, accelerate to a speed just below the BSR and keep steady until the fuel index is stable.

Once steady state sailing is attained, the speed setpoint is increased to a point above the barred speed range. This method ensures the highest possible speed of the water arriving at the propeller prior to the acceleration through the BSR, i.e. ensure a propeller curve as light as possible to accelerate along. Hopefully this extends the point at which the actual propeller curve encounters the torque limit to a point above the barred speed range.

This method will, compared to passing through the barred speed range along the torque limit of the engine, ensure an acceleration of the shafting as quickly as possible.

For further information on barred speed range passages, and recommendations on setting of the machinery telegraph, amongst others to aid passage of a barred speed range, please contact MAN Energy Solutions at MarineProjectEngineering2S@man-es.com.

Power limitations of main engines

The implementation of a power limitation on an engine can be relevant for different reasons. One application is to safeguard a retrofitted propeller optimised for a lower ship speed than the original, from the maximum torque of

the engine or to attain regulatory compliance, e.g. for EEXI, see Chapter 4.

The way to implement and effects of a power limitation depends on whether the engine is of camshaft (MC) or electronic (ME) control.

Impact of an index limitation for power limitation of MC engines

For MC engine with camshaft control of the fuel injection a power limitation is attained by limiting the maximum fuel index, i.e. limiting the maximum amount of fuel that can be injected per firing.

A fuel index limitation is de facto a limitation of the maximum engine torque, and fuel index is limited so that the sought power is attained along the engine layout curve as depicted on Fig. 3.18. Limiting the engine power by a torque limitation implies that at engine speeds below the speed corresponding to the sought power on the layout curve, the load diagram of the engine will be restricted as the engine torque is limited.

Once the torque limitation reaches the intersection with the original torque limit of the engine, the original torque limitation prevails. The difference between the original and torque/power limited load diagram is marked on Fig. 3.18.

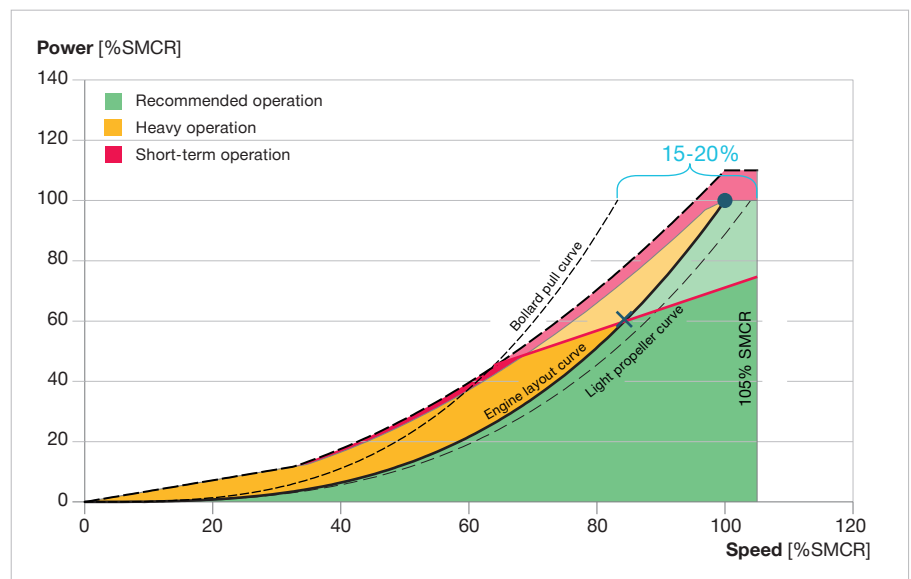


Fig. 3.18: Impact to the engine load diagram of a fuel index limitation for an MC engine to attain a 60% power limitation on the engine layout curve

The narrower load diagram resulting of an index limitation implies that acceleration capabilities of the ship can be reduced, depending on the extent of heavy running of the bollard pull curve and its intersection with the new load limitations. This is important to consider with respect to passage of a barred speed range, as well as it for a permanent limitation must be considered with respect to minimum propulsion power, see Chapter 4. For an overridable power limitation, an assessment of the impact towards manoeuvrability and minimum propulsion power is not required as the limitation can be lifted in such conditions.

Impact of a power limitation of ME engines

On ME engines, with electronic control of the fuel injection, a direct power limitation can be implemented. A direct power limitation is possible, as the engine per revolution, based on the work performed on the gas in the cylinder, can calculate the developed power directly.

As the power developed by the engine is known, it is not necessary to implement limitations directly to the fuel index. Instead, the fuel index is adjusted per firing, in order not to exceed the limited engine power. Hereby, limitations towards the heavy running capabilities of the engine are avoided as illustrated in Fig. 3.19.

However, depending on the extent of the power limitation, acceleration capabilities may still be affected, as well as it is still necessary to evaluate the minimum propulsion power criteria for permanent limitations.

For propeller retrofits, it is important to consider that the engine torque on an ME engine is not limited beyond the limitations implied by the power limitation. The original torque limitation of the engine will prevail and must be considered when evaluating the strength of the retrofitted propeller.

Extensions to the standard engine load diagram for acceleration and encounters of adverse weather

The electronic control of the ME engine allows for individual control of parameters relevant to the combustion such as fuel injection timing, length, pressure profiles, exhaust valve opening and closing times etc. This allows for optimising the combustion parameters to extent the regular load diagram of the engine in specific situations, while at the same time taking precautions not to overload the engine.

Dynamic limiter function (DLF)

As explained on the two previous pages, in the sections on acceleration, the location of the encounter of the heavy propeller curve and engine load limitations is decisive for the rate at which

the engine can accelerate. In order to aid quick acceleration and improve manoeuvring capabilities, the DLF functionality has been developed for ME engines.

The *DLF standard* system adjusts the engine operating parameters with respect to fuel injection for maximum torque when required and for maximum 30 minutes, see Fig. 3.20. The DLF calculates the air available in the engine cylinder before each firing. When the mass of available air is calculated, the engine control system can proceed to calculate how much fuel can be injected until either the minimum acceptable air excess ratio is reached (the DLF lambda limiter) or the maximum intermittent torque allowable at the actual speed is reached (the DLF torque limiter).

If *DLF full* is applied, further improvements towards torque can be attained by utilising the electronic control of the exhaust valve as well. By closing the exhaust valve earlier the air amounts available for combustion is increased. Furthermore, the DLF full opens the exhaust valve earlier to increase the flow of energy across the turbo charger in order to build up scavenge air pressure faster, further increasing air available for combustion.

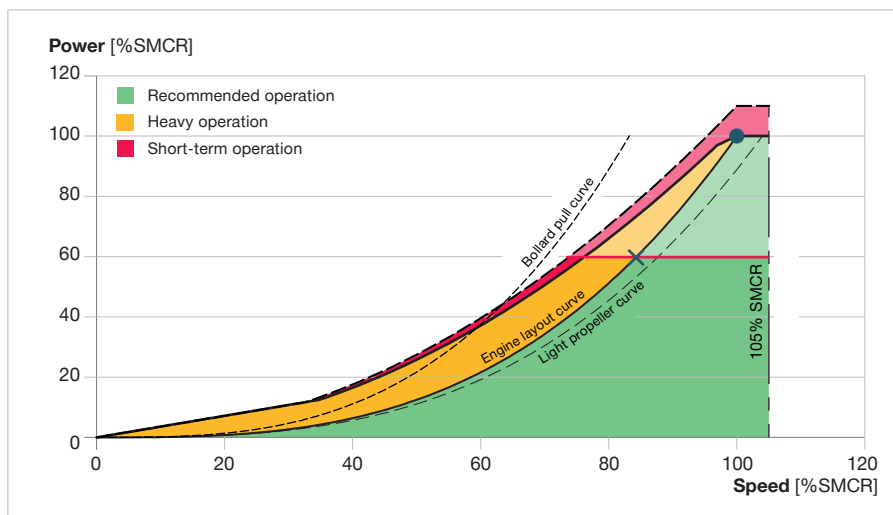


Fig. 3.19: Impact to the engine load diagram of a 60% power limitation for an ME engine

The ambient conditions will affect the maximum available index per firing. When the DLF functionality has been active for 30 minutes it will gradually roll back to the normal fuel index limiters and load diagram, see Fig. 3.20. DLF will then not be available until the engine components have had sufficient time to cool. This may take several hours. The efficiency of the engine reduces while DLF is active.

The capabilities of the DLF are attained solely by the electronic control of the combustion parameters, and does not require extra components. The DLF standard functionality is applied for 5 and 6-cylinder engines per standard, as these in general experience the highest relative location of the barred speed range. For further information, see the paper “Dynamic limiter function”.

Adverse weather condition (AWC) functionality

The AWC functionality is developed along the same principles of DLF, though with the difference that the extension of the load diagram by the optional AWC functionality is available as long as required in an emergency. Fig. 3.21 shows an illustration of an engine load diagram with the AWC functionality. The AWC function extends the operating area in the range from 60% to 97% engine speed, with the engine working at up to 100% torque, at 80% of the engine speed.

The aim of the area of the AWC extension to the load diagram is to make it possible for the engine to follow a typical bollard pull propeller curve up to 80% engine speed for regular propulsion plants of bulk carriers and tankers.

In principle, the AWC functionality increases the amount of fuel injected into the combustion chamber, which increases the torque output of the engine. In order not to overload the engine, the AWC function, amongst other initiatives, delays the fuel injection, which limits the peak pressure and temperature in the combustion chamber. Thermal loads of piston crown, exhaust valve, cylinder liner and cylinder cover are hereby reduced and kept below the temperatures attained at the SMCR.

The AWC functionality is not to be considered a replacement for an adequate light running margin. Frequent exposure to adverse weather conditions with utilisation of the AWC will reduce guiding overhaul intervals like other special engine configurations. The avoidance of adverse weather encounters is still to be sought by good seamanship, weather routing, etc.

When ordering an engine, it shall be informed if AWC is desired for that specific engine. For further information on availability for specific engines, see the paper “Adverse Weather Condition functionality and minimum propulsion power”. Alternatively, contact MAN Energy Solutions at MarineProjectEngineering2S@man-es.com.

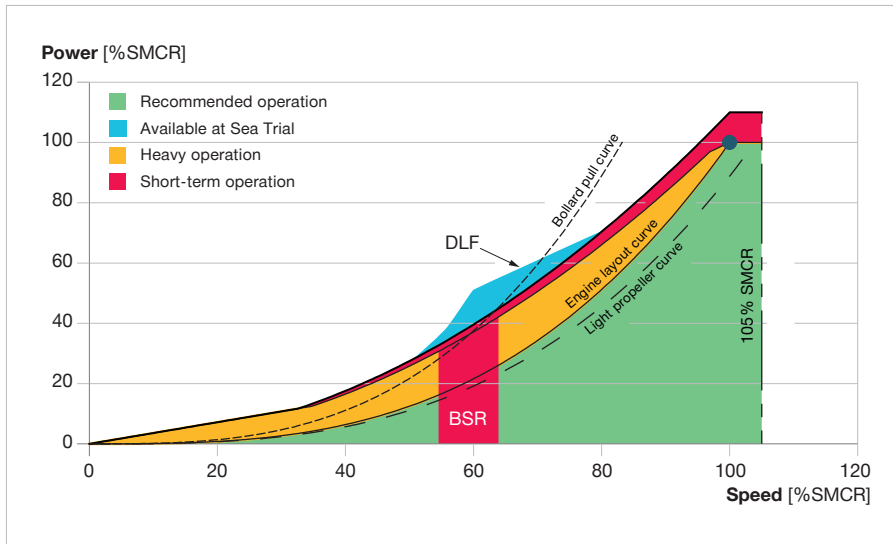


Fig. 3.20: Improved heavy running capabilities from DLF during acceleration

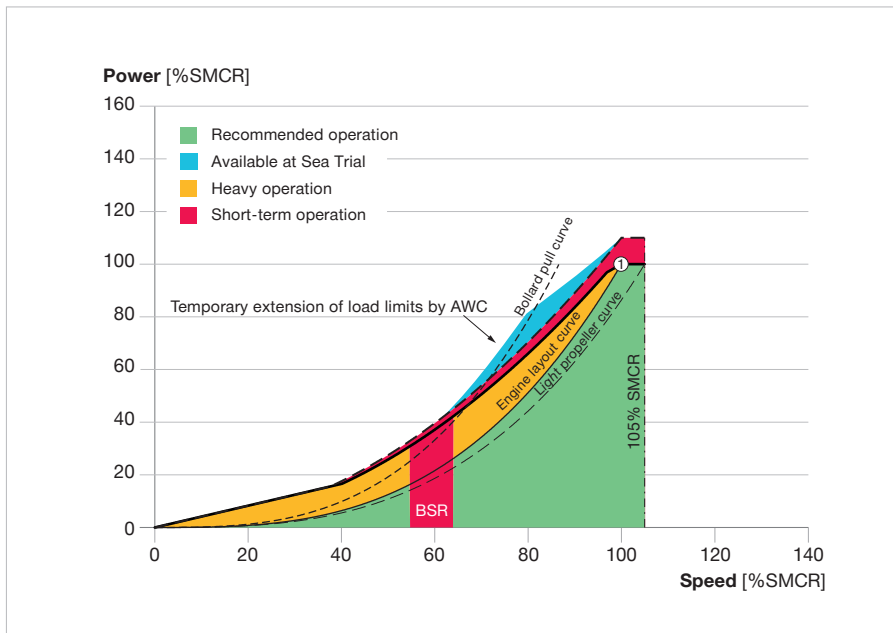


Fig. 3.21: Illustration of an engine load diagram with the AWC active. From the right, the light propeller curve, engine layout curve and the bollard pull curve

Degradation of light running margin on a ship in service, example

As described in the previous section “Light running margin (rpm margin)” (p. 33) it is necessary to design with a margin from the light propeller curve to the engine layout curve through SMCR. This is in order to have a margin for conditions not as ideal as sea trial conditions / service conditions for which the propeller is laid out.

Encounters of adverse weather will increase the extent of propeller heavy running, see “Minimum propulsion power” in Chapter 4 as well. It is however not the only reason for a heavier running propeller curve.

Over time the hull and propeller becomes fouled, dents are introduced to the hull be encounters with the quay-side, repaints may be conducted without removing the old paint completely, as well as the hull itself may rust with increasing roughness as a result, all increasing the skin friction.

This leads to an increase in friction and a heavier running propeller. The fouling can be limited by introducing biocides to the paint of the ship and/or removed by mechanical means in the form of a cleaning/polishing, especially after times of idling. Even if the hull is cleaned, experience however show that it can be hard to bring back the hull to original conditions hereby.

This is illustrated in Fig. 3.22 where the light running margin of an actual Kamsarmax bulk carrier is plotted over time. As seen, the light running margin varies not only with the loading condition of the ship (due to the variation in wetted surface and hence resistance) but also over time with various events happening to the hull.

For the first one-and-a-half year after delivery it appears that the biocide of the paint is sufficient to keep the level of fouling at a minimum, only a propeller cleaning is performed. Hereafter the LRM begins to degrade until a hull cleaning is performed whereafter the

LRM increases for some time, likely from the sailing smoothening out any patches of fouling possibly left in the cleaning.

Yet a propeller polishing is performed before the LRM slowly degrades again. According to experience from online onboard data monitoring of engines, so it will continue until the ship goes to dry-dock. Here the LRM can be close to completely restored to its original state, depending on the level of work performed herein and extent of dents, rust, etc. accumulated by the hull since delivery.

Considering this in-service increase of resistance, it is for a plant with a fixed pitch propeller, or controllable pitch propeller following a set combinator curve, important to have designed the propulsion plant with an adequate light running margin, of 4% to 7%, up to 10% in special cases.

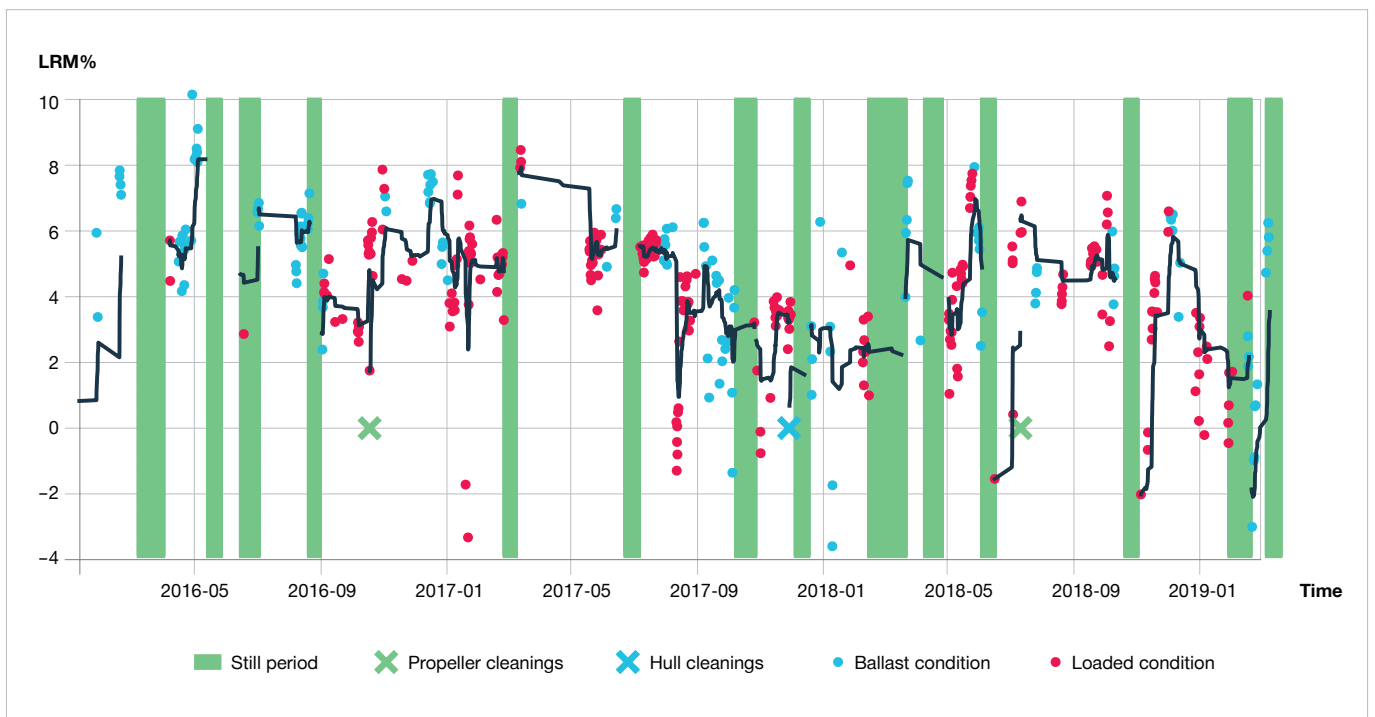


Fig. 3.22: Development to light running margin over time for an actual Kamsarmax bulk carrier

Power functions and logarithmic scale for engine diagrams

Historically, and before the introduction of computers, it was practical to display engine *layout* and *load* diagrams in logarithmic scale. Logarithmic scale is still commonly used in the industry, and their use can be beneficial to the experienced designer, and bring additional clarification.

The effective brake power P_B of an engine is proportional to the mean effective pressure (mep) and engine rate of rate of revolution, n . When using c as a constant, P_B may then be expressed as follows:

$$P_B = c \times \text{mep} \times n^i \tag{EQ 39}$$

This means that for constant mep, the power is proportional to the rotational speed of the engine, $i = 1$:

$$P_B = c \times n^1 \text{ (for constant mep)} \tag{EQ 40}$$

When only considering frictional resistance, as described in the section “Propeller Law and speed power curves” in Chapter 2, the power demanded for propelling a ship with a fixed pitch propeller at a speed V is proportional to the cubic of this, $i = 3$:

$$P_{\text{prop}} \propto c \times V^3 \tag{EQ 41}$$

As described in Chapter 2 the exponent for calculating the power required for propelling the ship at a speed V can be higher than 3 when including wave making resistance etc.

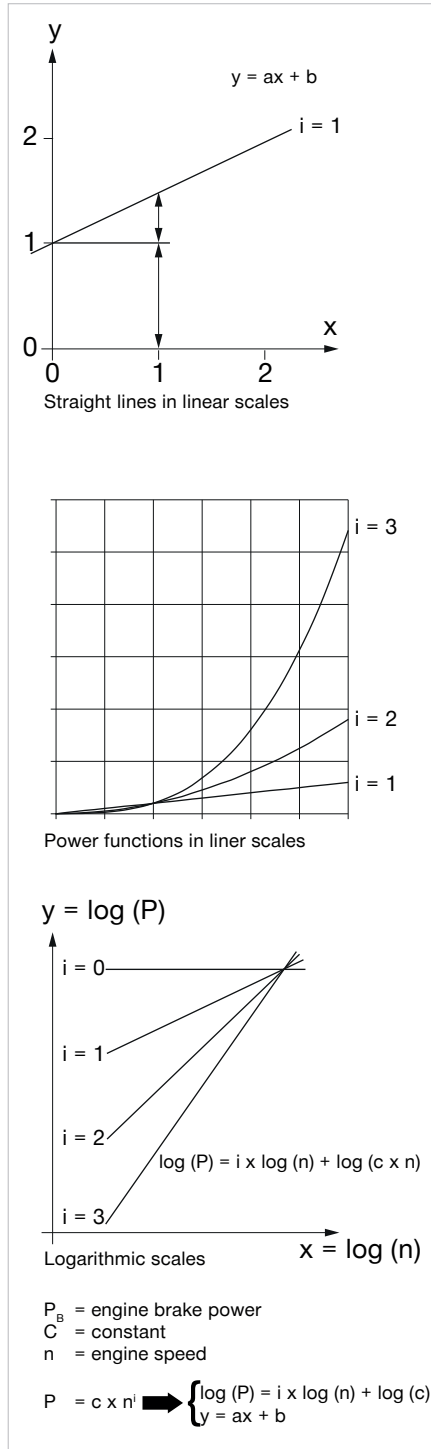


Fig 3.23: Linear and power functions in linear and logarithmic scale

Fig. 3.23 depicts P_B and P_{prop} in a normal linearly scaled coordinate system and in logarithmic scale. The beauty of the logarithmic scale is that a power function in logarithmic scale will be a linear line, the slope of which depends on the exponent i of the power function, according to the principal formula:

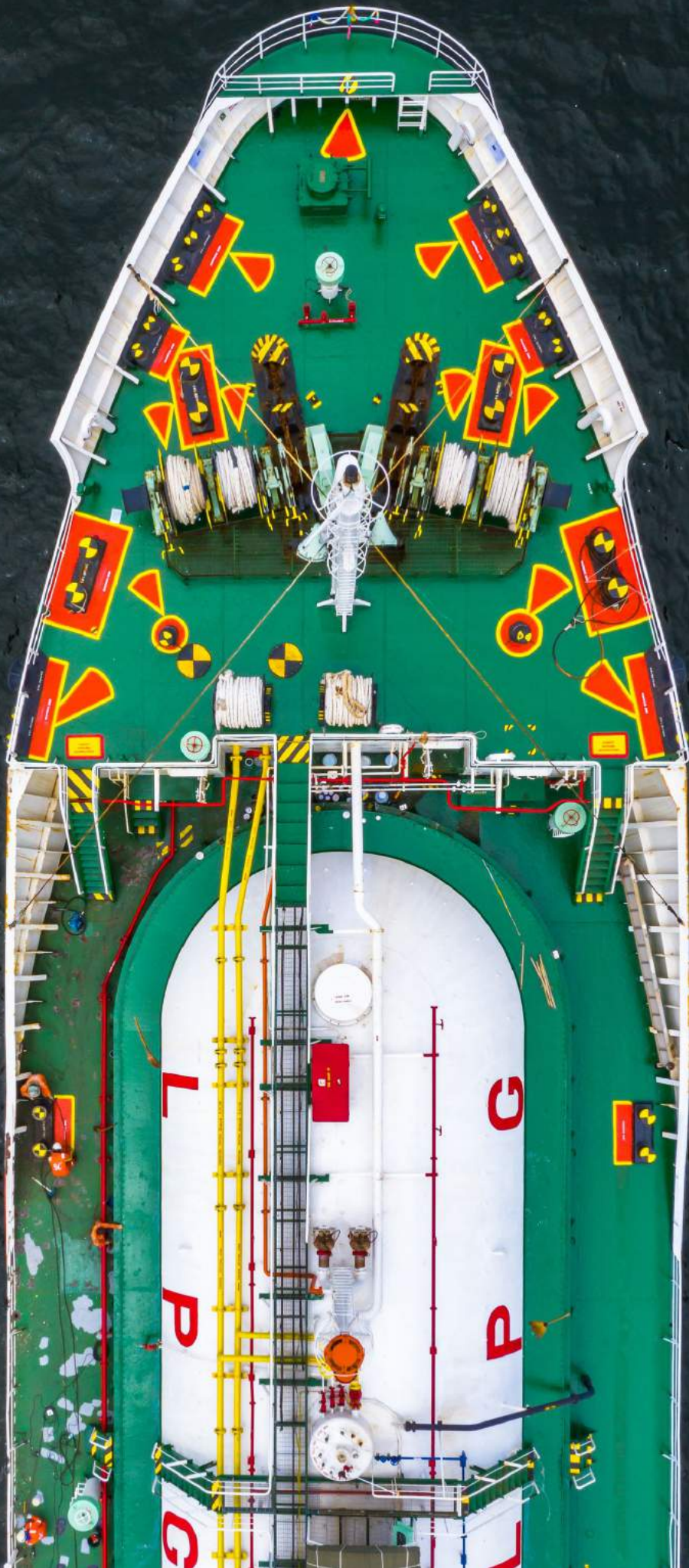
$$P_B = c \times n^i \tag{EQ 42}$$

Resulting in the logarithmic scale

$$\log(P_B) = i \times \log(n) + \log(c) \tag{EQ 43}$$

This means that the P_B for constant mep will follow lines of $i = 1$ in the logarithmic scale and P_{prop} will follow lines of $i = 3$.

Logarithmic lines of $i = 1$ are equivalent to regular linear lines, and as such the shape of the engine *layout* diagram is the same regardless of applying logarithmic scales or not, only the shape of the *load* diagram will change.



Chapter 4

Environmental regulations

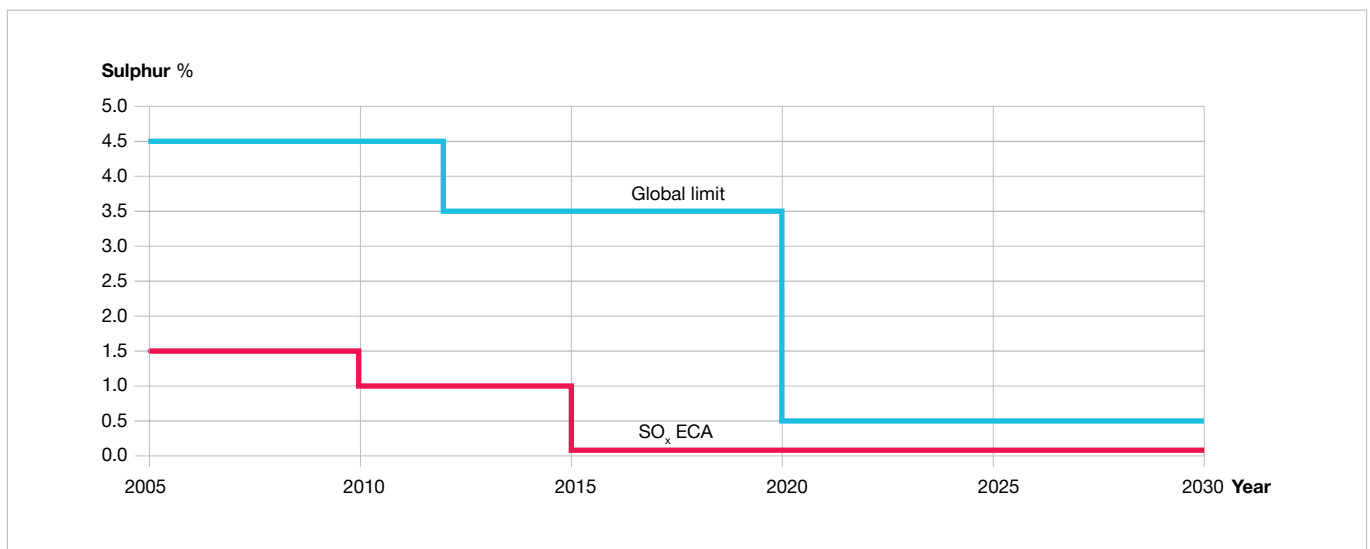


Fig. 4.01: Limits for sulphur emissions

Regulations limiting the emission of sulphur oxides (SO_x) and nitrogen oxides (NO_x) have been implemented during the latest decades. Special emission control areas (ECA) have been declared, further limiting SO_x and NO_x emissions in specific areas.

Measures towards fulfilling these regulations are briefly described in the subsequent sections on SO_x and NO_x. For in-depth knowledge, the reader is advised to consult MAN Energy Solutions' "Emission Project Guide", Ref. [4.1]. This is continuously updated and can be downloaded from our homepage → Two-Stroke → Project-Guides.

With the energy efficiency design index (EEDI) and Carbon Intensity Indicator (CII) the emission of greenhouse gases is set in focus and sought limited,

as described in a section of their own. As an effect of implementing EEDI, the IMO has also made recommendations on minimum propulsion power, described at the end of this chapter.

Sulphur oxides

Sulphur in fuel leads to emission of SO_x and particulate matter (PM). The IMO has set a global limit on sulphur emissions from all ships, gradually to be lowered as seen in Fig. 4.01. From 2020, a global limit of 0.5% applies, and a limit of 0.1% already applies locally in the SO_x-ECAs.

At the time of writing (2023), the sulphur content of HFO is approx. 2-3.5% depending on origin and significantly lower, approx. 0.1%, for MGO, and somewhere in between for MDO. The ECA

sulphur cap has led to the introduction of very low-sulphur fuel oil (VLSFO) and ultra low-sulphur fuel oil (ULSFO) of 0.5% and 0.1% sulphur content respectively. As low-sulphur fuels typically have different properties with regard to the lubrication of fuel components, special care must be taken as described in the paper "Guidelines for operation on fuels with less than 0.1% sulphur".

Alternative fuels such as LNG, LPG and methanol contain an insignificant amount of sulphur.

The IMO permits the use of fuels with a higher sulphur content if technical measures can be applied to reduce the SO_x emissions to a level equivalent to using low sulphur fuel, the main option for this is SO_x scrubbers.

SO_x scrubbers

Scrubber technology has been known for decades, as inland emissions of SO₂, e.g. from power plants, have been regulated. The primary motivation for using SO_x scrubbers in a maritime application is that HFO is significantly cheaper than low-sulphur fuels. For a large ship, this difference can turn a scrubber investment into a good business case, naturally requiring that the space for the system can be allocated.

Wet scrubbers are typically applied for marine applications, using either seawater in an open loop or freshwater with additives in a closed loop. Typically, both options are included in a hybrid solution, see Fig. 4.02.

Open loop operation offers low running costs, as seawater is fed directly to the scrubber, neutralising the SO_x only due to the natural alkalinity of seawater. The water is then led back to the sea. The discharge criteria set by the IMO guidelines is met by the high water flow through the scrubber. Power for pumping the seawater will be the largest running cost.

A closed loop system must be used if the alkalinity of the seawater is too low, the seawater is too dirty, or where local legislation prohibits open loop opera-

tion. Typically, NaOH is added in order to form sulphate with the sulphur. Sulphate accumulates in the scrubber water amongst the particulate matters from the combustion. Water is formed in the combustion, and constitutes a constant supply of fresh water, while water is bled off from the loop to be cleaned in a special unit, before being discharged to the sea. Closed loop running costs are higher due to the constant addition of chemicals, even if the

reduced flow reduces pumping costs.

With regard to fulfilling the EEDI requirements, it is important to note that a slightly increased electric load from the pollution reducing measures does not affect the index attained. The electrical consumption to use in the EEDI calculations are based on the power of the main engine. For the CII, the slight increase to electric load will however have a small impact.

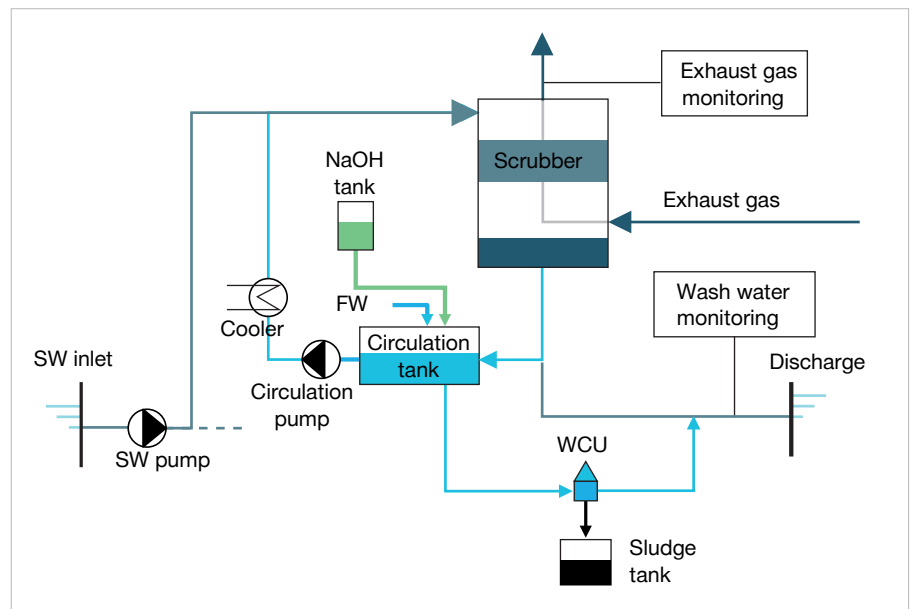


Fig. 4.02: Hybrid scrubber system

Nitrogen oxides

IMO has regulated NO_x emissions since 2000, implementing limits in various Tiers, I, II and III. Tier II has applied globally for ships which had their keel laid after 2011. Tier III applies in NO_x-ECA-areas only, in the North American ECA from 2016 and in the North European ECA from 2021, see “Emission control areas for SO_x and NO_x”. The NO_x emission limits are a function of the rated engine speed, see Fig. 4.03.

Both NO and NO₂ is included in NO_x, and especially NO₂ is harmful. NO_x can be formed by different processes resulting in either fuel, thermal, or prompt

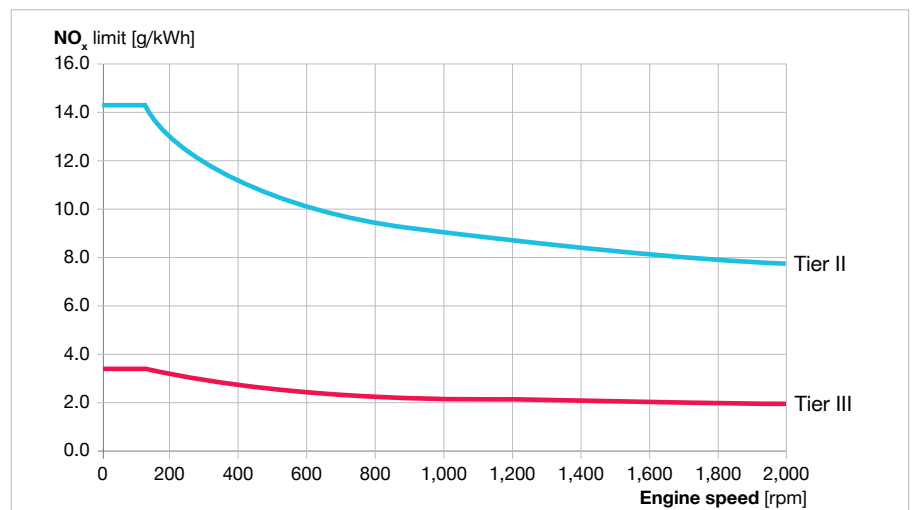


Fig. 4.03: Limits on NO_x emissions depending on engine speed

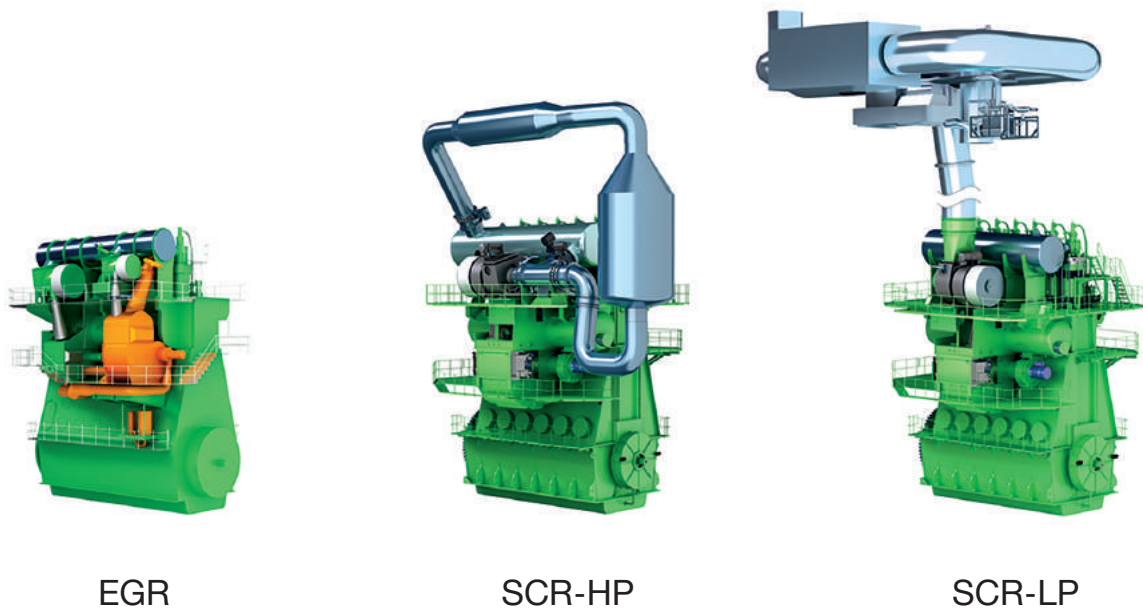


Fig. 4.04: Illustration of different NO_x reducing measures

NO_x, see Ref. [3.1]. Thermal NO_x is the main source in a diesel cycle engine.

Temperature and especially peak temperature during the combustion is the main parameter governing the amount of NO_x formed, but the timespan at peak temperature is of course also important.

Sufficient control of the temperature for fulfilling Tier II can be achieved by adjusting engine parameters such as injection timing, injection pressure, exhaust valve timing, etc.

Fulfilling Tier III limits require specific NO_x reducing technologies, described in the following sections about EGR and SCR.

Exhaust gas recirculation

Tests show that the amount of NO_x formed is related to the amount of oxygen found in the combustion chamber. The EGR-plant substitutes some of the fresh scavenge air with exhaust gasses that have a lower oxygen content. The exhaust gas is led through a cooling and cleaning cycle before re-entering the scavenge air receiver.

Due to the recirculated exhaust gas, more of the gasses in the chamber must be entrained in the combustion process, i.e. the flame must broaden to

entrain sufficient amounts of oxygen to burn the injected fuel. Entraining more gas means that the heat capacity of the combustion zone is increased, i.e. more gas must be heated to burn the fuel, which lowers the peak temperature of the combustion. The increased mass and specific heat capacity of the CO₂ and H₂O in the recirculated gas compared to O₂ and N₂, in fresh air, also contributes to increasing the heat capacity of the combustion zone.

An EGR system placed before the turbocharger is a high-pressure (HP) system, whereas a low-pressure (LP) system is placed after the turbocharger. HP EGR is most commonly used in marine applications.

When recirculating the exhaust gasses, the amount of fresh air that must be provided from the turbocharger decreases. The turbocharger must be capable of handling this condition, either by a bypass or if multiple turbochargers are installed, by cutting out one.

Using an EGR system to achieve Tier II is an option to improve Tier II SFOC (specific fuel oil consumption). Instead of optimising the combustion parameters for fulfilment of Tier II, these can be optimised for maximum efficiency. This has been termed EcoEGR.

Selective catalytic reduction

SCR does not interfere with the combustion process, but instead treats the exhaust gas according to the chemical reactions described in the “Emission project guide”, Ref. [4.1].

Since ammonia (NH₃) is poisonous in its pure form, it is stored and added in the form of urea, which is an aqueous solution of NH₃. The urea is reduced to ammonia in the system prior to the actual SCR catalyst.

An SCR system requires an elevated temperature in order to activate the catalyst elements. Furthermore, the sulphur content of the fuel sets limits for the minimum temperature, as sulphur reacts with ammonia to form ammonium bisulphate (ABS) at low temperatures. If the temperature is too low, this sticky substance can build up in the catalyst elements. Often, the ABS-imposed temperature limit is higher than the temperature required for the elements to perform the reduction.

SCR plants for marine applications exist both in a high (before the turbocharger) and low-pressure (after the turbocharger) variant. The benefit of the LP SCR is that it offers the designer better flexibility for arranging the installation, compared to the HP solution that must be positioned prior to the

turbocharger. Temperatures are lower after the turbocharger than before, which means that typically only low-sulphur fuel can be combined with a low-pressure SCR system.

Especially at low load, the application of SCR increases the SFOC due to the required minimum temperature of the exhaust gas. In the HP system, a cylinder bypass is installed to decrease the mass of air in the cylinders, thereby increasing the exhaust gas temperature, and reducing the efficiency of the engine. In the LP version it is required for some of the exhaust gas to bypass the turbocharger and directly heat the SCR elements, thus also decreasing efficiency.

Emission control areas

Emission control areas (ECA) can be declared for SO_x or NO_x, or for both types of emissions. Fig. 4.05 shows the existing ECA zones. The SO_x ECA limits of 0.1% sulphur apply to all

ships both in the North American and Northern Europe SO_x- and NO_x-ECA. The Mediterranean is designated SO_x-ECA from 2025. In the North American ECA, Tier III NO_x limitations are applicable for new ships built after 2016, and in Northern Europe after 2021.

Any abatement technology reducing the emission of SO_x and NO_x below the limits set will be accepted, given that the relevant IMO guidelines are followed.

Energy efficiency design index

In order to ensure the reduction of greenhouse gasses (GHG) from shipping, the IMO have introduced the energy efficiency design index (EEDI) as an amendment to annex VI of MARPOL, Ref. [4.2].

The principle of EEDI is to compare the emission of GHG from new ships with a baseline of existing ships built from 2000 to 2010, see Fig. 4.06.

A reduction factor of the index required for new ships is prescribed. It increases the requirement over time, as generally illustrated in Table 4.01 for large ships, Ref. [4.2]. Relaxations for small ships are made, and for general cargo ships as well as reefers, phase 2 only requires a reduction of 15%.

As the EEDI regulations are continuously evaluated, the reader is advised to consult the latest resolutions. As of 2023 these are available on:

www.imo.org → Our Work → Marine Environment → Pollution Prevention → Air Pollutant and GHG Emissions → Index of MEPC Resolutions and Guidelines related to MARPOL Annex VI → Guidelines related to Energy Efficiency of Ships.



Fig. 4.05: Existing SO_x & NO_x emission control areas around North America and North Europe, and SO_x emission control area in the Mediterranean

Phase	0, Jan 2013 -	1, Jan 2015 -	2, Jan 2020 -	3, Jan 2025 -
Reduction factor, X [%]	0	10	20	30

Table 4.01: EEDI reduction factors for ship types above certain thresholds except container ships and LNG carriers. See [4.2].

Calculation of required EEDI

The EEDI is as implied by the name a design index, evaluating the capabilities of the design and a certification attained upon delivery. A ship must attain an EEDI value lower than a required value, based on the baseline established for the ship type, corrected with the required reduction factor (X) as stated in Table 4.01.

$$\text{Reference line value} = a \times b^{-c} \tag{EQ 44}$$

Here, a & c are baseline parameters, Ref. [4.2], and b is the maximum deadweight of the ship given in tonnes. For container ships 100% dwt is applied as well.

$$\text{Required EEDI} = \left(1 - \frac{X}{100}\right) \times \text{Reference line value} \tag{EQ 45}$$

If the design of the ship falls into more than one category, the required value will be the lowest one.

Calculation of attained EEDI

The EEDI expresses the CO₂ emissions relative to the societal benefits of the transport work performed, giving a simplified version of the EEDI equation:

$$\text{EEDI} \approx \frac{\text{CO}_2}{\text{Transport work}} \tag{EQ 46}$$

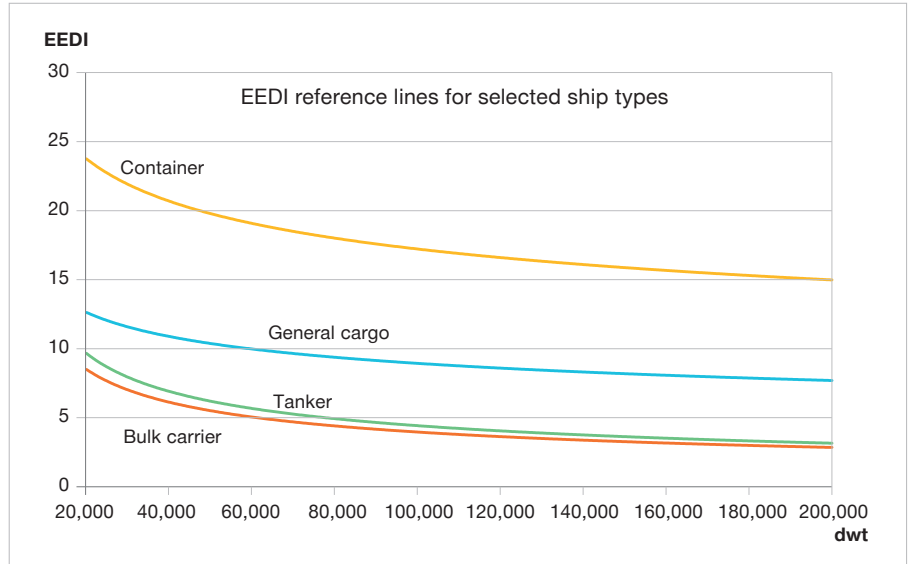


Fig. 4.06: EEDI reference lines for selected ship types

The CO₂ emissions relative to the transport work can be expressed as the relation of total power $\sum P$ times the specific fuel consumption (SFC) times the carbon content of the fuel type, C_F, taken relative to the capacity times the speed by which this is moved:

$$\text{EEDI} \approx \frac{\sum P \times C_F \times \text{SFC}}{\text{Capacity} \times V_{ref}} \tag{EQ 47}$$

This equation is still a simplification of the overall equation for calculating the index, Ref. [4.3], as seen at the bottom of the left page. This equation is hereafter referred to as the EEDI-equation.

In general, the power of the main engine (P_{ME}) and the specific fuel consumption (SFC) are to be taken at 75% MCR, in g/kWh, also providing the reference ship speed, V_{ref}, at 75% MCR.

For passenger ships, for example a cruise liner, but not a ro-pax, the capacity is equal to the gross tonnage. For container ships, the capacity is set equal to 70% of the maximum deadweight. For all other ships the capacity is equal to the maximum deadweight, Ref [4.3].

The non-dimensional conversion factor (C_F) between tonnes of fuel burned and tonnes of CO₂ produced accounts for

$$\frac{(\prod_{j=1}^n f_j) (\sum_{i=1}^{n_{ME}} P_{ME(i)} \cdot C_{FME(i)} \cdot SFC_{ME(i)}) + (P_{AE} \cdot C_{FAE} \cdot SFC_{AE}) + ((\prod_{j=1}^n f_j \cdot \sum_{i=1}^{n_{PTI}} P_{PTI(i)} - \sum_{i=1}^{n_{eff}} f_{eff(i)} \cdot P_{AEff(i)}) C_{FAE} \cdot SFC_{AE}) - (\sum_{i=1}^{n_{eff}} f_{eff(i)} \cdot P_{eff(i)} \cdot C_{FME} \cdot SFC_{ME})}{f_i \cdot f_c \cdot f_i \cdot \text{Capacity} \cdot f_w \cdot V_{ref} \cdot f_m}$$

Type of fuel	Carbon content	C _F , (t CO ₂)/ (t fuel)	Approx. LCV, kJ/kg
Diesel / Gas oil	0.8744	3.206	42,700
Light fuel oil, LFO	0.8594	3.151	41,200
Heavy fuel oil, HFO	0.8493	3.114	40,200
Liquefied petroleum gas, LPG	0.8213	3.015	46,000
Liquefied natural gas, LNG	0.7500	2.750	48,000
Methanol	0.3750	1.375	19,900
Ethanol	0.5217	1.913	26,800

Table 4.02: Carbon factor and lower calorific values for different fuels, as defined by the IMO, Ref. [4.3]. Note that LPG is a mixture of propane and butane, the values given here are for a 50/50 mixture. The primary content of LNG, pure methane, has an LCV of 50,000 kJ/kg

the GHG emission of different types of fuels, as shown in Table 4.02, Ref. [4.3].

In the EEDI-equation, f_{eff} refers to the availability of alternative energy generating measures. Correction factors f_i , f_c , f_m , and f_w relates to specific calculations for the ship type and the systems installed onboard, such as ice classed ships, cranes, ramps, etc., and is not treated here, see Ref. [4.3].

EEDI reducing measures

Speed reduction

As explained in “Propeller law and speed power curves” in Chapter 2, the power required to propel the ship is proportional to the speed of the ship by the power of about 3 to 4, $P \propto V^{3 \text{ to } 4}$. This means that if speed is increased from, for example 20 to 21 knots, the required power (placed in the numerator of the EEDI equation) is increased by as much as 25% even if the speed (placed in the denominator) is only increased by 5%.

Accordingly, a small reduction in speed, may result in a large reduction in power and hereby in EEDI. When reducing the speed, and thus the power installed, the designer must make sure that the ship can still manoeuvre safely even in harsh conditions.

Reducing power required

Various steps can be taken to minimise the power required at a given speed. Details on the influence of optimum propeller size and shaft speed are discussed in Chapter 2. By optimising hull lines and adding energy saving devices additional reductions can be achieved.

Changing fuel type

As seen in Table 4.02, both the carbon factor (C_F) and heating values will influence the amount of CO_2 produced. Higher heating values will result in smaller masses of fuel burned and, hereby, smaller amounts of CO_2 generated, and vice versa. When heating values are included, an EEDI reduction of, e.g. 23%, is attained for LNG and 8% for methanol. Pilot oil is injected to ignite most alternative fuels. The amount of this must be included in the final EEDI.

Decreasing specific fuel consumption

For example, a shaft generator can be installed on the main engine to reduce the SFC for producing electric energy. Application of waste heat recovery systems would have a similar effect. Additionally, EcoEGR for Tier II can be considered.

If in the early design phases a ship dimensioned with a four-stroke main engine cannot attain an EEDI lower than required, the implementation of a two-stroke engine with a lower SFC could, depending on the layout of the ship, be a way to secure EEDI compliance.

Capacity

Increasing the capacity while maintaining the total displacement of the ship can also reduce the EEDI. Reducing the lightweight is of most significance to ships with a large lwt/dwt ratio, e.g. $\text{lwt}/\text{dwt} > 1.5$ such as ro-pax ships, and of nearly no significance to bulk carriers and tankers, see Table 1.01 (p. 8).

For most ship types, it is generally worth considering the above-mentioned reducing measures prior to this option.

EEDI and light running margin

Due to the EEDI, there is a tendency towards installing less powerful engines,

see Fig. 4.07. The effect of this can be illustrated by an example of a car that has been fitted with an engine with less power than usual.

The car would have a lower top speed and accelerate slower, and the uphill running capability would be reduced. In those situations, the reduced power would have to be compensated for by using a lower gear ratio. However, a ship with an engine coupled directly to a fixed pitch propeller cannot shift gear. So, to cope with a reduced main engine power, the engine and propeller can be designed with a lower gear ratio, i.e. higher light running margin.

In Fig. 4.07, the *absolute* margin from the same propeller curve to the load limitations of two different SMCR ratings, compliant for EEDI phase 2 and 3 respectively are shown with resulting engine load diagrams. Even if the *relative* light running margin is the same, the *absolute* margin from the propeller curve to the load limits reduce.

Consequently, as the ship is the same, this may result in relatively reduced acceleration capabilities and a higher degree of heavy running for the EEDI phase 3 compliant rating. To counterbalance this characteristic of reduced

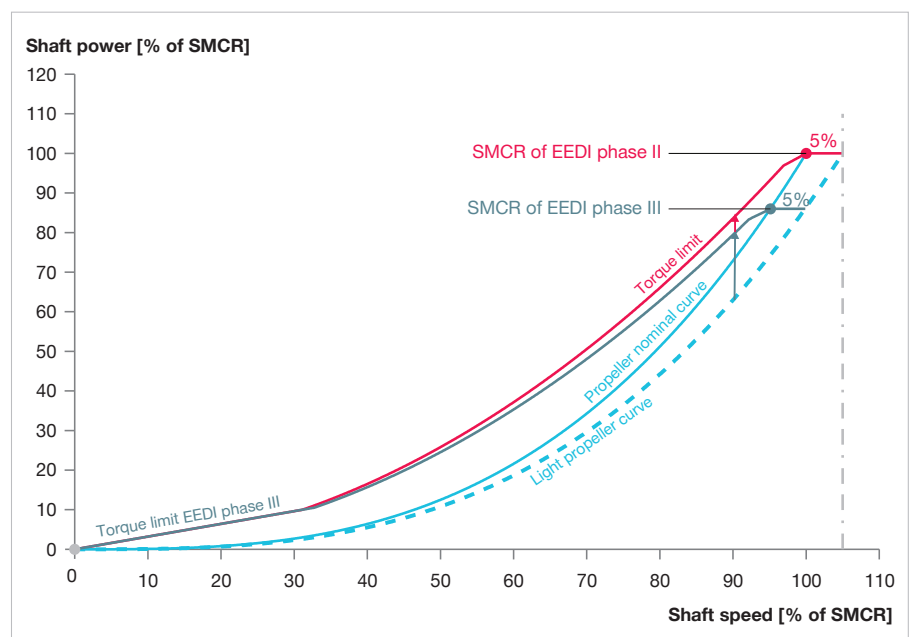


Fig. 4.07: *Absolute* margin between the light propeller curve and the torque limit for the same relative light running margin for an example of two ratings, EEDI phase 2 and 3 compliant respectively

power for EEDI Phase 3 propulsion plants, it is recommended to increase the *relative* light running margin to attain the same *absolute* margin as for known designs, in order to attain similar manoeuvring capabilities.

In the example in Fig. 4.07, the light running margin has to be increased from 5% for the EEDI phase 2 compliant rating to 7% for the phase 3 compliant rating, if the same absolute margin from the light propeller curve to the torque limit is to be maintained. This can be attained in two ways without increasing the engine power: Either by reducing the SMCR speed while maintaining a constant propeller curve, i.e. no changes to propeller pitch, as depicted on Fig. 4.08. Or alternatively, if the SMCR speed is maintained, by reducing the propeller pitch, see “Light running margin” in Chapter 3.

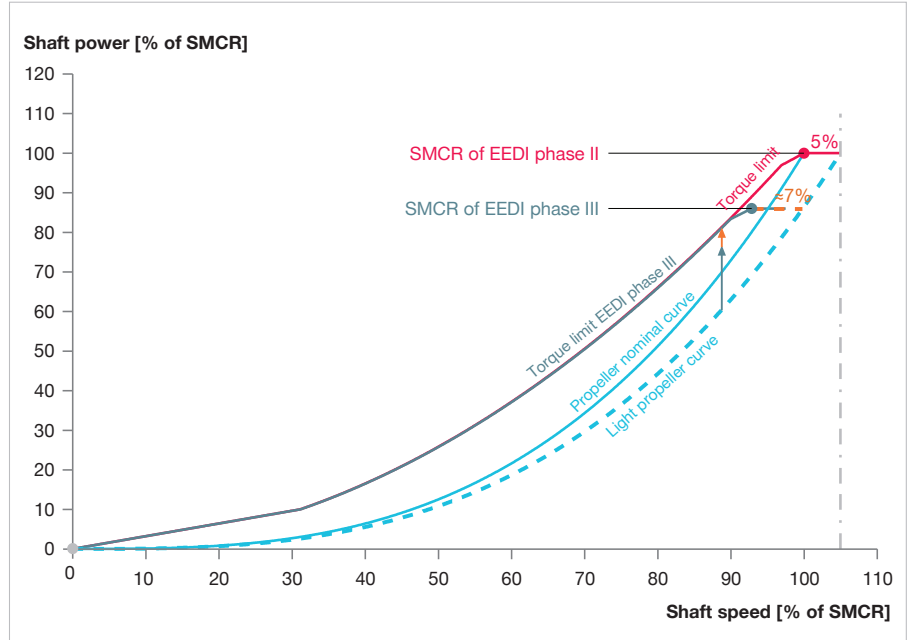


Fig. 4.08: Increase of the *relative* light running margin for the power compliant for EEDI phase 3, by a reduction of the SMCR speed

Energy efficiency existing ship index

The energy efficiency existing ship index (EEXI) was adopted by the IMO in 2022 in order to bring existing ships to a level corresponding to the EEDI in phase for new ships as per 1st of April 2022. I.e. EEDI phase 2 for all other ships than container ships and LNG carriers for which phase 3 applies from this date. A few differences exist amongst the EEDI phase 2 reduction rates and EEXI reduction rates depending on the capacity, see [4.2].

At the time of writing (2023) the EEXI is a one-time certification, phases for any future tightening of the EEXI reduction rates have not been established.

The EEXI is calculated according to the same equation and principles of the EEDI. Hereby, the EEXI is reduced by the same methods as the EEDI, described in the previous section. The most typical method to attain compliance with the EEXI is to install a power limitation. The power limitation can be either overridable in the form of the overridable power limitation (OPL) or permanent with the engine power limitation (EPL) features.

For an overridable OPL the EEXI is calculated at 83% of the limited power compared to the 75% of SMCR applied for determining the vessel EEXI in its present, unlimited, condition. This implies that for an OPL the first $(1-75/83) \times 100 \approx 10\%$ does not bring any reduction to the EEXI compared to the original SMCR power. For a permanent EPL the EEXI is calculated at 75% of the power limited value similar to the EEDI, see [4.5].

Irrespective if overridable or permanent, the method of the power limitations implementation depends if the fuel injection is mechanically controlled by a camshaft (MC) or electronically controlled (ME), see the section “Power limitations of main engines” in Chapter 3.

Due to the nature of the fuel index (torque) limitation implemented for MC engines, the heavy running capabilities of the engine is restricted below the val-

ue of the power limitation, see “Impact of an index limitation for power limitation of MC engines”. For ME engines only the power of the engine is limited, not the torque, nor the heavy running capabilities below the set power limit, see “Impact of a power limitation of ME engines”.

As a result of the restrictions to the load diagram the impact towards the ships capabilities towards manoeuvring and maintaining a minimum course keeping speed in adverse weathers of a permanent power limitation must be evaluated; see the later section “Minimum propulsion power”.

Carbon intensity indicator

The CII has been adopted by the IMO in 2022 to assess and promote operational efficiency. Unlike the EEDI that at delivery certifies the “technical” efficiency of the ship in a specific condition, the CII is an annual assessment of the operational efficiency, i.e. how much fuel is used relative to the transport work performed, where the ships capacity is used as a proxy for actual cargo carried.

The baseline for assessing the CII is established by the capacity transport-

ed and fuel consumed reported to the IMO data collection system, DCS, for year 2019. The reference line for assessing a ships level of efficiency at the CII introduction in 2023 is reduced by 5% from the baseline followed by 2% annual reduction from 2024 to 2026, i.e. 11% in total for 2026 compared to 2019. For 2027 the reduction rates are not yet decided (as per 2023), see Fig. 4.09.

Depending on the CII rating attained, the ship is certified as an A, B, C, D or E graded ship. If the ship for three consecutive years is graded as a D or for one year as an E ship, a corrective plan will have to be made and approved by authorities.

A series of correction factors exist for calculating the CII for various types of ships. A description of those lies beyond the scope of this paper, see [4.6].

As CII is an operational index, both technical efficiency, state of maintenance, operational profile / distribution of ship speed, idling, and waiting time in port etc. affects the final CII score. However, an efficient ship with a low EEDI will, all else being equal, have a better CII than a ship with a higher EEDI.

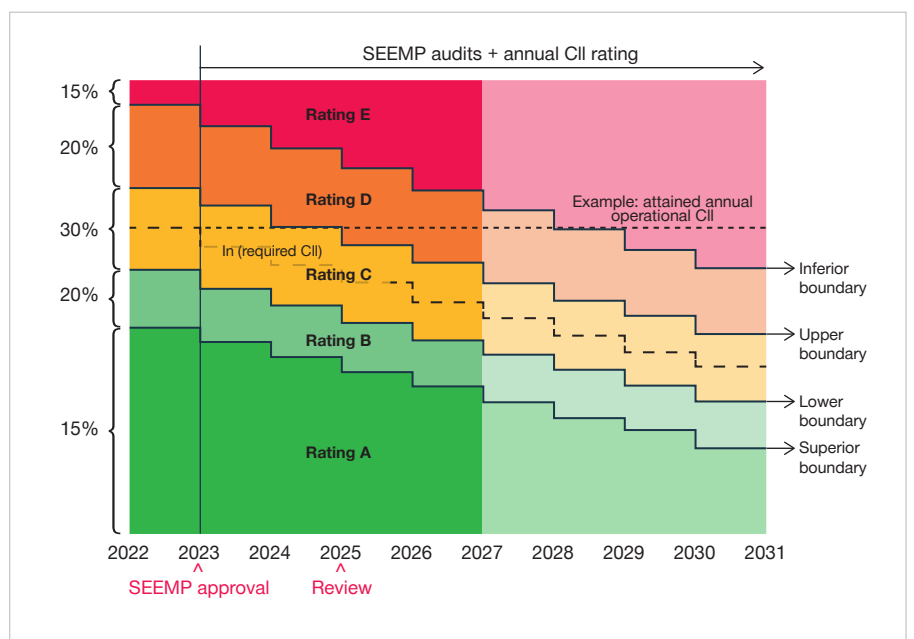


Fig. 4.09: Reduction rate for CII

Minimum propulsion power

While lowering a ship’s installed power has been acknowledged as a common method to obtain a lower EEDI value, it has also raised a concern that it could result in underpowered ships with reduced manoeuvrability in heavy weather. As a result of this, the IMO has published an assessment method for determining the minimum propulsion power required to maintain the safe manoeuvrability of ships in adverse conditions, Ref. [4.4], for bulk carriers, tankers, and combination carriers. The guideline was finalised by the IMO in 2021 and replaces the interim guideline.

The evaluation of minimum propulsion power can be performed by assessment level 1 or assessment level 2.

Assessment level 1

Assessment level 1 allows calculation of the minimum power line value based on ship type and deadweight, with value a and b according to Ref. [4.4]:

$$\text{Minimum Power Line Value} = a \times \text{dwt} + b \tag{EQ 47}$$

However, if the propulsion power installed is below the given minimum power line value of assessment level 1, then an evaluation on the ship’s design must be performed according to assessment level 2. In practice, most ships on traditional bunker attaining EEDI phase 3 compliance by a power reduction will have to be assessed by level 2, as the EEDI phase 3 compliant SMCR power will be below the value determined by level 1.

Assessment level 2

Assessment level 2 evaluates the specific capabilities of the propulsion plant, considering the open water diagram of the specific propeller (see Fig. 2.08), load diagram of the specific engine (see Fig. 3.10) as well as the added wave resistance in conditions specified by [4.4].

The added wave resistance from the conditions as defined in Table 4.03 can be established in two ways. Either by an emperic expression

$$R_{\text{add}} = 1,336 (5.3 \times V_{\text{ship}}) \times \left(\frac{B \times T}{L_{\text{PP}}} \right)^{0.75} \times H_s^2 \tag{EQ 48}$$

where B is the breadth of the ship and T the draught at maximum capacity. Alternatively, by use of a spectral method, considering the transfer function of the added resistance and wave spectrum. The transfer function can be determined either by seakeeping (model tank) tests or by a semi-empirical meth-

od as specified by [4.4].

In assessment level 2 it is evaluated if the mean power and rotational speed required of the propeller to maintain a minimum maneuvering speed of two knots can be accommodated within the continuous load limits of the main engine. As such, assessment level 2 accesses the torque capabilities of the engine compared to the heavy running propeller rather than the maximum power of the engine: For an FPP plant, the torque limit will be the limiting factor rather than the maximum power of the engine, see Fig. 4.10 for an example of a calculation according to assessment level 2.

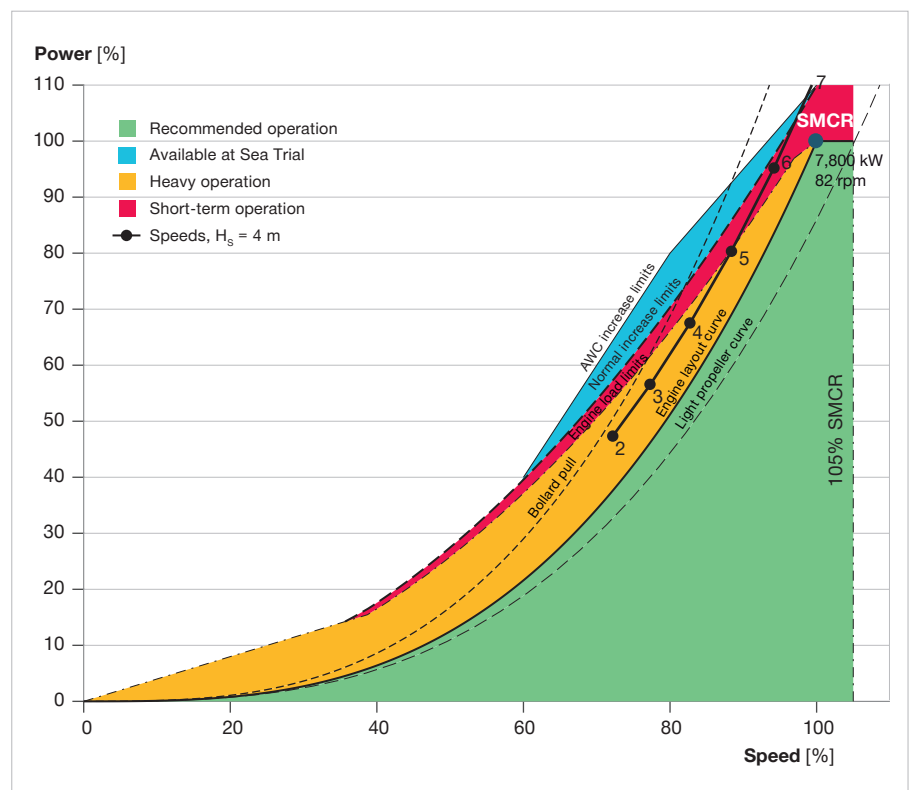


Fig. 4.10: Heavy propeller curve resulting from conditions of Table 4.03 for an example EEDI phase 3 compliant Kamsarmax bulk carrier, 82000 dwt, Lpp = 225 m, and SMCR 7800 kW at 82 rpm with 5% LRM. Integers along the resulting heavy propeller curve indicates the ship speed in knots for a example significant wave height of 4.0 meters. Wageningen B series applied for establishing the open water diagram.

If the AWC functionality is applied, the continuous load limits of the engine is extended, see “Extensions to the standard engine load diagram for acceleration and encounters of adverse weather” in Chapter 3. For further details towards the resistance calculations, determination of propeller power and speed, as well as examples see [4.7].

If the ship cannot fulfil the criteria to any of the assessment levels, various options can be considered. Alternative fuels, that lower the EEDI, will allow for a more powerful engine. A lighter propeller can be applied, hull lines and the bow can be refined to minimise resistance in general and from interaction with waves specifically, etc. Attaining

compliance by optimisation of the hull form will require individual model tank seakeeping tests.

Ship length L_{pp} [m]	Sig. wave height, H_s [m]	Peak wave period, T_p [s]	Mean wind speed, V_w [m/s]
Less than 200	4.5	7.0 to 15	19.0
$200 \leq L_{pp} \leq 250$	Linear interpolation	7.0 to 15	Linear interpolation
More than 250	6.0	7.0 to 15	22.6

Table 4.03: Adverse conditions applied to ships defined as the threshold value of ship size for assessment level 2 in which a minimum course keeping speed of 2 knots must be attained [4.4]. Most severe peak wave period to be investigated.

Chapter 5

Examples of engine selections for selected ship types

This chapter exemplifies the selection of main engine(s) for selected ship types based on the engine selection spirals for FP- and CP-propellers.

All calculations are performed with simple, open access tools, to underline the exemplarity of the calculations.

Three ships are considered:

- MR tanker, 50,000 dwt, FPP, with/without PTO, methanol
- Container carrier, 24,000 teu, FPP with PTO, LNG
- Ro-ro, 6000 lm, twin screw CPP with PTO, LNG

Furthermore the reader is advised to consult the example given for a 320,000 dwt VLCC in the separate paper “Propulsion of VLCC” and similar papers.

Example 1 - MR tanker

This example uses a 50,000 dwt MR tanker, and includes considerations on

EEDI phase 3 from 2025 and minimum propulsion power.

The tanker is designed for operation on methanol in North America or North

Europe, applying NO_x reducing measures.

The principal parameters of the MR tanker are shown in Table 5.01.

Deadweight, scantling	50,000 dwt
Deadweight, design	44,000 dwt
Length oa. L_{OA}	185 m
Length bp. L_{PP}	177 m
Breadth	32.2 m
Depth to main deck	19.1 m
Draught, scantling, T_s	12.8 m
Draught, design, T_d	11.6 m
Displacement, scantling	59,700 t
Lightweight	9,700 t
lwt/dwt	0.19
Block coefficient, C_B scantling	0.82
Block coefficient, C_B design	0.81
Design speed	14.0 kn
Froude number at design speed	0.18
Propeller diameter, d	6.8 m

Table 5.01: Principal parameters of example 1

1. Calm water resistance and propulsion coefficients

There are various methods for determining the calm water towing resistance. In this case, the Ship-DESMO program is used, Ref. [2.5] which is based on Ref. [1.2]. The calculated resistance is often validated and optimised by a towing tank test at a later stage of a project.

Apart from the towing resistance, it is necessary to determine the wake fraction coefficient and the thrust deduction coefficient used to establish the hull and rotative efficiency as described in Chapter 2. For a first estimate the following formulas could be used, see also Table 2.02 (p. 22).

$$w = 0.5 \times C_B - 0.05 = 0.35 \text{ and } \eta_H = \left(\frac{1-t}{1-w} \right) = 1.2$$

$$t = 0.27 \times C_B = 0.22 \Rightarrow \eta_H = \left(\frac{1-t}{1-w} \right) = 1.2$$

EQ 49

2. Light propeller curve

The light propeller curve is calculated for the design condition, based on the calm water towing resistance, propulsion coefficients, and the propeller characteristics, see Fig. 5.01. Preliminary values for propeller data could be obtained from the Wageningen B-series or another propeller-series. For more accurate values of resistance and propeller characteristics, tank test data, or CFD analysis of the actual ship design can be applied.

Considering that the propeller must be submerged when the MR tanker is sailing in ballast, the maximum propeller diameter is set to $d = 6.8 \text{ m}$, $d / T_d = 0.59$ with four blades.

The shafting efficiency is set to 99% as the engine is located aft and the shaft is short.

At an initial design speed of 14.0 knots, the light propeller curve demands 5,750 kW at 86.3 rpm.

3. Propulsion margins

Initially, a sea margin of 15% and an engine margin of 10% is set for the ship.

The light running margin is set to 5%.

The combined inclusion of margins result in an SMCR = 7,350 kW at 89.0 rpm, Fig. 5.01, see p. 33 for the relevant equations.

4. SMCR on engine layout diagram

Using the CEAS calculation tool, which can be accessed from the MAN Energy Solution website → Two-stroke →

CEAS Engine Calculations, the SMCR is plotted on the engine layout diagram of various possible engines, one of which is illustrated in Fig. 5.01.

This allows plotting of consumption values as a function of engine load, which can be accessed from the MAN Energy Solution website → Two-stroke →

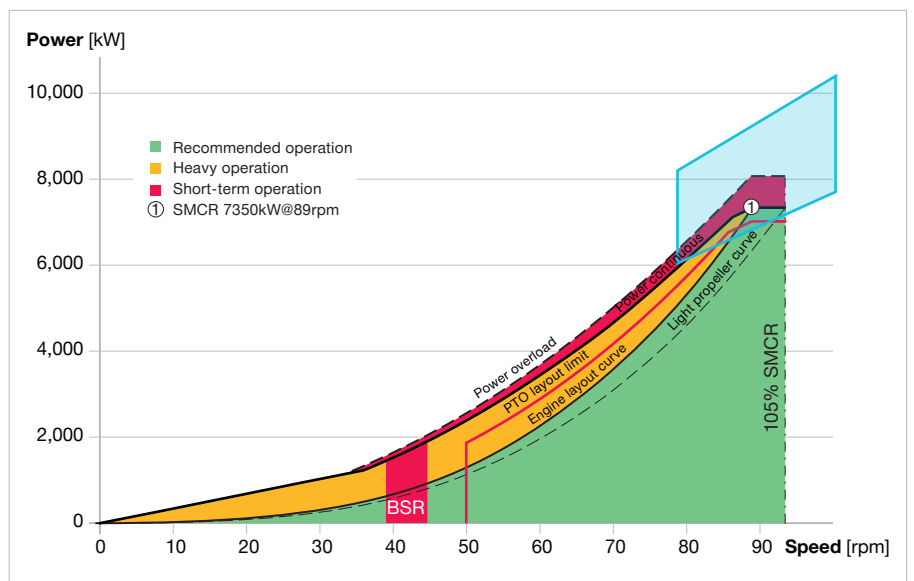


Fig. 5.01: Light propeller curve, margins and layout curve for SMCR = 7,350 kW with load diagram and layout diagram for a potential engine for a 50,000 dwt MR tanker. Maximum available PTO power at 75% MCR is approx. 1,050 kW

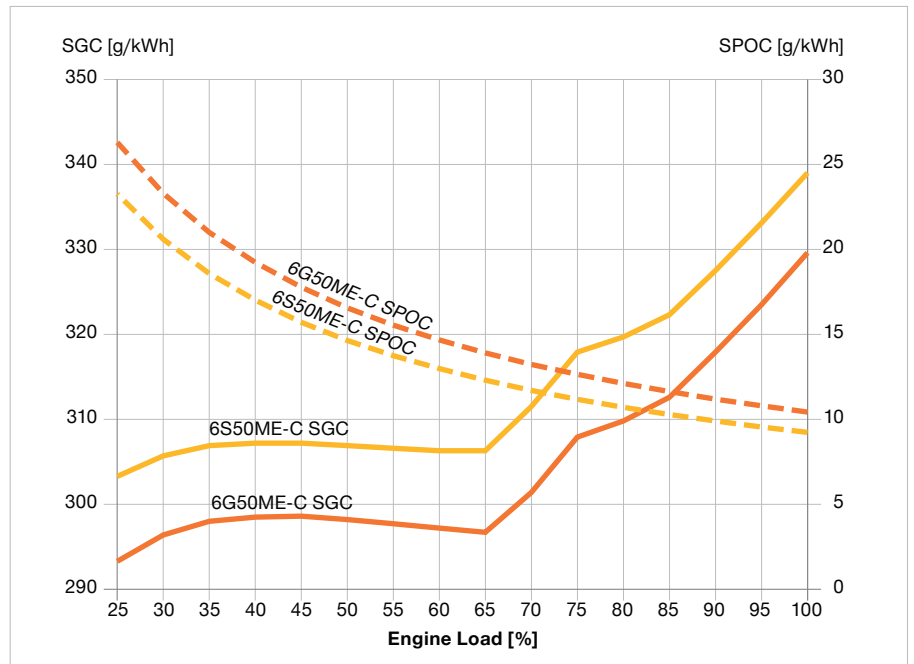


Fig. 5.02: Specific gas consumption (methanol) and specific pilot oil consumption excluding tolerances of possible engines for a 50,000 dwt MR tanker in Tier II mode and a SMCR of 7,350 kW at 89 rpm, as of 2023. Values may change, please use CEAS for specific values

5. Select engine

Usually, the most derated engine will result in the lowest fuel consumption over the full range but also the highest initial cost as well as the largest engine dimensions.

For LGIM engines SCR is not available as Tier III technology. In Tier II mode, which is of significance to EEDI calculations, EGR offers the potential of implementing EcoEGR, which reduces the consumption further.

The optimum choice of engine will depend on the priorities of the project. A sensible compromise between operational (OPEX) and capital (CAPEX) expenses could in this case be the 6G50ME-C9. The 6G50ME-C9 will be used for the first iteration through the engine selection spiral.

6. Passage of barred speed range

Quick passage of a barred speed range can in some cases be a challenge for 5 and 6-cylinder engines. Here, a 7-cylinder engine is employed and, therefore, the BSR is expected to be passed quickly because the BSR is placed at a relatively low rpm relative to SMCR-speed and the required propeller power therefore is quite low.

For this example ship, the highest rpm in the BSR is estimated to be at 50% of SMCR speed, see Fig 5.01. The location of the BSR and the ability to pass it quickly should be evaluated specifically for each project.

The barred speed range power margin (BSR_{PM}) is calculated as described in the corresponding step in the FPP selection spiral in Chapter 3, and is well above the recommendation of minimum 10%.

7. Standard engine load diagram

The selected SMCR and the resulting load diagram is included in Fig. 5.01.

8. Compliance with regulation

The operational profile of an MR tanker operating near North America or North Europe will involve operation within NO_x -ECA zones. An EGR solution is selected as the NO_x reducing measure in this example, one of the reasons being

the saving potential offered by EcoEGR. By methanol as fuel SO_x compliance in any area is attained. If operated in fuel mode, ULSFO fuel is needed to maintain compliance within SOX-ECA whereas VLSFO is needed in fuel mode for global operation.

With regard to EEDI, the ship considered here is to be built to phase 3 standards (30% reduction from the EEDI reference line) implemented from 2025.

With a capacity of 50,000 dwt, the required EEDI can be calculated by first establishing the reference line value for a tanker, as set by Ref. [4.3], see equation 50.

With the reduction from phase 3 resulting in a required EEDI, see equation 51.

Through the same power prediction method as applied in step 1, applying Ref. [2.5], the reference speed at 75% engine load and 100% capacity utilisation in trial condition is established, $V_{ref} = 14.10$ knots.

The attained index calculated is based on the EEDI equation in Chapter 4, in this case for MDO. The methanol and pilot oil consumption of the main engine at 75% MCR in Tier II mode is used for the calculation. The consumption is obtained through CEAS, and the 6% tolerance on this number is included in the calculations. In this example the SFO- C_{AE} of a smaller single fuel auxiliary engine at 50% load is estimated to 220 g/kWh MDO including tolerance. The

electric power to use in the EEDI equation is calculated to 368 kW, Ref. [4.3].

As seen, the MR tanker fulfills the phase 3 requirements for EEDI as the attained value of 4.22 > 4.34. Had the MR tanker, of the speed capabilities considered here, been for traditional bunker, the EEDI would have been 8% higher due to the higher carbon content to LCV ratio of traditional bunker compared to methanol, see Chapter 4. A power reduction would be required if EEDI phase 3 compliance is to be attained for traditional bunker for this example.

The MR tanker does not fulfil the MPP requirements at assessment level 1 (7,350 kW < 9,220 kW), and will instead have to be evaluated by assessment level 2, which based on experience should be possible, provided that the light running margin of the design is within the general recommendations.

An often relatively simple solution to further reduce EEDI is to install a PTO, as this both reduces the SFOC for generating electric power, and allows for some of the main engine power to be allocated to the electric power production. This allocation of main engine power leads to a reduction in reference speed. A PTO is especially relevant for a dual fuel ship, as the PTO will allow the main engine, operated by the alternative fuel, to cover the onboard electric consumption while at sea. This can possibly reduce the need for dual fuel gensets.

$$BSR_{PM} = \frac{P_L - P_P}{P_P} \times 100 = \frac{1,900 - 1,400}{1,400} \times 100 = 35\% \quad \text{EQ 50}$$

$$\text{Reference line value} = a \times b^{-c} = 1218.8 \times 50000^{-0.488} = 6.21 \quad \text{EQ 51}$$

$$\text{Required EEDI} = \left(1 - \frac{X}{100}\right) \times \text{Reference line value} = \left(1 - \frac{30}{100}\right) \times 6.21 = 4.34 \quad \text{EQ 52}$$

The required rated electric “name plate” output of the PTO to be able to cover 368 kW in the EEDI calculation is $445 / 0.75 / 0.75 = 657$ kW. The engine selection spiral can be re-entered at step 7 in order to ensure that the margin between the light propeller curve and the PTO_{layout limit}. With a PTO, the EEDI_{PTO} of the MR tanker is 3.94.

Other EEDI reducing measures could also be considered. For instance a Kappel propeller, rudder bulb, and/or a wake equalising duct, could also be relevant, in order to reduce required power for a given ship speed, and thereby the EEDI.

Considerations on such energy saving devices, further derating, and possibly additional speed reductions will be required to meet EEDI phase 3, if alternative fuels are not considered as in this example.

Example 2 - container carrier

This example considers a 24,000 teu container carrier for LNG as fuel, illustrating the inclusion of a PTO for ships with a high electric consumption. The principal parameters of the container carrier are shown in Table 5.02.

1. Calm water resistance

Various measures exist for determining the calm water resistance. Here, the Ship-DESMO program is used, Ref. [2.5] which is based on Ref. [1.2].

2. Light propeller curve

The light propeller curve is determined using the same methods as in example 1.

Considering limitations of propeller casting and the fact that the propeller must be submerged in all conditions, the maximum diameter of the propeller has been set to $d = 10.7$ with 5 blades. This is on the upper edge of current designs with a d/T_d - ratio of 0.74.

3. Propulsion margins

Initially a sea margin of 20% is set for the ship with an engine margin of 15%. Relative high margins are desirable in order to be able to catch up delays.

$$\text{Attained EEDI} = \frac{\text{SMCR} \times 0.75 \times (C_{F,PO} \times \text{SPOC} + C_{F,Alt.} \times \text{SGC}) + P_{AE} \times C_{F,AE} \times \text{SFOC}_{AE}}{\text{capacity} \times V_{ref}} \quad \text{EQ 53}$$

$$\text{Attained EEDI} = \frac{7,350 \times 0.75 \times (3.206 \times 15.8 + 1,375 \times 321.2) + 368 \times 3.206 \times 220}{50,000 \times 14.1} = 4.22 \quad \text{EQ 54}$$

$$\text{Minimum Power Line Value} = a \times \text{dwt} + b = 0.0652 \times 50,000 + 5,960.2 = 9,220 \text{ kW} \quad \text{EQ 55}$$

Deadweight, scantling	228,000 dwt
Deadweight, design (80%)	182,000 dwt
Length oa. L_{OA}	400 m
Length bp. L_{PP}	385 m
Breadth	60.5 m
Depth to main deck	30.5 m
Draught, scantling, T_s	16.5 m
Draught, design, T_d	14.0 m
Displacement, scantling	292,000 t
Lightweight	64,000 t
lwt/dwt	0.28
Block coefficient, C_B scantling	0.74
Block coefficient, C_B design	0.73
Design speed	22 kn
Froude number at design speed	0.184
Propeller diameter, d	10.7 m

Table 5.02: Principal parameters of example 2

The light running margin is initially set to 4%, the lowest recommendable value, due to the slender hull lines of this ship and the corresponding relatively low increase in resistance in heavy weather.

The result is an SMCR point at 63,000 kW and 79 rpm.

4. SMCR on engine layout diagram

Using the CEAS online calculation tool, the SMCR is plotted on the engine layout diagram of various possible engines, see Fig. 5.03.

5. Select engine

Depending on the priorities of the project, the optimum engine can be selected based on the CEAS reports, see Fig. 5.04. In this case the 11G95ME-C10-GI-EGRTC is selected as a compromise between minimum LNG consumption, pilot oil consumption, engine dimensions as well as maintenance.

When evaluating the lower fuel consumption of a derated engine, it is important to consider the increased lubrication oil consumption from added cylinders as well as for dual fuel engines the added pilot oil consumption. The pilot oil amount is absolute per cylinder why the pilot oil fraction for the same engine power increases with the cylinder number, see Fig. 5.04.

Besides illustrating the difference in pilot oil consumption by cylinder number Fig. 5.04 indicates the impact of various technologies on the engine. The tier II consumption of LPSCR and EGR is identical, apart from when the turbo charger cut out (TCCO) made possible by the EGR is applied to optimise the performance at lower loads.

In addition Fig. 5.04 illustrates the impact of selecting a GI-optimisation compared to a standard tuning where there are no differentiation between oil and gas mode. The GI-optimisation implies a penalty for oil mode and must be selected based on an evaluation of expected bunker availability etc.

With TCCO and GI-optimisations the possible engines attains efficiencies

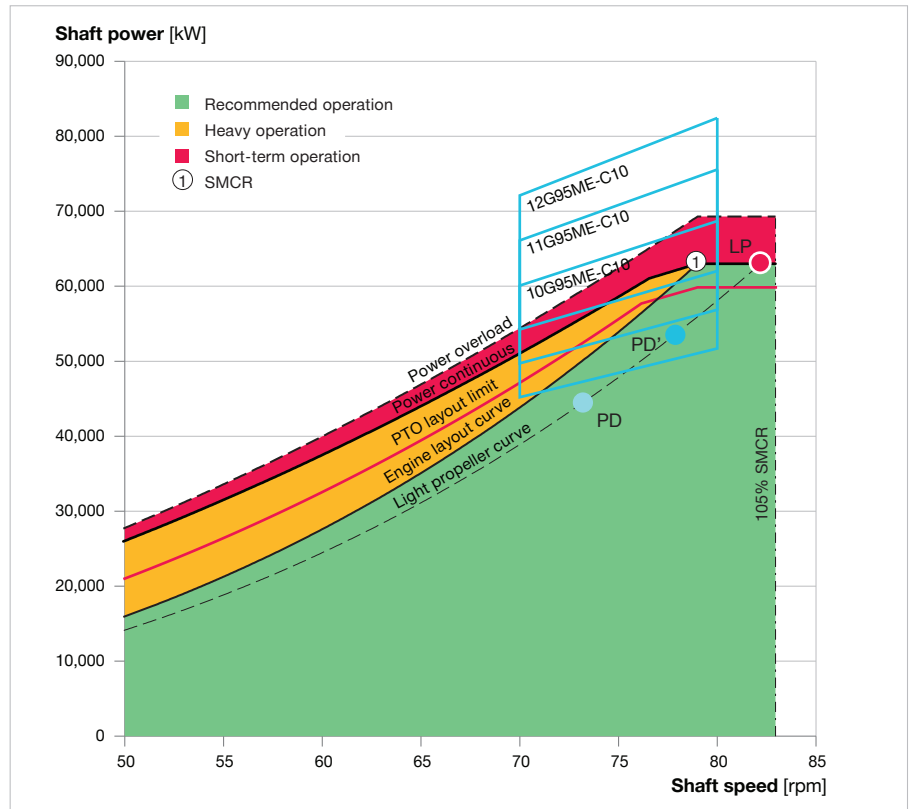


Fig. 5.03: Layout diagrams for selected engines possible and load diagram for the rating of 63,000 kW at 79 rpm for the example 24,000 teu container carrier

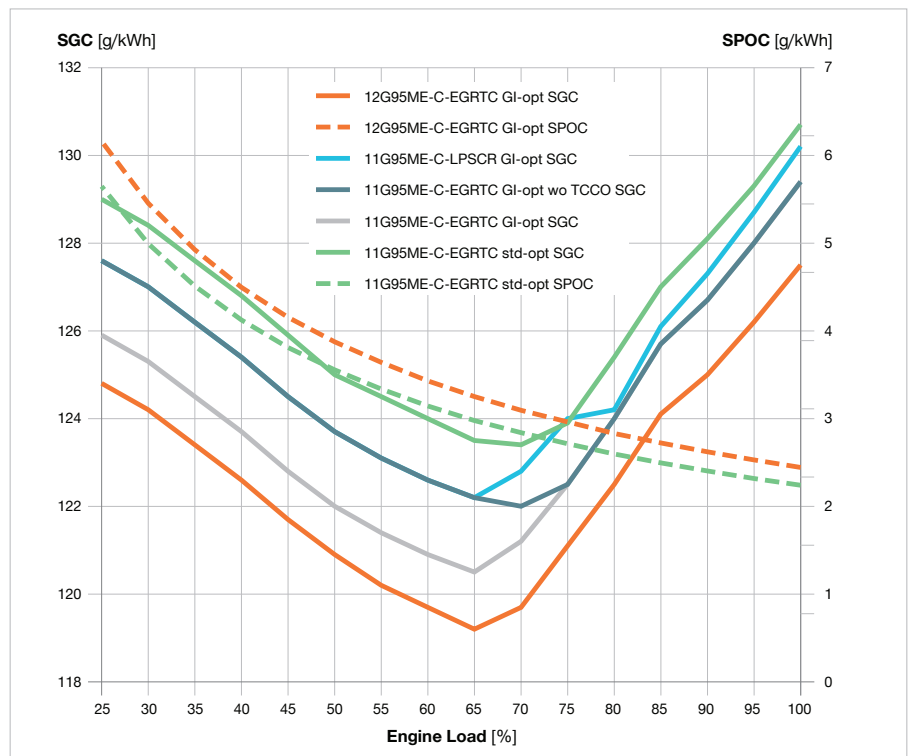


Fig. 5.04: Tier II SGC and SPOC of selected possible engines with Tier III equipment and possible GI optimisations as well as turbo charger cut out (TCCO) for the rating of 63,000 kW at 79 rpm. Values may change, please use CEAS for specific values.

above 58% at 65% engine load. If a waste heat recovery plant is added, plant efficiencies well above 60% are within reach.

6. Passage of barred speed range

The barred speed range will, when considering the many cylinders of the engine and the long shaft line for such a ship, be located at a low rpm. The BSR power margin will be large and the BSR passage will therefore be quick.

7. Standard engine load diagram

As a PTO is desired, the engine *load* diagram is of special interest in this case. A 6-MWe PTO is sought included. The maximum power demanded by the light propeller curve and PTO combined is to be designed to the $PTO_{\text{layout limit}}$, see Chapter 3 “Engine load diagram & considerations of PTO”.

When considering the difference between the $PTO_{\text{layout limit}}$ and the light propeller curve (see Fig. 5.04) over the full shaft speed-range as it is plotted on Fig. 5.05, the availability of PTO power can be investigated. When operating along the light propeller curve and using, for example, 75% MCR for propulsion, the engine will operate at 74.5 rpm on the light propeller curve. Fig. 5.05 shows that 7,700 kWm is available for a PTO at this speed, and can accommodate a 6 MWe generator, including the generator efficiency of 0.9, resulting in 6,666 kWm load on the shaft.

If it is desired to increase the PTO power available or to minimise the ratio of heavy operation (yellow area on Fig. 5.05) while the PTO is engaged, the engine selection spiral is re-entered at step 4. For a fixed propeller curve the SMCR speed can be decreased or the SMCR power increased to increase the margin from the light propeller curve to the $PTO_{\text{layout limit}}$ or for a fixed SMCR the propeller pitch can be reduced.

8. Compliance with regulation

Compliance with global SO_x regulations are achieved by the application of LNG as a fuel. EGR is selected to make it possible to trade globally. Furthermore, EGR for the G95 engine offers

the possibility for a turbo charger cut-out at low loads, improving the performance of the engine in part load as reflected by Fig. 5.04.

The reference EEDI is calculated, with phase 3 (50%) reduction, Ref. [4.3].

The reference speed at 70% dead-weight utilisation (for container carriers only) and 75% MCR in trial condition is calculated to 22.4 knots, and 22.1 knots with PTO.

The attained index is calculated based on the EEDI equation in Chapter 4. The method is similar to example 1, the PTO is included along with the 6% tolerance on the combined heat rate of the pilot oil and gas consumption. As seen below, the attained EEDI of 5.15 is well below the required EEDI.

As the specific gas consumption of the engine is stated for pure methane with an $LCV_{\text{methane}} = 50 \text{ MJ/kg}$, the specific gas consumption must be corrected to correspond to the LCV value of LNG stated by the IMO, $LCV_{\text{LNG}} = 48 \text{ MJ/kg}$, in order to apply the carbon factor of LNG, $C_{F,\text{LNG}} = 2.75$, as determined by the IMO. This has been included in the values applied in the equations, as reflected in the EEDI section of the CEAS report.

As of 2028, the IMO has not specified rules for container carriers with regard to minimum propulsion power. A container carrier has a significantly higher design speed than bulk carriers and tankers, and is hereby considered to have, sufficient installed power for all relevant conditions.

$$\text{Required EEDI} = a \times b^c = 174,22 \times 159,600^{-0.201} \times \left(1 - \frac{50}{100}\right) = 15.22 \times \left(1 - \frac{50}{100}\right) = 7.61 \quad \text{EQ 56}$$

$$\text{Attained EEDI} = \frac{\left(\left(63,000 - \frac{1,825}{0.75}\right) \times 0.75 + 1,825\right) \times 3.206 \times 4.4 + 2.75 \times 134.7}{159,600 \times 22.1} = 5.15 \quad \text{EQ 57}$$

PTO power available [kWm]

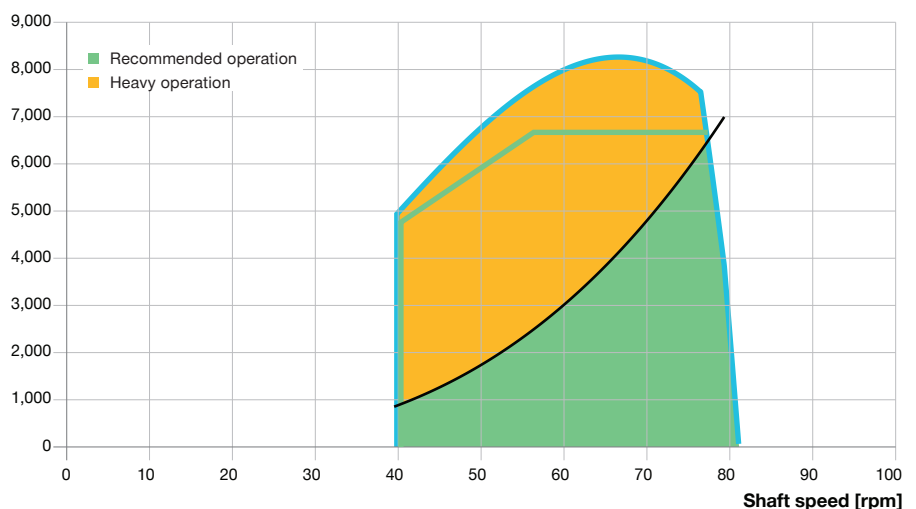


Fig. 5.05: PTO availability over the full speed range for the rating of 63,000 kW at 79 rpm with 4% light running margin. Colours reflect the colour of the load diagram for the specific power, see Fig. 5.03.

Example 3 - ro-ro cargo

A ro-ro cargo ship with CP-propellers and PTO is considered, including the positive influence on EEDI by applying LNG as fuel. The principal parameters of the 6,000 lm ro-ro cargo ship are shown in Table 5.03.

1. Calm water resistance

Again the Ship-DESMO program is used for establishing the calm water resistance, Ref. [2.5].

2. Possible propeller operation for CPP & required power

The ship is equipped with two CP-propellers, and it is assumed that the control system is capable of controlling the pitch independently of propeller rpm.

As an initial estimate, the power required has been calculated for a FP-propeller and since corrected for an assumed 1.5% less effectiveness due to the larger hub of the CP propel-

ler. The application of a well-designed rudder bulb (see Chapter 2) would in most cases reduce the difference between FPP and CPP efficiency significantly, as a rudder bulb eliminates the low pressure/drag behind the hub.

The draught is limited because the cargo is light, which also limits the maximum size of the propeller.

Considering that there will be no significant difference between ballast and loaded condition, as cargo amounts are assumed to be equal on both crossings, and the fact that the lightweight constitutes the major part of the displacement, the propeller size is set relatively large to $d = 6.1$ m with 4 blades. This gives a ratio of $d/T_d = 0.79$, which will require special considerations when designing the aft hull lines.

Twin-screw ships can be designed as a regular hull or as a twin-skeg hull, in this case the first option is selected.

The transmission efficiency is estimated at 99%. The propeller design point (P_D) without any margins is located at $P_D = 10,025$ kW at 117 rpm per shaft for a ship speed of 22 knots.

Deadweight, scantling	15,000 dwt
Deadweight, design	14,000 dwt
Length oa. L_{OA}	228 m
Length bp. L_{PP}	220 m
Breadth	33 m
Depth to main deck	10.5 m
Draught, scantling, T_s	8.0 m
Draught, design, T_d	7.7 m
Displacement, scantling	34,000 t
Lightweight	19,000 t
lwt/dwt	1.27
Block coefficient, C_B scantling	0.57
Block coefficient, C_B design	0.57
Design speed	22 kn
Froude number at design speed	0.24
Propeller diameter, d	6.1 m

Table 5.03: Principal parameters of example 3

3. CPP operating principles for inclusion of PTO

As the ro-ro ship is intended for a large capacity of reefer units, a PTO is intended on each shaft.

In order to maximise the flexibility of the ro-ro ship and minimise the fuel consumption as much as possible, a solution allowing for variable rpm is selected. This is at the cost of including power electronics, for the conversion of the variable electric frequencies generated by the PTO to the constant frequency of the ship's electric grid.

4. Propulsion margins for CPP

Initially, a sea margin of 25% is set for the ship with an engine margin of 15%. The ro-ro ship is intended for scheduled traffic in the North Sea and therefore a large sea margin is included in order to avoid or catch up delays.

If a fixed combinator curve is followed, a rather high LRM, of e.g. 7% if possible, would be relevant as heavy seas can be encountered in the intended operation area, as well as the ship is intended for PTO operation. As the CPP control system is assumed to be able to control the pitch independently of shaft speed, depending on the extent of heavy running, no light running margin is required in the design of a dynamic combinator curve.

Using the margins, the SMCR power and rpm requirements are calculated.

5. Engine layout diagram with SMCR for CPP

The following engines are possible candidates for this project based on the power and rpm requirements calculated:

- S50ME-C9-GI with L_1 at 125 rpm and
- S50ME-C8-GI with L_1 at 127 rpm.

A high load pitch increase is a typical feature for CP-propellers with a combinator curve. The high load pitch increase is typically applied for the last 10 to 15% power, see Fig. 5.06, left. In order to account for the slightly lower L_1 speed of the S50ME-C9-GI engine design, high load pitch increase is applied to a larger extent for this design, see Fig. 5.06, right.

As the pitch is increased at high loads, it will be slightly off the design pitch and result in a small reduction in efficiency. For reasons of simplicity further considerations of this have been omitted in this example.

6. Select engine for CPP

In CEAS there is an FPP option with fuel consumption given along the engine layout curve, and a CPP option with fuel consumption given for con-

stant speed / generator curve operation at the SMCR speed.

In this simple example, the fuel consumption along a conceptual combinator curve can be calculated by interpolating between the SFOC on the engine layout curve and the SFOC on the constant speed (equal to SMCR-speed) curve. Both curves can be obtained through CEAS, the result is shown in Fig. 5.07 for Tier III mode. Alternatively, please contact MarineProjectEngineering2S@man-es.com for estimations of fuel consumptions different from the curves available in CEAS.

Fig. 5.07 illustrates the difference in specific gas consumption (SGC) and specific pilot oil consumption (SPOC) from following the engine layout curve, as for CEAS FPP values, or from following a generator curve from CEAS CPP values. The S50ME-C9 has a pilot oil fraction of 1.5% while the S50ME-C8 operates with a fraction of 3%.

Both the SGC and SPOC increases with lower loads at a higher rate for constant speed CPP operation compared to operation along a nominal FP propeller curve. For constant speed CPP operation the constant amount of pilot oil injected per firing means that pilot oil constitutes a relatively larger share of the total energy consumption as the

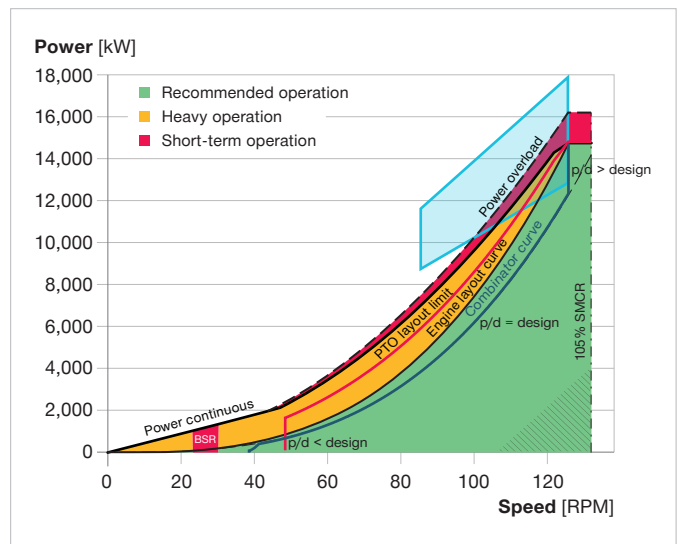
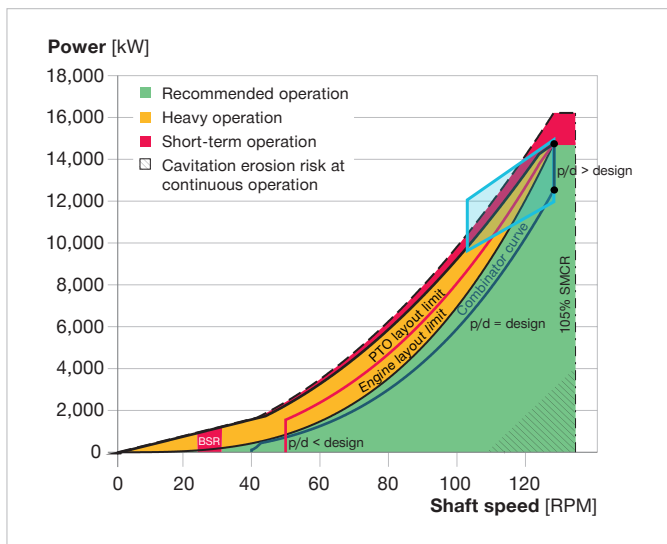


Fig. 5.06: The light propeller curve with conceptual combinator curves plotted on engine load diagram for specific ratings with the layout diagram of the S50ME-C8-GI and S50ME-C9-GI respectively

power is reduce at constant speed. The SFOC at low loads will also increase at a faster rate for constant speed CPP operation, due to the increased relative fictional losses in the engine for low power at constant speed.

The S50ME-C9-GI design will be approx. 5.5% more efficient overall and will be preferred. A significant margin is left to the S50ME-C8-GI design, even if a slight reduction in efficiency as a result of the extended high load pitch increase is considered.

7. Engine load diagram for CPP and considerations of PTO power

The difference between the selected combinator curve and the $PTO_{\text{layout limit}}$ is evaluated, see Fig. 5.06. This indicates up to approx. 3,000 kW capacity per shaft due to the high margins included in this example.

In situations at sea where the margins are exploited and all main engine power is utilised for propulsion, the auxiliary engines on-board must take over the electric load.

8. Compliance with regulation

The ro-ro ship is considered to be in need of compliance with both the NO_x and SO_x ECA regulations, as a typical area of operation would be northern Europe. The EEDI reference line with phase 3 (30%) reduction is calculated, Ref. [4.3]. Note that for ro-ro cargo ships the value of the parameter a set for phase 2 and 3 is different from the value set for phase 0 and 1.

For engines connected to CP propellers, the engine will have to be NO_x -certified according to the constant speed generator curve, irrespectively if a combinator curve is applied. This means that the SGC and SPOC of the generator curve is what will appear in the NO_x certificate and what is to be used in the calculation of the EEDI.

The electric consumption at sea is calculated to be 988 kW, Ref. [4.3]. The reference speed at scantling draught and 75% SMCR is calculated to be 22.73 knots without PTO and 22.47 knots with PTO, using Ref. [2.5].

The attained index is calculated based on the EEDI equation in Chapter 4, considering PTO, the 6% tolerance on the SFOC values, and the f_j correction factor for ro-ro cargo ships.

The calculated correction factor of $f_j = 0.3159$ applied to the main engine related term is only displayed here, the calculation is described in Ref. [4.3].

As the specific gas consumption of the engine is stated for pure methane with an $LCV_{\text{methane}} = 50$ MJ/kg, the specific gas consumption must be corrected to correspond to the LCV value of LNG stated by the IMO, $LCV_{\text{LNG}} = 48$ MJ/kg, in order to apply the carbon factor of LNG, $C_{F,\text{LNG}} = 2.75$, as determined by the IMO. This has been included in the values applied in the equations, as reflected in the EEDI section of the CEAS report.

For reference, the EEDI for MDO is calculated as well. A significant reduction is attained for LNG with MDO as pilot oil.

$$SMCR_{\text{power}} = PD \times \frac{\frac{100 + SM}{100}}{\frac{100 - EM}{100}} = 10,025 \times \frac{\frac{100 + 25}{100}}{\frac{100 - 15}{100}} = 14,750 \text{ kW} \quad \text{EQ 58}$$

$$SMCR_{\text{rpm}} = 117 \times \left(\frac{14,750}{10,025}\right)^{1/3} = 133 \text{ rpm}$$

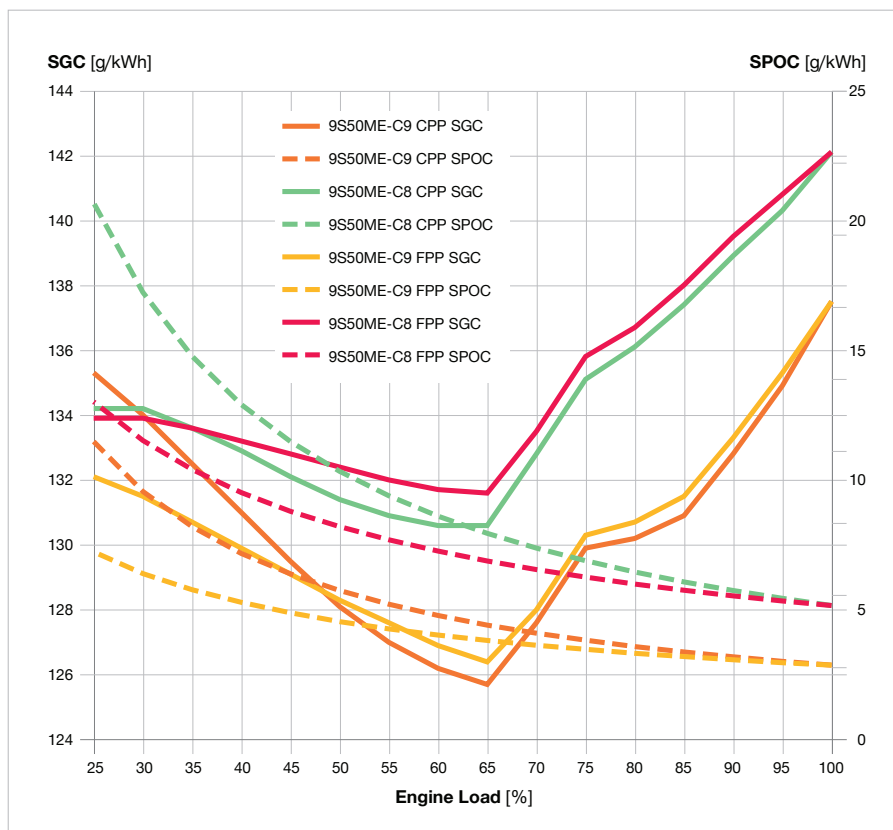


Fig. 5.07: Tier II SGC and SPOC of selected possible engines along the engine layout curve (CEAS FPP) and the generator curve (CEAS CPP). Values may change, please use CEAS for specific values

If the design speed needs to be kept at 22 knots due to a desired operational schedule, LNG is a good option for compliance with EEDI phase 3, reaching 40% reduction from the reference line.

$$\text{Required EEDI} = a \times b^c = 1686.17 \times 15,000^{0.498} \left(1 - \frac{30}{100}\right) = 14.03 \times \left(1 - \frac{30}{100}\right) = 9.82$$

EQ 59

If traditional fuels are employed EEDI phase 2 compliance can be attained. Energy saving devices and likely a reduction of sea and engine margins will be necessary for compliance with EEDI phase 3.

$$\text{Attained EEDI}_{\text{PTO, LNG}} = \frac{\left(\left(29,500 - \frac{987.5}{0.75}\right) \times 0.75 \times 0.3159 + 987.5\right) \times (3.206 \times 3.83 + 2.75 \times 143.2)}{15,000 \times 22.47} = 8.43$$

EQ 60

Similar to example 2, no considerations are currently required with regard to minimum propulsion power for this type of ship.

$$\text{Attained EEDI}_{\text{PTO, MDO}} = \frac{\left(\left(29,500 - \frac{987.5}{0.75}\right) \times 0.75 \times 0.3159 + 987.5\right) \times (3.206 \times 165.2)}{15,000 \times 22.47} = 11.0$$

EQ 61

Closing remarks

In practice, the calculated resistance of the ship will frequently be checked against the results obtained by testing a model of the ship in a towing tank. The experimental tank test measurements are also used for optimising the propeller and hull design along with CFD simulations.

The interaction between ship and main engine is important, in order to achieve the lowest possible fuel consumption for the specific ship design. Different paths for optimising the design can be taken by the ship designer. This also explains why two tender designs for the same ship never look the same.

When the ship's necessary power requirement, including margins, and the propeller's speed (rate of revolution, typically rpm) have been determined, the capabilities of different possible main engines can be investigated. MAN Energy Solutions' online engine calculation programme CEAS supports this.

The placing of the engine's load diagram, i.e. the choice of engine SMCR in relation to the engine's (ship's) operational propeller curve, must be made carefully in order to achieve the optimum propulsion plant.

The engine selection spirals for FP and CP propellers, respectively, will ease this optimisation, including considerations of a possible engine driven shaft generator.

Thanks to the flexibility of the layout and load diagrams for the MAN B&W two-stroke engines, a suitable solution will always be at hand.

For questions to specific cases MAN Energy Solutions can be contacted at MarineProjectEngineering2S@man-es.com.

References

Chapter 1

- [1.1] Harvald, Sv. Aa. and Guldhammer, H. E.: "Ship Resistance", revised edition, Akademisk forlag, 1974
- [1.2] Harvald, Sv. Aa.: "Resistance and Propulsion of Ships", Wiley & Sons, 1983
- [1.3] Holtrop, J. and Mennen, G.G.J.: "An approximate power prediction method", MARIN, 1982
- [1.4] Kitamura, F., Ueno, M., Fujiwara, T. & Sogihara, N.: "Estimation of above water structural parameters and wind loads on ships", Ships and Offshore Structures, vol. 12, 2017
- [1.5] Lackenby, H.: "The Effect of Shallow water on Ship Speed", The Shipbuilder and the Marine engine Builder, 1963
- [1.6] Berthelsen, F. and Nielsen, U.D.: "Prediction of ships' speed-power relationship at speed intervals below the design speed", Transportation Research Part D 99, 2021

Chapter 2

- [2.1] Tornblad, J.: "Fartygspropellar och Fartygs Framdrift", KaMeWa, 1985. In Swedish, EN: "Ship propellers and ship propulsion"
- [2.2] Carlton, J: "Marine Propellers and Propulsion", 3rd edition, Elsevier, 2012
- [2.3] Mewis, P. "Analysis of propeller losses", Hamburgische Schiffbau-Versuchsanstalt, HSVA, 2006
- [2.4] "DNV Fuel Saving guideline - For container ships", DNV and HSVA, 2012
- [2.5] Kristensen, H. O. "Ship-DESMO", 2017. Calculation tool by the Technical University of Denmark.

- [2.6] Breslin, J. P. & Andersen, P. "Hydrodynamics of Ship Propellers", Cambridge Ocean Technology Series, 1996.
- [2.7] DNV rules "Part 4 Systems and components, Chapter 2 Rotating machinery, general"
- [2.8] I.C. Clark "Ship Dynamics for Mariners", The Nautical Institute, 2005.

Chapter 3

- [3.1] Basshuysen, R. V. & Schaefer, F.: "Internal Combustion Engine Handbook", 2nd edition, SAE International, 2016
- [3.2] "Fifth Assessment Report", Intergovernmental Panel on Climate Change, IPCC, 2014
- [3.3] "Alphatronic 3000 - State-of-the-art propulsion control, product information", MAN Energy Solutions, 2017.

Chapter 4

- [4.1] "Emission project guide", MAN Energy Solutions, 2023
- [4.2] "MARPOL Annex VI", IMO
- [4.3] "2014 Guidelines on the method of calculation of the attained energy efficiency design index (EEDI) for new ships, as amended by resolution MEPC.263(83) and MEPC.281(70).", IMO, 2017
- [4.4] "Guidelines for determining minimum propulsion power to maintain the manoeuvrability of ships in adverse conditions, MEPC.1/Circ.850/Rev.3", IMO, 2021
- [4.5] "EEXI Implementation Guidelines, rec. no. 172", IACS 2022
- [4.6] "CII Guidelines, G1-5", IMO 2022
- [4.7] Holt, P. and Nielsen, U.D.: "Preliminary assessment of increased main engine load as a consequence of added wave resistance in the light of minimum propulsion power", Applied Ocean Research 108, 2021

List of abbreviations

AWC	adverse weather conditions	MARPOL	The International Convention for the Prevention of Pollution from Ships
BSR	barred speed range	MCR	maximum continuous rating
BSR _{PM}	barred speed range power margin	mep	mean effective pressure
CAPEX	capital expenditure	MPP	minimum propulsion power
CEAS	computerised engine application system	NCR	normal continuous rating
CII	carbon intensity indicator	NMCR	nominal maximum continuous rating
CP	controllable pitch	OPEX	operating expense
CPP	controllable pitch propeller	PD	propeller design point
DF	dual fuel	PM	particulate matter
DLF	dynamic limiter function	PTI	power take in (shaft motor)
dwt	deadweight tonnage	PTO	power take off (shaft generator)
ECA	emission control area	SCR	selective catalytic reduction
EEDI	energy efficiency design index	SFC	specific fuel consumption
EEXI	energy efficiency existing ship index	SFOC	specific fuel oil consumption
EGR	exhaust gas recirculation	SGC	specific gas consumption
EM	engine margin	SM	sea margin
FP	fixed pitch	SMCR	specified maximum continuous rating
FPP	fixed pitch propeller	SPOC	specific pilot oil consumption
GHG	greenhouse gasses	TCCO	turbocharger cut-out
IMO	International Maritime Organisation	WHR	waste heat recovery
LCB	longitudinal centre of buoyancy		
LCF	longitudinal centre of flotation		
LNG	liquefied natural gas		
LRM	light running margin		
lwt	lightweight tonnage		

MAN Energy Solutions

2450 Copenhagen SV, Denmark

P + 45 33 85 11 00

F + 45 33 85 10 30

info-cph@man-es.com

www.man-es.com

All data provided in this document is non-binding. This data serves informational purposes only and is not guaranteed in any way. Depending on the subsequent specific individual projects, the relevant data may be subject to changes and will be assessed and determined individually for each project. This will depend on the particular characteristics of each individual project, especially specific site and operational conditions.

Copyright © MAN Energy Solutions.
5510-0004-05ppr Apr 2023
Printed in Denmark.